THE UNIVERSITY OF ALBERTA

A MATHEMATICAL MODEL OF PRODUCTION THROUGH A STEAM STIMULATED ZONE

BY

MARCO A. LEAL

A THESIS

SUBMITTED TO THE FACULTY OF GRADUATE STUDIES

IN PARTIAL FULFILMENT OF THE REQUIREMENTS FOR THE

DEGREE OF MASTER OF SCIENCE

IN

PETROLEUM ENGINEERING

FACULTY OF ENGINEERING

DEPARTMENT OF CHEMICAL AND PETROLEUM ENGINEERING

EDMONTON, ALBERTA

APRIL, 1966

UNIVERSITY OF ALBERTA

FACULTY OF GRADUATE STUDIES

The undersigned certify that they have read, and recommend to the Faculty of Graduate Studies for acceptance a thesis entitled A MATHEMATICAL MODEL OF PRODUCTION THROUGH A STEAM STIMULATED ZONE submitted by Marco A. Leal in partial fulfilment of the requirements for the degree of Master of Science in Petroleum Engineering

ABSTRACT

An approximate mathematical model was formulated to describe the "push-pull" method of steam injection during the backflow period. Two example calculations, in which the method of Willman et al(23) was used to calculate the injection period,are included.

The thermal behavior of the strata surrounding the permeable sand was approximated by the one-dimensional heat flow equation. The overburden and underburden were considered as two sets of concentric, semi-infinite cylinders, and the permeable sand was assumed to have an infinite thermal conductivity in the vertical direction.

The temperature distribution in the sand was determined by numerically solving the total energy balance equation for the system. Darcy's law, employing plug flow, was used to compute the saturation distribution and composition of the fluid flowing at various time steps of the numerical solution.

With the exception of viscosity, all physical properties were assumed to be independent of temperature and were calculated at an average temperature.

Although a verification of the model was not possible, the general shape of the calculated back production versus time curves is similar to those observed in field operations(2).

ACKNOWLEDGEMENT

The author wishes to express his sincere appreciation for the guidance and encouragement of Dr. D.L. Flock, Professor, Department of Chemical and Petroleum Engineering, University of Alberta, under whose supervision this investigation was performed.

Acknowledgement and thanks are also owing to the Government of Colombia, and in the latter part to the National Research Council of Canada, for the financial aid that made this project possible.

TABLE OF CONTENTS

TABLE OF CONTENTS

APPENDIX II - THE COMPUTER PROGRAM

LIST OF FIGURES

INTRODUCTION

Statistics, reported by Boberg(2), indicate that, at the end of 1964, 60% of the active new-field projects for secondary recovery, in the United States, involved thermal processes, as compared with about 20% in 1958. This increased popularity of thermal recovery processes is primarily due to higher recovery of high viscosity oils obtained by reservoir heating.

The various thermal techniques proposed may be divided into four basic groups.

1. Electrical methods, in which an electrical heater is installed at the bottom of the hole to heat either the fluids being produced or the fluids being injected.
2. In situ combustion projects, in which part of the oil-in-place is ignited to heat the reservoir.
3. Hot-fluid injection methods, in which steam, hot water, hot air or hot gases are injected into the reservoir.
4. Nuclear explosion techniques.

The injection of hot fluids combines both flooding and thermal effects. These thermal effects have been identified as thermal expansion of the oil and viscosity reduction(23). Steam supplies a large heat of vaporization and, in addition, may cause steam distillation which further increases the recovery of oils with large fractions of steam-distillable components(23).

The major disadvantage of thermal projects is the large heat loss to the strata surrounding the permeable reservoir. For example, calculations of the thermal efficiency, using the method of Marx et al(16), indicate that the heat losses, after five months of injection into a 10-feet thick, circular reservoir, may be as high as 80% of the heat injected. Further analysis shows that most of the heat present in the steam and hot water portions of the sand does not reach the oil bank ahead of the intermediate cold water zone. This behavior of the injection process led to the idea of reversing the direction of flow by stopping injection and producing through the injection well, to recover some of the heat stored in the sand. In addition, if conditions are such that the rate of back production is high, the reservoir sand may behave as a heat sink with respect to the surrounding strata. This alternating process of injection of steam and production of oil has been called the "push-pull" or "huff-and-puff" method of steam injection.

To date, no theoretical study of this process has been published. The purpose of this work is to present an approximate approach to the problem of predicting the back flow.

THEORY AND LITERATURE SURVEY

Heat Losses

Saturated steam is injected into a horizontal, homogeneous, isotropic oil reservoir of constant thickness (see Figure 1a). The heating of the flooded sand and the loss of heat to the surrounding strata causes steam condensation and gradual cooling of the hot water. Three distinct thermal zones may be visualized: a water zone at reservoir temperature, a hot water zone at temperatures varying from reservoir to steam temperature and the steam zone at the saturated steam temperature.

The temperature distribution in the flooded sand has the shape represented by the continuous line in Figure 1C. This representation neglects the variation of steam temperature with distance in the steam zone, due to a decrease in pressure with an increase in distance from the point of injection.

To calculate the position of the various zones at any given time, it is necessary to take into account the following effects:

1. The wellbore heat losses.
2. The heat losses to overburden and underburden.
3. The heat required to heat the flooded sand.

An overall heat balance for the system may be written as

Rate of heat injection at sand face	=	Rate of heat injection at surface	-	Rate of wellbore heat losses
	=	Rate of heat losses to overburden and underburden	+	Heating rate of flooded sand

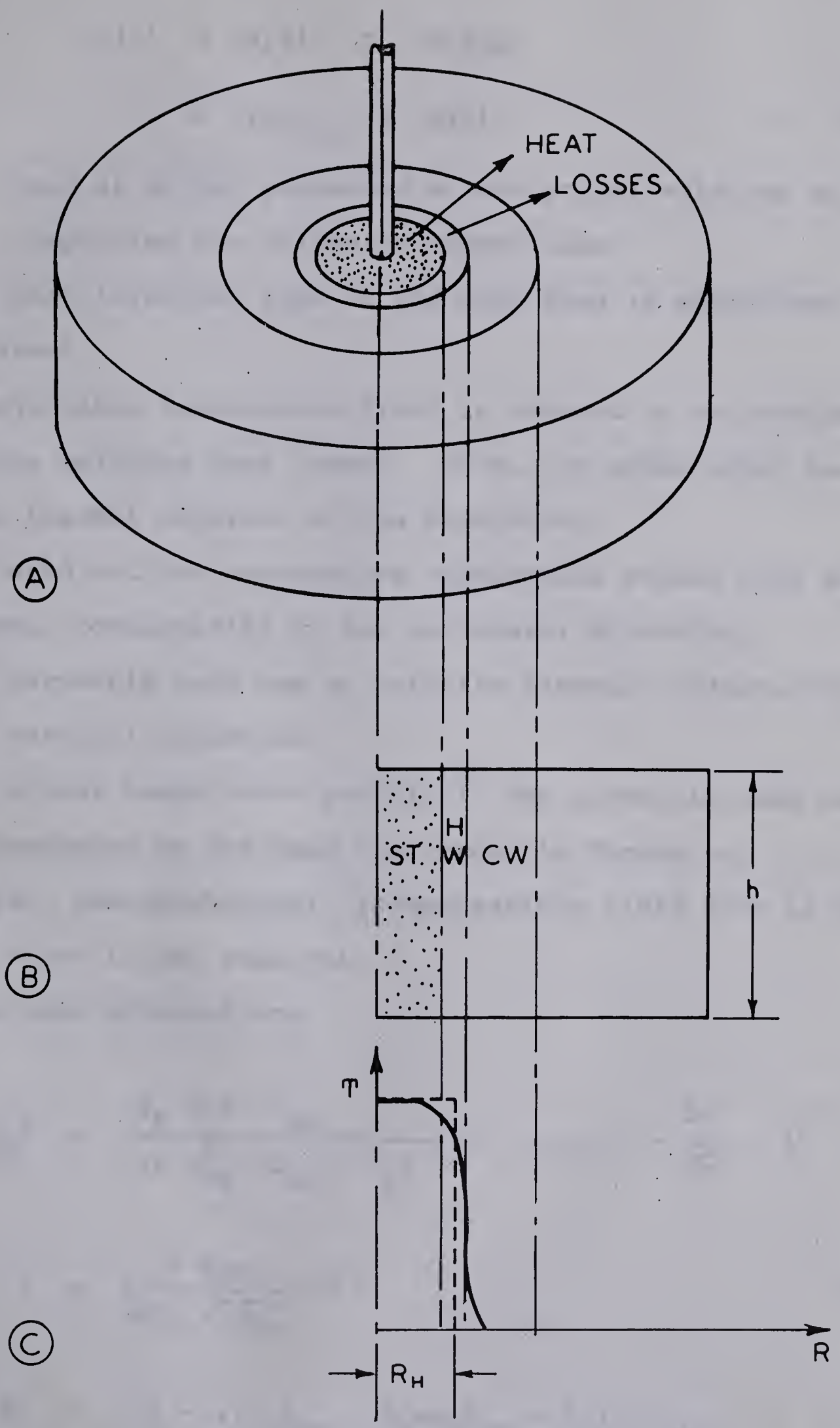

DIAGRAM OF THE PHYSICAL SYSTEM

FIG. 1

$$H_f(t) = H_i(t) - (H_L)_{WB}$$

$$= (H_L)_{OB} + H(t) \qquad (1)$$

Marx et al(16) presented an analytical solution to the problem, employing the following assumptions:

1. The heat injection rate at the sand face is maintained constant.
2. A negligible temperature field is created in the overburden by the wellbore heat losses. Thus, the underburden has the same thermal behavior of the overburden.
3. The sand and the surrounding impermeable strata have zero thermal conductivity in the horizontal direction.
4. The permeable sand has an infinite thermal conductivity in the vertical direction.
5. The actual temperature profile in the permeable sand may be approximated by the dashed line shown in Figure 1C.
6. Radial, one-dimensional, incompressible fluid flow is taking place in the reservoir.

The solutions obtained are

$$R_H^2 = \left(\frac{H_F\, M'h\, \alpha_{OB}}{4\pi\, k_{OB}^2\, (T_{ST} - T_i)}\right)\left(e^{\upsilon^2}\ \text{erfc}\ \upsilon + \frac{2\upsilon}{\sqrt{\pi}} - 1\right) \qquad (2)$$

where

$$\upsilon = \left(\frac{2\, k_{OB}}{M'h\, \sqrt{\alpha_{OB}}}\right) t^{1/2} \qquad (3)$$

$$M' = \left|(1 - \phi)\rho_r C_{pr} + S_w \phi \rho_w C_{pw} + S_o \phi \rho_o C_{po}\right| \qquad (4)$$

$$(H_L)_{OB} = H_f \left(1 - e^{\upsilon^2} \operatorname{erfc} \upsilon\right) \qquad (5)$$

The radii for the steam and hot water zones may be calculated from the "effective radius" R_H.

Equation 2 was modified by Willman et al(23) to establish formulations for the saturation distribution in the sand during the steam injection process.

Lauwerier(11) obtained an analytical solution for the hot water injection case with the same assumptions made by Marx et al. Spillette(22) examined contributions, in Russian literature, of Avdonin(1) and Rubinshtein(20), for hot water injection, and solved a general model employing assumptions 1 and 6 only. The results of these studies, dealing with hot water injection, are applicable to the analysis of the hot water zone advancing ahead of the steam.

The Controlling Heat Transfer Mechanism in Porous Media with A Flowing Fluid

The theoretical prediction of the temperature distribution in the permeable reservoir sand during injection or back production is simplified if controlling heat transfer mechanisms can be selected. Two physical models were studied for the selection of the predominant mechanisms: 1) a semi-infinite porous body through which hot water flows in a linear direction, and, 2) a cylindrical model in which the hot water injected at $r = 0$ flows in the radial direction. These two models are represented in Figure 2. The solid and fluid temperatures in

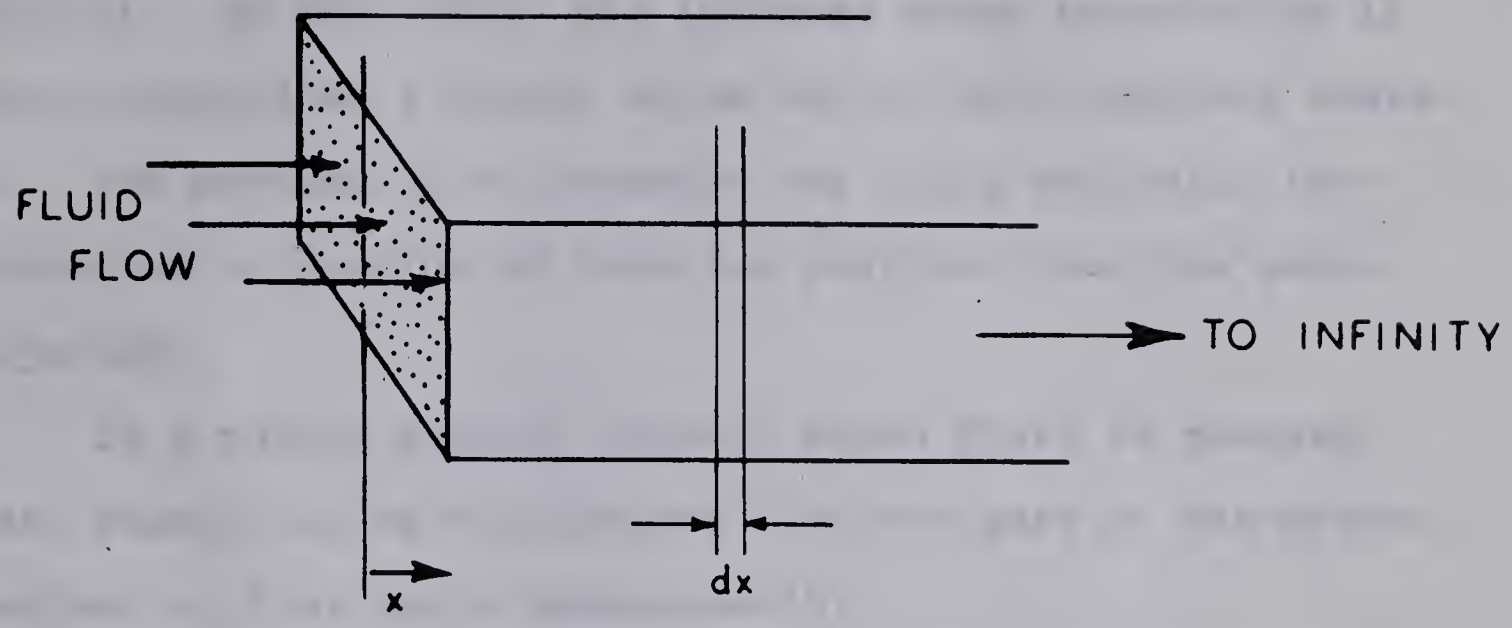

LINEAR MODEL

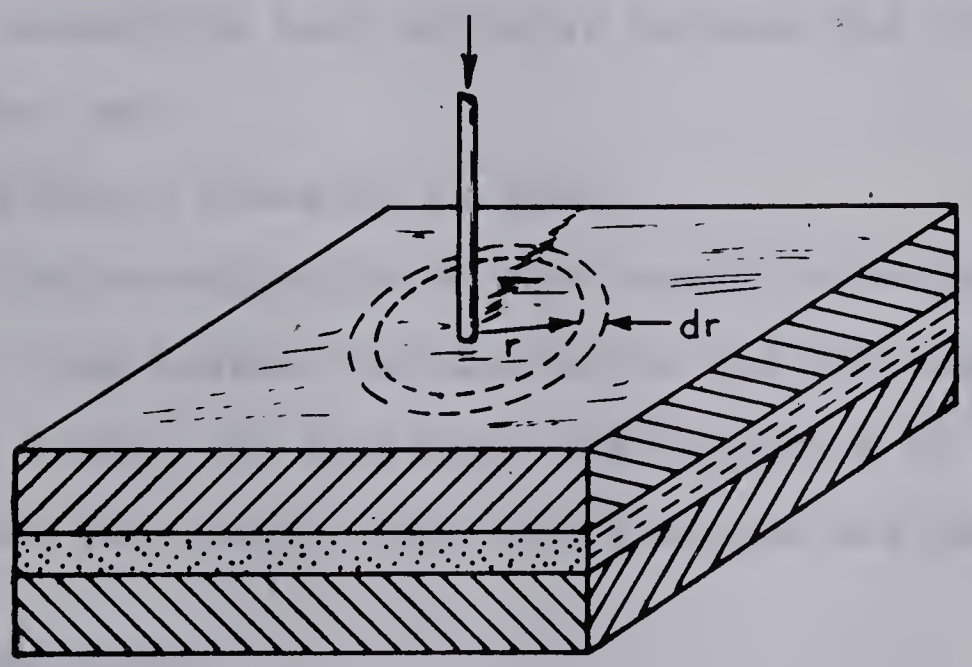

CYLINDRICAL MODEL

PHYSICAL MODELS USED FOR STUDYING THE CONTROLLING HEAT TRANSFER MECHANISMS.

FIG. 2

both models are initially equal to the same constant value throughout. At time zero, the injected water temperature is suddenly changed to a higher value and is held constant thereafter. The problem is to describe the fluid and solid temperatures as a function of time and position from the point of injection.

In a porous medium, through which fluid is passing, thermal energy can be transferred from one part of the system to another by four basic mechanisms(5):

1. the physical movement of the fluid which carries its own thermal energy;
2. the conduction of heat through the solid and fluid phases;
3. the convective heat transfer between the solid and fluid phases, and
4. the radiant transfer of heat.

The contribution of the fourth mechanism, radiant heat transfer, was assumed negligible in all the papers reviewed for this study. In addition, the variation of the physical properties with temperature and pressure was neglected.

The Linear Model

Hadidi(6) suggested the following assumptions:

1. An instantaneous thermal equilibrium between the injected fluid and the model fluid and sand is always attained, that is, the convective heat transfer coefficient is infinite, and

2. the heat transferred by conduction in the sand and in the fluid is negligible.

The differential equation for this model and its solution are

$$(\rho_r C_{pr}(1 - \phi) + \rho_w C_{pw}\phi) \frac{\partial T}{\partial t} = v\rho_w C_{pw}\phi \frac{\partial T}{\partial x} \quad (6)$$

$$V_F = \frac{dx}{dt} = \frac{v\rho_w C_{pw}\phi}{\rho_r C_{pr}(1 - \phi) + \rho_w C_{pw}\phi} = \text{constant} \quad (7)$$

$$X_F = V_F t \quad (8)$$

According to this approach, the temperature of the outlet fluid would vary with time in the manner illustrated by Curve 1 in Figure 3. However Preston et al(11) found that the corresponding outlet fluid temperature profile had the characteristic S-shape shown in the same figure.

Hausen(7) and Schumann(21) independently derived equations describing the process under the assumption that "mechanism 2", heat conduction from point to point within either phase, may be neglected. The corresponding equations are

$$\rho_w C_{pw}\phi \frac{\partial T_w}{\partial t} = -v\rho_w C_{pw}\phi \frac{\partial T_w}{\partial x} - ha(T_w - T_r) \quad (9)$$

$$\rho_r C_{pr}(1 - \phi)\frac{\partial T_r}{\partial t} = ha(T_w - T_r) \quad (10)$$

The solutions to Equations 9 and 10, which are integrals containing Bessel functions, have been evaluated by numerical or

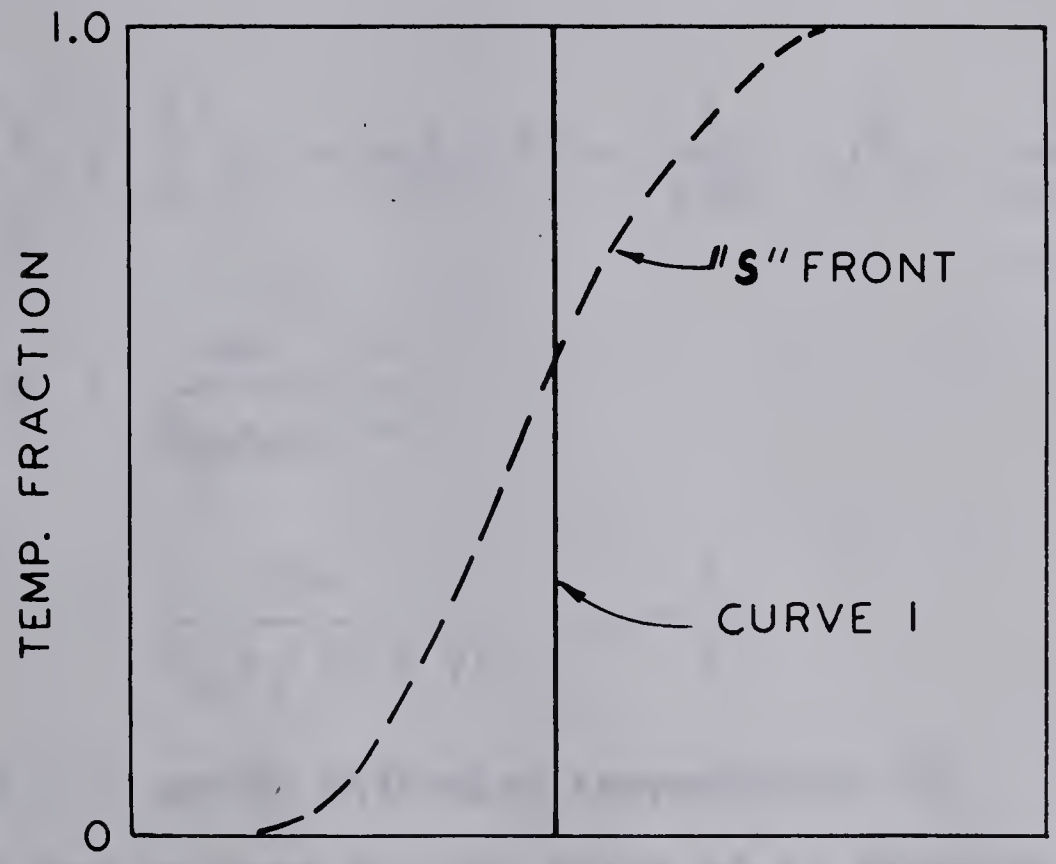

LINEAR MODEL -
OUTLET FLUID TEMP. VS. TIME

FIG. 3

graphical methods. Klinkenberg(9) found that the exact solutions may be approximated, within fixed limits, by probability integrals. The fit was made by choosing the appropriate upper limits of integration. Klinkenberg proposed the approximations:

$$\frac{T_w - T_i}{T_l - T_i} \simeq \frac{1}{2}\left[1 + \text{erf}\left(\sqrt{Z} + \frac{1}{8\sqrt{Z}} - \sqrt{Y} + \frac{1}{8\sqrt{Y}}\right)\right] \quad (11)$$

$$\frac{T_r - T_i}{T_l - T_i} \simeq \frac{1}{2}\left[1 + \text{erf}\left(\sqrt{Z} - \frac{1}{8\sqrt{Z}} - \sqrt{Y} - \frac{1}{8\sqrt{Y}}\right)\right] \quad (12)$$

where

$$Y = \frac{ha}{C_{pw}\rho_w\phi}\,\frac{x}{v} \quad (13)$$

$$Z = \frac{ha}{C_{pr}\rho_r\,(1-\phi)}\left(t - \frac{x}{v}\right) \quad (14)$$

T_l = water injection temperature, °F

Equation 12 may be used for any value of Z, Equation 11 for $Z > 1$ provided $Y > 2$ in both cases. The maximum error under these conditions is less than $\pm 1\%$.

Preston et al(19) applied the Hausen and Schumann model to studies of packed columns to determine the effect of the flow rate, the column length and the sand size on the convective heat transfer coefficient,ha. The water velocity, based on the effective flow area, varied from 2 to 25 feet per hour, the sand size from 20 to 170 U.S. mesh and the column length from

6.03 to 24 inches. The convective heat transfer coefficient was found to be independent of the sand size and the length of the column, but dependent on the fluid velocity raised to the 1.8 power, according to the equation

$$ha = 54.5\ v^{1.82} \tag{15}$$

It should be remarked that ha, calculated by applying Equations 9 and 10 is fictitious, if the conduction mechanism is not negligible.

Jenkins et al(8) essentially made the opposite assumption concerning the mechanism of heat transfer. These authors considered conduction to be an important mechanism and assumed negligible heat flow by convection between the solid and the fluid. Consequently, the system can be described by one differential equation:

$$(\rho_r C_{pr}(1 - \phi) + \rho_w C_{pw}\phi)\ \frac{\partial T}{\partial t} = - v\rho_w C_{pw}\phi\ \frac{\partial T}{\partial x} + k\ \frac{\partial^2 T}{\partial x^2} \tag{16}$$

where

$$k = k_w\phi + k_r(1 - \phi)$$

The solution to Equation 16 is

$$\frac{T - T_i}{T_1 - T_i} = \frac{1}{2}\left[\operatorname{erfc}\left(\frac{x}{2\sqrt{\alpha t}} - \sigma\sqrt{\alpha t}\right) + e^{2x\sigma}\operatorname{erfc}\left(\frac{x}{2\sqrt{\alpha t}} + \sigma\sqrt{\alpha t}\right)\right] \tag{17}$$

where

$$\sigma = \frac{vC_{pw}\rho_w}{2\alpha\ (\phi\rho_w C_{pw} + (1 - \phi)C_{pr}\rho_r)}$$

Equation 17 was found to fit the experimental results of Preston et al when an average thermal conductivity of 1.0 BTU/hr. ft.°F was used. Any contribution of the convective mechanism, which may be present in this value for the thermal conductivity, was neglected.

Kunii et al(10) carried out experimental work on heat transfer in linear beds of glass beads and sand through which fluids were flowing. The data were interpreted in terms of an apparent or effective thermal conductivity, k_e. The use of an effective thermal conductivity implies that the system possesses a single, mean temperature at every point. The mathematical model of Kunii et al, however, differs from that of Jenkins et al in the sense that k_e does include any effect of the convective heat transfer mechanism, if present. Correlations for k_e vs Reynolds numbers based on particle diameter were given for five different fluids: helium, nitrogen, air, carbon dioxide and liquid water. To accurately measure values for k_e at low flow rates was difficult. This is specially true for the sand-water system, for which only one correlation for modified Reynolds numbers less than 0.005 was presented. The values of k_e were found to increase significantly with the mass velocity of the fluid.

Green et al(5) derived a general set of differential equations for the linear model with all three heat transfer mechanisms included. These equations are

For the water phase

$$\rho_w C_{pw} \phi \frac{\partial T_w}{\partial t} = - v \rho_w C_{pw} \phi \frac{\partial T_w}{\partial x} + k_w \phi \frac{\partial^2 T_w}{\partial x^2} - ha(T_w - T_r) \quad (18)$$

For the solid phase

$$\rho_r C_{pr} (1 - \phi) \frac{\partial T_r}{\partial t} = k_r (1 - \phi) \frac{\partial^2 T_r}{\partial x^2} + ha\ (T_w - T_r) \quad (19)$$

Equations 18 and 19 were written in dimensionless form by choosing the parameters:

$$\lambda = \left(\frac{ha}{k_w \phi}\right)^{1/2} \frac{\alpha_w}{v} \quad (20)$$

$$T^* = \frac{T - T_i}{T_1 - T_i} \quad (21)$$

$$Y = \left(\frac{ha}{k_w \phi}\right)^{1/2} x \quad (22)$$

$$\eta = \left(\frac{ha}{k_w \phi}\right)^{1/2} vt \quad (23)$$

T_1 = injection temperature, °F

and solved with different parametric values to study their effects. The systems studied were water flowing through silica beads and through glass beads. At λ values of 0.114 or less, the numerical solutions were found to approach the

curves assuming $k_w = k_r = 0$, implying that the convective mechanism essentially controls the profile shape. When λ was equal to 0.342 or higher, the numerical solutions more closely approach those solutions based on the assumption of $T_w = T_r$. In the intermediate λ range, both mechanisms of heat transfer control the temperature profile. Green et al have explained how the above numerical calculations may be used to select a value for the effective thermal conductivity, k_e, for describing a given system by a single equation. They applied the procedure to the data of Preston et al(19) and found that k_e depended on the fluid velocity, v. A relationship between k_e and v for the systems silica-water, silica-ethyl alcohol and glass-iso-octane was presented in graphical form. The velocity range studied was 0 to 22 feet per hour. The greatest deviation between calculated and predicted k_e's was about 20%.

The Cylindrical Model

The multidimensional physical model constructed and operated by Malofeev(13,14) had a sand section of 1 inch high, 28 inches long and 9 inches wide. The surrounding impermeable strata were simulated by clay layers, each 5 inches thick. A series of five experiments were performed at different hot water injection rates.

Spillette(22) calculated the thermal behavior of Malofeev's physical model for three water superficial injection

velocities: 0.52, 2.07 and 4.14 feet per hour. The method of the characteristics, as applied in reference 17, was used to solve the energy balance equation, based on the Jenkins et al(8) physical model. That is, the convective transport of heat was accounted for by the assumption of instantaneous thermal equilibrium between the sand and the fluid.

This literature review on the controlling heat transfer mechanisms in porous media containing flowing liquids has shown that

1. there is a difference of opinion concerning the liquid velocity at which the convective heat transfer mechanism essentially controls the transport of heat, and
2. the concept of apparent or effective thermal conductivity provides the simplest correlation basis, whether the convective transport of heat is negligible or not.

THE PHYSICAL MODEL FOR BACK PRODUCTION

The physical model was represented by a porous cylinder of radius R and thickness h through which radial, incompressible fluid flow occurred in a horizontal plane. The fluid and solid temperatures were assumed equal to the same initial constant value throughout. At time zero, a mixture of oil and water at a lower temperature, was injected, at constant pressure and temperature, into every point of the external cylindrical surface. The following assumptions were also made:

1. The impermeable strata had zero thermal conductivity in the horizontal direction and a finite thermal conductivity in the vertical direction.
2. The permeable reservoir sand had a finite thermal conductivity in the horizontal direction and an infinite thermal conductivity in the vertical direction.
3. The solution gas in the reservoir fluids was assumed to be negligible.
4. The heat transfer process within the permeable sand was described by using an average effective thermal conductivity selected from reference 5. The value for the effective thermal conductivity was held constant.
5. The fluids entering the hot cylinder were not heated by conductive heat transfer through the sand before reaching the boundary r = R.
6. Values of the physical properties were estimated at

average conditions of temperature and pressure and were assumed to remain constant. The oil and water viscosities were considered to be known functions of temperature.

Other assumptions concerning the calculations for the heat flux through the flat surfaces of the cylinder and the fluid distributions are given in the following pages.

To derive the energy balance equation, consider a cylindrical element of cross-sectional area dA and height h, which are depicted schematically in Figures 4A and 4C. The total energy balance may be written as follows:

Heat in by conduction during dt	+	Heat in by bulk flow during dt	±	Heat in or out by conduction through the flat surfaces during dt		
= Heat out by conduction during dt	+	Heat out by bulk flow during dt	+	Enthalpy change of element during dt		

or algebraically in the form

$$q_r dt + v\rho_f C_{pf} \phi 2\pi (r + dr) h T_{r+dr} dt \pm \dot{q} dt$$

$$= q_{r+dr} dt + v\rho_f C_{pf} \phi 2\pi r h T_r dt + 2\pi r h dr\, d(\rho C_p T)$$

Rearranging

$$(q_r - q_{r+dr}) dt + v\rho_f C_{pf} \phi 2\pi h [(r + dr) T_{r+dr} - r T_r] dt$$

$$\pm \dot{q} dt = 2\pi h\, r\, dr\, d(\rho C_p T) \qquad (24)$$

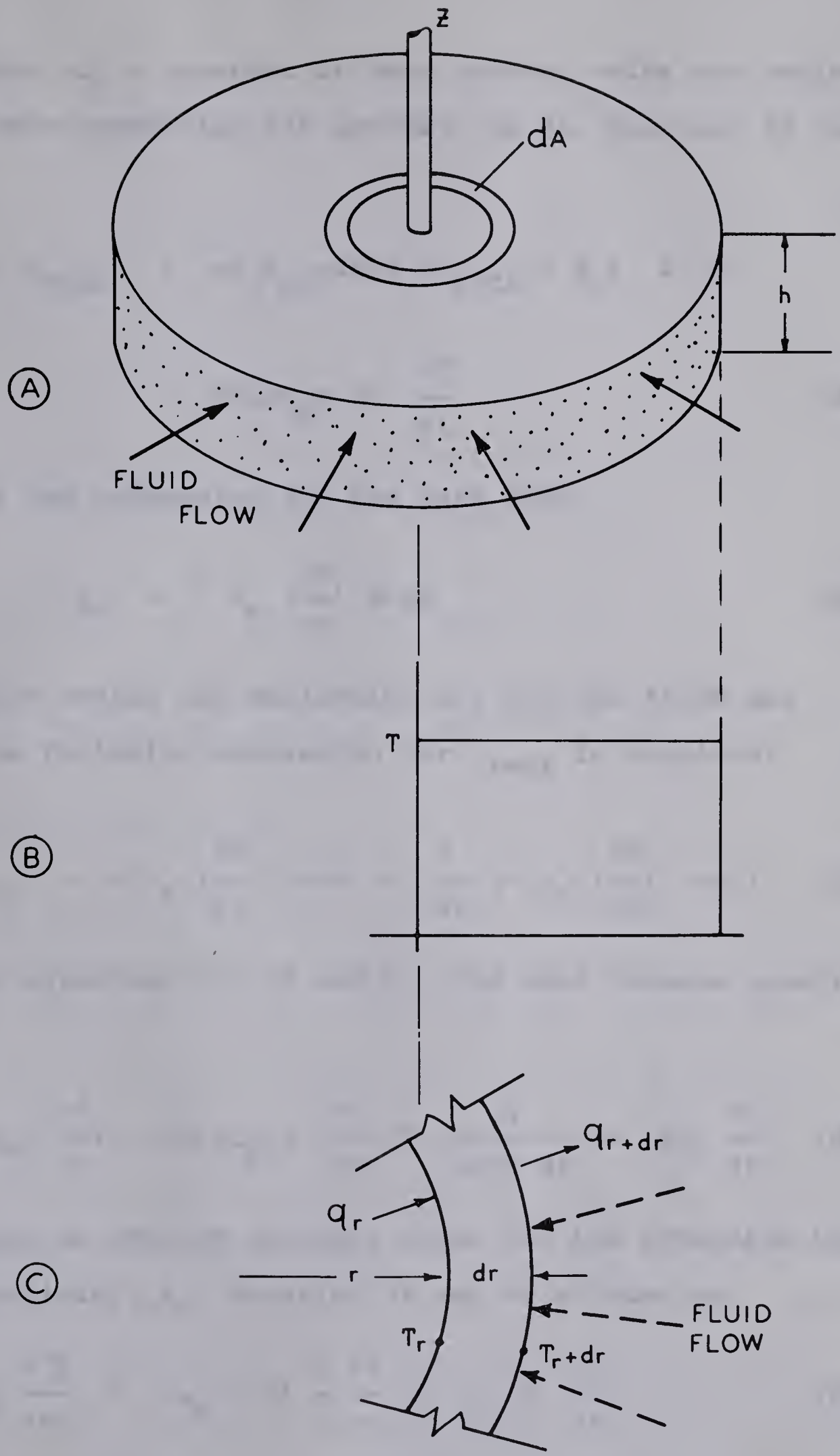

PHYSICAL MODEL FOR BACK-PRODUCTION.

FIG. 4

By assuming ρC_p = constant at some average value and neglecting the term containing the product, dr dt, Equation 24 becomes

$$(q_r - q_{r+dr}) + v\rho_f C_{pf} \phi 2\pi rh\,(T_{r+dr} - T_r) \pm \dot{q}$$

$$= 2\pi h \rho C_p r\, dr \frac{\partial T}{\partial t} \qquad (25)$$

Expanding the expression for the heat flux:

$$q_r = - k_e \left(\frac{\partial T}{\partial r}\right) 2\pi rh \qquad (26)$$

in a Taylor series and neglecting all but the first two terms, the following expression for q_{r+dr} is obtained:

$$q_{r+dr} = - k_e \left(\frac{\partial T}{\partial r}\right) 2\pi rh + \frac{\partial}{\partial r}\left[- k_e \left(\frac{\partial T}{\partial r}\right) 2\pi rh\right] \qquad (27)$$

Combining equations 25, 26 and 27, the heat balance equation becomes:

$$\frac{1}{r}\frac{\partial}{\partial r}\left[k_e r \left(\frac{\partial T}{\partial r}\right)\right] + v\rho_f C_{pf} \phi \frac{\partial T}{\partial r} \pm \frac{\dot{q}}{2\pi hr\, dr} = \rho C_p \frac{\partial T}{\partial t} \qquad (28)$$

By choosing an average constant value for the effective thermal conductivity, k_e, Equation 28 may be written as

$$\alpha_e \frac{\partial^2 T}{\partial r^2} + (\alpha_e + M) \frac{1}{r}\frac{\partial T}{\partial r} \pm C = \frac{\partial T}{\partial t} \qquad (29)$$

where

$$M = \frac{v r \rho_f C_{pf} \phi}{\rho C_p} \qquad (30)$$

$$C = \frac{q_T}{\rho C_p h} \tag{31}$$

$$q_T = \frac{\dot{q}}{dA} \tag{32}$$

$$\alpha_e = \frac{k_e}{\rho C_p} \tag{33}$$

The following set of boundary conditions were chosen:

1. $T = T_i = \text{constant}$ when $r = R_H$

2. $\frac{\partial T}{\partial r} = 0$ when $r = 0$

3. $T = T_{ST}$ when $t = 0$ for $0 < r < R_H$

Calculation of the C Term

To calculate the heat losses or gains through the flat surfaces of the cylindrical model, a knowledge of the temperature distribution existing in the overburden and in the underburden at the end of the steam injection process is necessary. This temperature profile is a function of R and t, implying that the C term in Equation 29 is not a constant. The impermeable strata was divided into a series of concentric cylinders within which C was assumed to be constant. Equation 29 was solved numerically using the boundaries of these cylinders as grid points. This approach allowed the use of different C's for different grids and thus, took into account

the dependence of C on R.

The computation of C for every cylinder was done by assuming one-dimensional heat flow from the sand during injection. A summary of the relevant equations follows.

Consider a cylindrical element with an inner radius r_j and an outer radius r_{j+1} where, j and j+1 are subscripts indicating the j and the (j+1) grid intersections in the r-direction. The temperature profile in the cylinder after injection is given by the solution of the equation

$$\frac{\partial^2 T}{\partial Z^2} = \frac{1}{\alpha_{OB}} \frac{\partial T}{\partial t} \qquad (34)$$

with the boundary conditions,

1. $T = T_{ST}$ when $Z = 0$
2. $T = T_i$ when $Z = \infty$
3. $T = T_i$ when $t = 0$ for any Z

The solution is

$$T - T_i = (T_{ST} - T_i) \operatorname{erfc} \left(\frac{Z}{2\sqrt{\alpha_{OB} t_j}}\right) \qquad (35)$$

The injection time for each cylinder, t_j, was calculated by the method of Willman et al(23), by subtracting the time necessary for the steam to reach the distance r_j from the combined injection and soaking time, t_I.

Equation 34 was then solved using Equation 35 as the initial condition to determine the temperature distribution

in the overburden cylinder during the back-flow period. Hence, the new boundary conditions for Equation 34 are

1. $T_S = T_S(t)$ when $Z = 0$

2. $T = T_i$ when $Z = \infty$

3. $T = T_i + (T_{ST} - T_i)\ \mathrm{erfc}\ \left(\frac{Z}{2\sqrt{\alpha_{OB} t_j}}\right)$ when $t = 0$ for any Z

The subscript S emphasizes that the given condition is valid at $Z = 0$ only.

The solution is given by Carslaw and Jaeger(3) as

$$T - T_i = \frac{1}{2\sqrt{\pi \alpha_{OB} t}} \int_0^{\infty} (T_{ST} - T_i)\ \mathrm{erfc}\ \left(\frac{Z'}{2\sqrt{\alpha_{OB} t_j}}\right) \quad x$$

$$\left(e^{-\frac{(Z-Z')^2}{4\alpha_{OB} t}} - e^{-\frac{(Z+Z')^2}{4\alpha_{OB} t}}\right) dZ'$$

$$+ \frac{2}{\sqrt{\pi}} \int_{\frac{Z}{2\sqrt{\alpha_{OB} t}}}^{\infty} \theta_S(\zeta)\ e^{-\xi^2}\ d\xi \qquad (36)$$

where

$$\theta = T - T_i$$

$$\theta_S(\xi) = T_S\ \left(t - \frac{Z^2}{4\alpha_{OB}\xi^2}\right) - T_i$$

$$\zeta = t - \frac{Z^2}{4\alpha_{OB}\xi^2}$$

The temperature of the element at Z = 0 (see Figure 5), $\theta_S(t) = T_S(t) - T_i$, must be expressed as a function of time before attempting to integrate Equation 36. $\theta_S(t)$ was approximated by a step function as follows:

$$\theta_S(t) = \theta^{(1)} = \text{constant for} \quad 0 < t < \tau_1$$
$$\theta_S(t) = \theta^{(2)} = \text{constant for} \quad \tau_1 < t < \tau_2$$
$$\theta_S(t) = \theta^{(3)} = \text{constant for} \quad \tau_2 < t < \tau_3$$
$$\cdots\cdots$$
$$\theta_S(t) = \theta^{(N)} = \text{constant for} \quad \tau_{N-1} < t < \tau_N$$

Figure 6 shows the schematic representation of the step function approximation. The second integral of Equation 36 becomes

$$\frac{2}{\sqrt{\pi}} \int_{\frac{Z}{2\sqrt{\alpha_{OB}t}}}^{\infty} \theta_S(\zeta) e^{-\xi^2} d\xi = \theta^{(1)} \operatorname{erfc} \frac{Z}{2\sqrt{\alpha_{OB}t}}$$
$$+ (\theta^{(2)} - \theta^{(1)}) \operatorname{erfc} \frac{Z}{2\sqrt{\alpha_{OB}(t - \tau_1)}}$$
$$+ (\theta^{(3)} - \theta^{(2)}) \operatorname{erfc} \frac{Z}{2\sqrt{\alpha_{OB}(t - \tau_2)}} + \cdots$$
$$+ (\theta^{(N)} - \theta^{(N-1)}) \operatorname{erfc} \left(\frac{Z}{2\sqrt{\alpha_{OB}(t - \tau_{N-1})}}\right) \qquad (37)$$

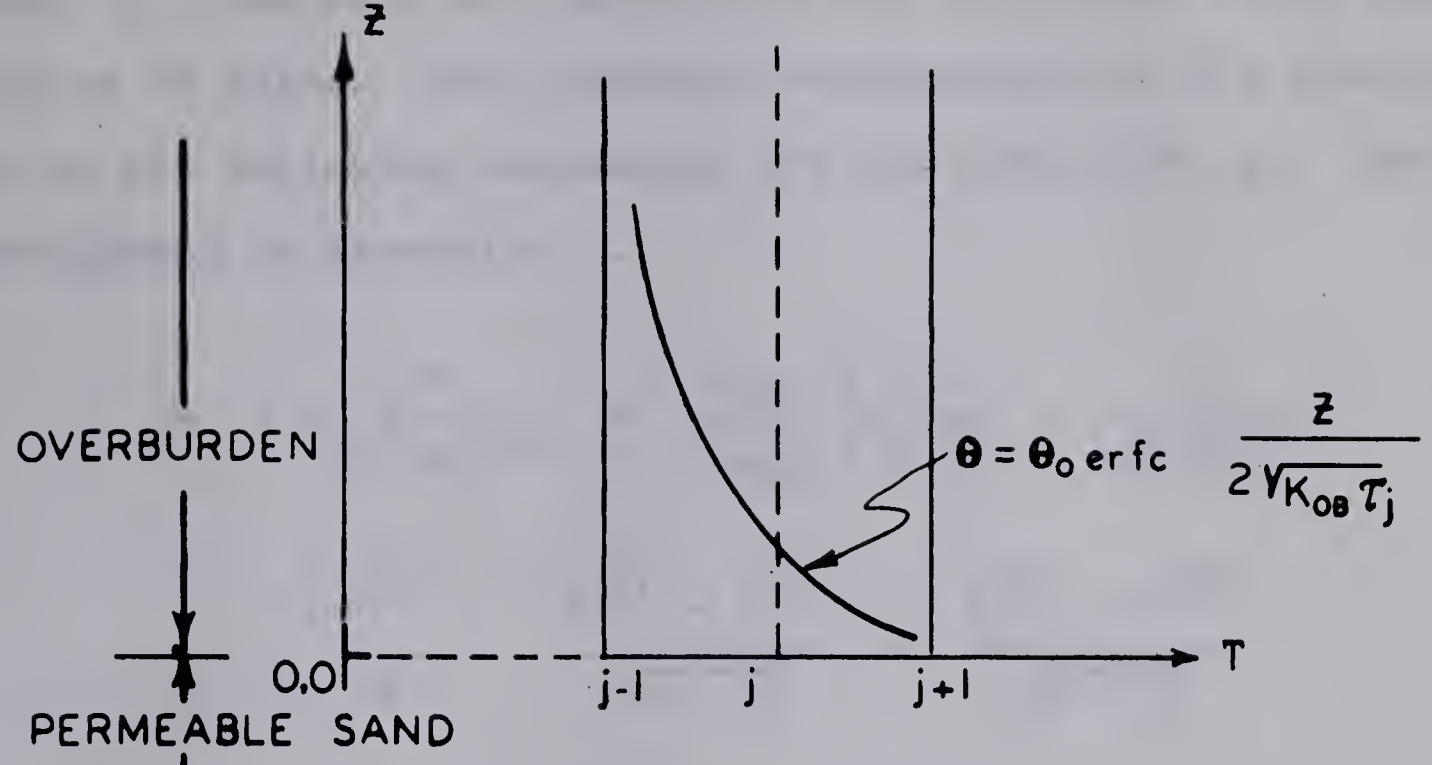

FIG. 5 TEMP. PROFILE IN OVERBURDEN ELEMENT AFTER STEAM INJECTIÓN (k horizontal = 0).

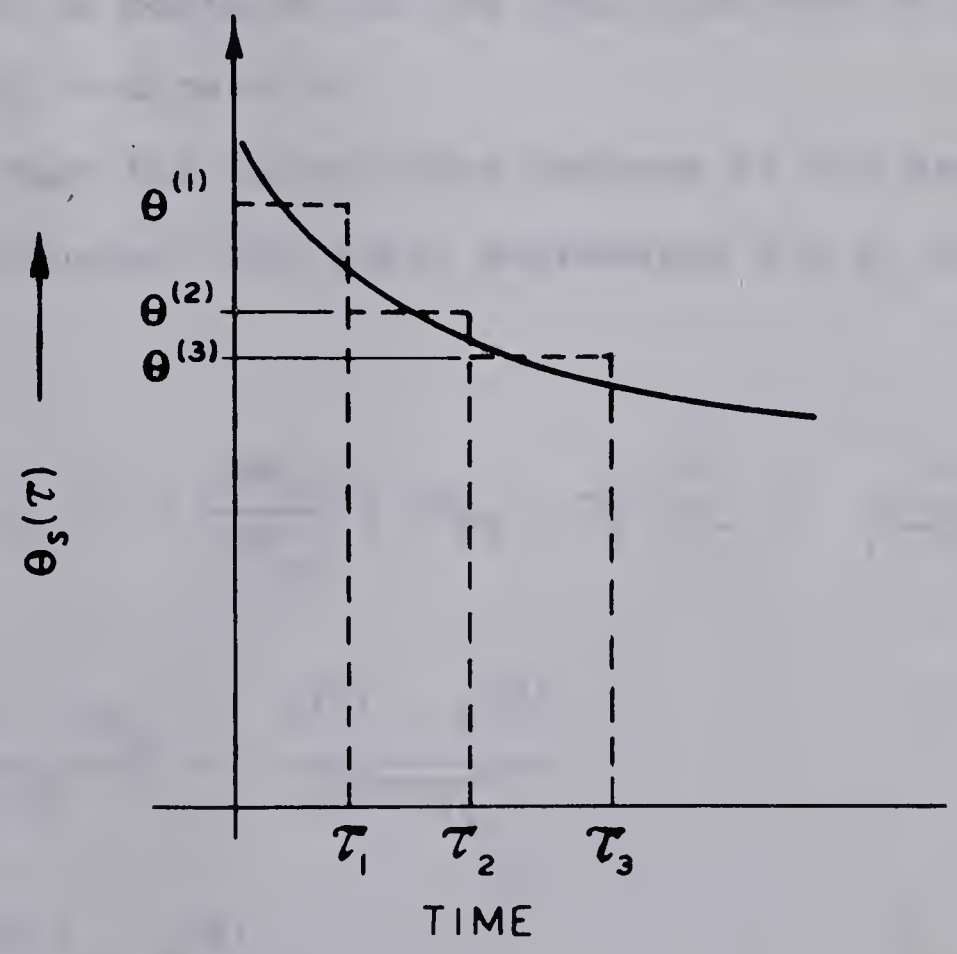

FIG. 6

APPROXIMATION FOR $\theta_s(\tau)$

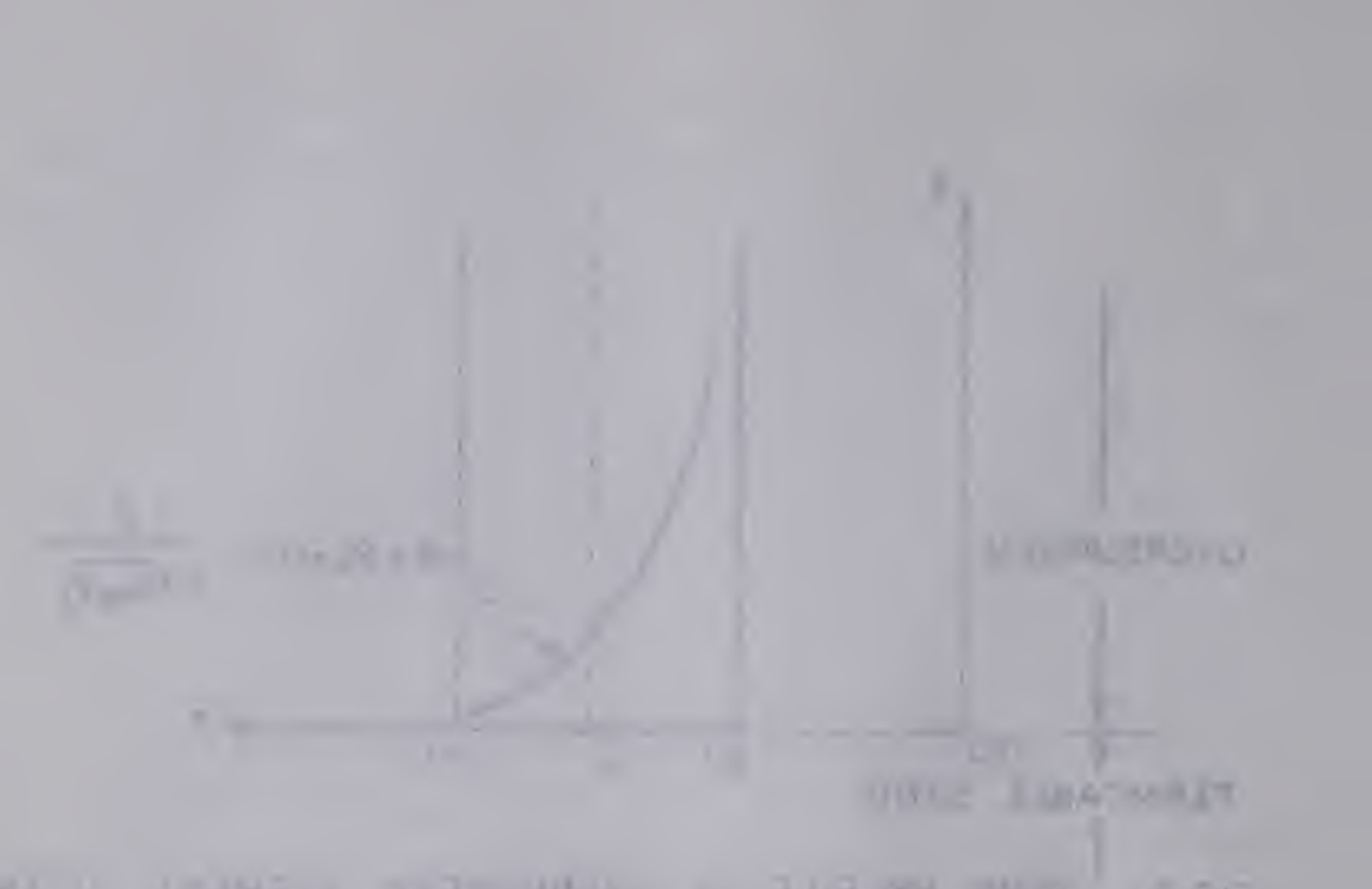

The first integral appearing in Equation 36 was not evaluated directly. Instead, its derivative was calculated using integration by parts. The algebraic manipulation of the equation led to the following expression for the heat flux, q_1, (see development in Appendix 1).

$$q_1 = + k_{OB}\left(\frac{\partial \theta}{\partial Z}\right)_{Z=0} = \frac{k_{OB}}{\sqrt{\pi \alpha_{OB}}}\left[\theta_o\left(\frac{1}{\sqrt{t}} - \frac{1}{\sqrt{t + t_j}}\right)\right.$$

$$- \frac{\theta^{(1)}}{\sqrt{t}} + \frac{\theta^{(1)} - \theta^{(2)}}{\sqrt{t - \tau_1}} + \frac{\theta^{(2)} - \theta^{(3)}}{\sqrt{t - \tau_2}}$$

$$\left. + \ . \ . \ . + \frac{\theta^{(N-1)} - \theta^{(N)}}{\sqrt{t - \tau_{N-1}}}\right] \qquad (38)$$

where q_1 was taken as positive if the heat flux was in the negative (downward) Z-direction.

Assuming that the underburden behaves in the same manner as the overburden, the final expression for q_T was found to be

$$q_T = q_1 + q_2 = + \frac{2k_{OB}}{\sqrt{\pi \alpha_{OB}}}\left[(T_{ST} - T_i)\left(\frac{1}{\sqrt{t}} - \frac{1}{\sqrt{t + t_j}}\right)\right.$$

$$- \frac{T^{(1)} - T_i}{\sqrt{t}} + \frac{T^{(1)} - T^{(2)}}{\sqrt{t - \tau_1}} + \ . \ . \ .$$

$$\left. + \frac{T^{(N-1)} - T^{(N)}}{\sqrt{t - \tau_{N-1}}}\right] \qquad (39)$$

where t = total back production time

τ_1 = first back production time increment

$(\tau_2 - \tau_1)$ = second back production time increment

$(\tau_3 - \tau_2)$ = third back production time increment

. . . . . .

$(\tau_N - \tau_{N-1})$ = n^{th} back production time increment

The term C was calculated for every cylindrical element at every time step using Equations 31 and 39.

Calculation of M

The term M appearing in Equation 29 was defined by Equation 30. In field units it becomes

$$M = \frac{0.03720\ W\rho_f C_{pf}}{h\rho C_p} \tag{40}$$

where

$$\rho_f = X_w\rho_w + x_o\rho_o \tag{41}$$

$$C_{pf} = X_w C_{pw} + X_o C_{po} \tag{42}$$

$$\rho C_p = \rho_r C_{pr}(1 - \phi) + \rho_f C_{pf}\phi \tag{43}$$

An examination of Equations 40 to 43 showed that expressions for the rate of back production and the composition of the mixture of oil and water flowing had to be determined before solving Equation 29 for the temperature profile. Neither of these two variables is a known function of time

and both are dependent on the temperature distribution existing in the reservoir at any time. In addition, the rate of back production is dependent on the fluid saturation distribution prevailing in the reservoir, which is also a function of time. A numerical approach was chosen for solving Equation 29 which facilitated the stepwise change of values of these variables with time. The procedure followed will be explained in a step-by-step fashion for the sake of clarity.

a) Calculation of the Initial Rate of Back Production

A schematic representation of the saturation distribution during steam injection(23) is shown in Figure 7. The "actual" saturation distribution may be approximated by taking average values in each zone as shown in the same Figure. The initial rate of back production was calculated from the equation:

$$W_i = \frac{0.007080\ h\Delta P}{\frac{1}{\lambda_{co}} \ln \frac{r_e}{R_{oi}} + \frac{1}{\lambda_{cW}} \ln \frac{R_{oi}}{R_{HW}} + \frac{1}{\lambda_{HW1}} \ln \frac{R_{HW}}{R_H} + \frac{1}{\lambda_{HW2}} \ln \frac{R_H}{R_{ST}} + \frac{1}{\lambda_{ST}} \ln \frac{R_{ST}}{r_e}}$$

where

$$\lambda = \lambda_o + \lambda_w = \frac{k_{ro}k}{\mu_o} + \frac{k_{rw}k}{\mu_w} \qquad (44)$$

This equation may be simplified to

$$W_i = \frac{0.00708\ h\Delta P}{\frac{1}{\lambda_{co}} \ln \frac{r_e}{R_{oi}} + \frac{1}{\lambda_{cW}} \ln \frac{R_{oi}}{R_{HW}}} \qquad (45)$$

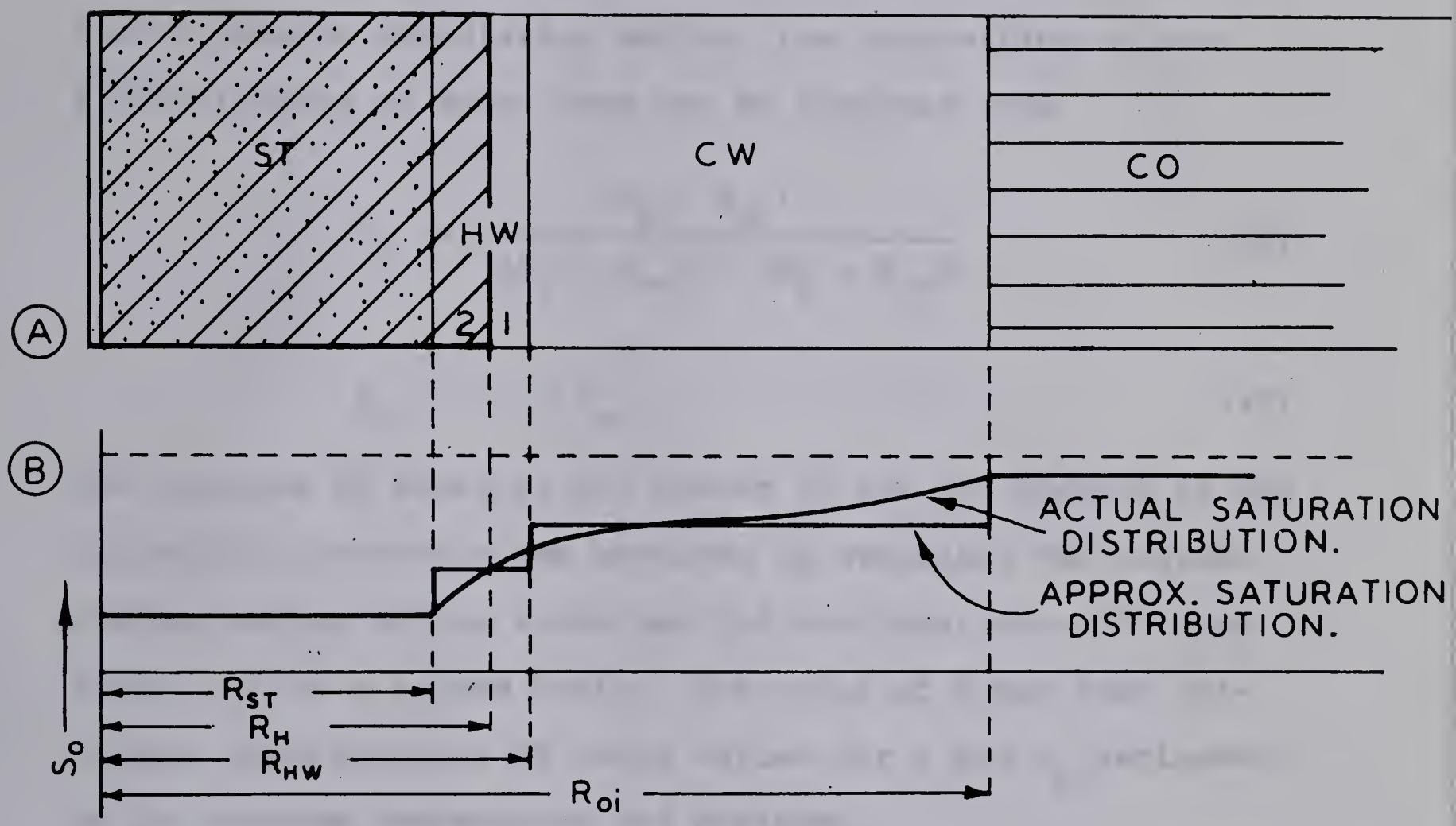

APPROXIMATION FOR THE SATURATION DISTRIBUTION

FIG. 7

due to the small contribution of the neglected terms for small values of back production

b) Composition of the Fluids Flowing in the Hot Cylindrical Reservoir

Assuming that any fluid with a saturation exceeding the corresponding irreducible saturation is displaced by the fluids flowing immediately behind, the composition of the fluids flowing at every zone may be computed from

$$X_w = \frac{(S_w - S_{wr})}{(S_w - S_{wr}) + (S_o - S_{or})} \qquad (46)$$

$$X_o = 1 - X_w \qquad (47)$$

The fraction of water or oil moving in the hot portion of the cylindrical reservoir was obtained by averaging the corresponding values in the steam and the hot water zone "2" (see Figure 7a) on a volume basis. The value of M was then calculated from Equation 40 using values for ρ and C_p estimated at the average temperature and pressure.

c) Calculation of the Temperature Profile

After choosing a small time increment, Δt, for which M is assumed constant, Equation 29 was numerically solved. The temperature distribution was calculated in the following manner.

The hot part of the cylindrical reservoir was divided in m elements of equal (Δr), as shown in Figure 8b (m+1 grid intersections) and expressions for an equal number of C's

were established according to Equations 31 and 39. These expressions are of the form

$$C_p = a - b\, T_p^{(1)} \tag{48}$$

where

a, b are positive constants

$T_p^{(1)}$ = temperature of element p when $t = \Delta t$

Equation 29 was replaced by finite differences using third order correct approximations for the distance derivatives and the Crank-Nicholson approach for the time derivative. The approximations for the distance derivatives are

$$\frac{dT_j}{dr} = \frac{-2T_{j-1} + 6T_{j+1} - 3T_j - T_{j+2}}{6(\Delta r)} \tag{49}$$

at $j = 2$ (See Figure 8B)

$$\frac{dT_j}{dr} = \frac{T_{j-2} - 6T_{j-1} + 3T_j + 2T_{j+1}}{6(\Delta r)} \tag{50}$$

at $j = 3, 4, \ldots, m$

$$\frac{d^2T_j}{dr^2} = \frac{T_{j+1} - 2T_j + T_{j-1}}{(\Delta r^2)} \tag{51}$$

At $r = 0$, $\frac{1}{r}\frac{\partial T}{\partial r}$ becomes indeterminate since both r and $\frac{\partial T}{\partial r}$ approach zero. Taking the limit,

$$\lim_{r \to 0} \frac{1}{r}\frac{\partial T}{\partial r} = \left(\frac{\partial^2 T}{\partial r^2}\right)_{r=0}$$

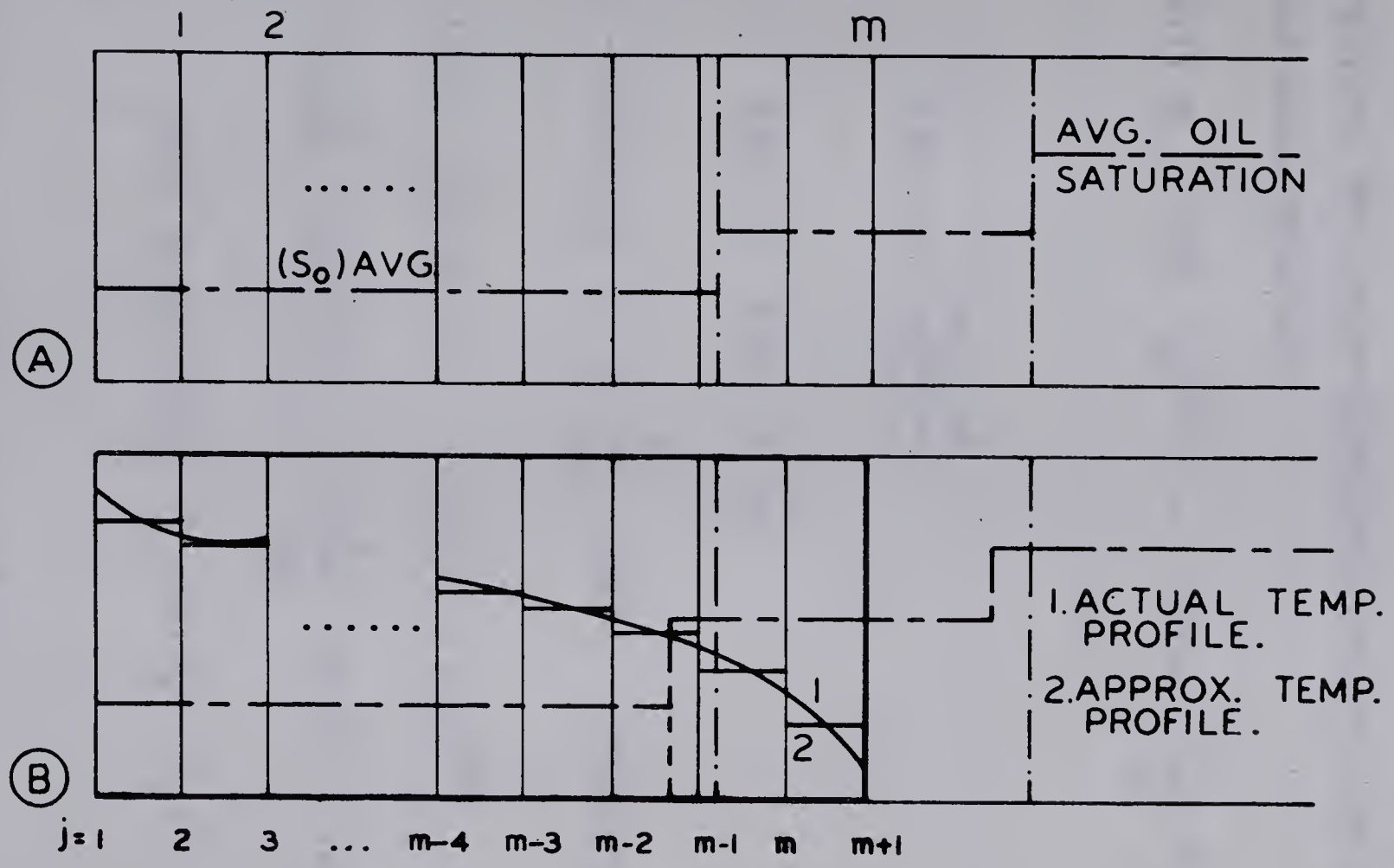

USE OF THE TEMPERATURE PROFILE FOR COMPUTING THE BACK FLOW RATE.

FIG. 8

and Equation 29 becomes at r = 0 (j=1)

$$(2\alpha_e + M)\frac{\partial^2 T}{\partial r^2} = \frac{\partial T}{\partial t} \tag{52}$$

Replacing the finite differences approximations in Equation 29 and applying the Crank-Nicholson Method, the following expressions were obtained:

$$\{ -X(1)\ T_1 + Y(1)\ T_2\}^{n+1} = \{|Y(1) - \frac{1}{\Delta t}|\ T_1 - Y(1)T_2\}^n \tag{53}$$

at j = 1

where

$$Y(1) = \frac{2\alpha_e + M}{\Delta r^2} \tag{54}$$

$$X(1) = Y(1) + \frac{1}{\Delta t} \tag{55}$$

$$\{|X(2) - 2Y(2)|T_1 + |-\frac{2}{\Delta t} - 2X(2) - 3Y(2)|T_2$$

$$+ |X(2) + 6Y(2)|T_3 - Y(2)T_4 + C_2\}^{n+1}$$

$$= \{-|X(2) - 2Y(2)|T_1 - |\frac{2}{\Delta t} - 2X(2) - 3Y(2)|T_2$$

$$- |X(2) + 6Y(2)|T_3 + Y(2)T_4 - C_2\}^n \tag{56}$$

at j = 2

$$\{|Y(J)|T_{j-2} + |X(J) - 6Y(J)|T_{j-1}$$

$$+ |-\frac{2}{\Delta t} - 2X(J) + 3Y(J)|T_j + |X(J) + 2Y(J)|T_{j+1} + C_j\}^{n+1}$$

$$= \{|-Y(J)|T_{j-2} - |X(J) - 6Y(J)|T_{j-1}$$

$$-|\frac{2}{\Delta t} - 2X(J) + 3Y(J)|T_j - |X(J) + 2Y(J)|T_{j+1} - C_j\}^n \quad (57)$$

at $j = 3, 4, \ldots, m$

where,

$$X(J) = \frac{\alpha_e}{\Delta r^2}, \quad J = 2,m \quad (58)$$

$$Y(J) = \frac{\alpha_e + M}{6(J-1)\Delta r^2}, \quad J = 2,m \quad (59)$$

n represents the time level at which the temperatures and coefficients are being calculated. For the first time increment n = 0

Applying the initial condition,

$$(T_j)^\circ = T_{ST} \qquad \text{at} \quad j = 1,m$$

$$(T_{j+1})^\circ = \frac{T_{ST} + T_i}{2} \quad (60)$$

By writing Equations 53, 56 and 57 (written for every point from j = 3 to j = m) a set of linear algebraic equations was obtained. In matrix notation, the set of equations is of the type:

$$\left|\begin{array}{cccccccccccc} a_{11} & a_{12} & 0 & 0 & 0 & 0 & 0 & \ldots & 0 & 0 & 0 \\ a_{21} & a_{22} & a_{23} & a_{24} & 0 & 0 & 0 & \ldots & 0 & 0 & 0 \\ a_{31} & a_{32} & a_{33} & a_{34} & 0 & 0 & 0 & \ldots & 0 & 0 & 0 \\ 0 & a_{42} & a_{43} & a_{44} & a_{45} & 0 & 0 & \ldots & 0 & 0 & 0 \\ \cdot & \cdot & \cdot & \cdot & \cdot & \cdot & \cdot & \cdot & \cdot & \cdot & \cdot \\ 0 & 0 & 0 & 0 & 0 & 0 & 0 & \ldots & a_{m,m-2} & a_{m,m-1} & a_{m,m} \end{array}\right|^{n+1} \left|\begin{array}{c} T_1 \\ T_2 \\ \cdot \\ \cdot \\ \cdot \\ T_m \end{array}\right|^{n+1}$$

$$= \left|\begin{array}{cccccccccccc} a_{11} & a_{12} & 0 & 0 & 0 & 0 & 0 & \ldots & 0 & 0 & 0 \\ a_{21} & a_{22} & a_{23} & a_{24} & 0 & 0 & 0 & \ldots & 0 & 0 & 0 \\ a_{31} & a_{32} & a_{33} & a_{34} & 0 & 0 & 0 & \ldots & 0 & 0 & 0 \\ 0 & a_{42} & a_{43} & a_{44} & a_{45} & 0 & 0 & \ldots & 0 & 0 & 0 \\ \cdot & \cdot & \cdot & \cdot & \cdot & \cdot & \cdot & \cdot & \cdot & \cdot & \cdot \\ 0 & 0 & 0 & 0 & 0 & 0 & 0 & \ldots & a_{m,m-2} & a_{m,m-1} & a_{m,m} \end{array}\right|^{n} \left|\begin{array}{c} T_1 \\ T_2 \\ \cdot \\ \cdot \\ \cdot \\ T_m \end{array}\right|^{n}$$

The right hand side of this system is known. The elements of the m x m matrix on the left hand side may be calculated using the appropriate equations. The solution for the T-vector yields the temperature distribution.

d) New Saturation Distribution

The composition of the fluids flowing in the reservoir is essentially controlled by the saturation distribution. In addition, since the cooling rate of the reservoir sand is dependent on the composition of the cooling fluids, the temperature distribution also depends on the saturation profile. This dependence is stressed by the fact that the heat capacity

cf oil is approximately one half of the heat capacity of water.

The displacement mechanism for mixtures of oil and water displacing mixtures of oil and water of different compositions at different temperatures has not been studied yet. The procedure followed in the calculation of the saturation distribution as a function of time is detailed in an example problem and may be described as follows.

The hot portion of the reservoir was divided in m cylindrical elements of equal Δr and the oil (or water) saturation in every element was changed in a stepwise manner with respect to time. The following calculation steps were carried out:

1. Values for the irreducible water and oil saturations were selected from known relative permeability curves.
2. The volume of the liquids with saturations in excess of the pertinent irreducible saturation was calculated for every element in the reservoir.
3. The composition of the fluids being displaced from every zone was calculated using Equation 46.
4. By assuming a "piston-like displacement" mechanism, the oil saturation in the last element of the steam zone was changed to a higher value

$$S_o = S_{oi} + (1 - S_{or} - S_{wr})_{ST}(X_o)_{HW} \quad (61)$$

when the total volume of the fluids produced in the wellbore

was equal to the total displaceable pore volume of the last element in the steam zone and that of the hot water zone at the steam temperature.

Subsequent stepwise changes in the oil saturation of the steam zone were made in a similar manner. For example, the oil saturation of the second element was set equal to the saturation given by Equation 61 when the total volume of fluids produced was equal to the total displaceable pore volume of the first and second elements and that of the hot water zone at the steam temperature. A piston-like displacement mechanism was also assumed to occur in the cold water and cold oil zones. The oil saturation in the "flushed-out" steam and hot water zones was subsequently changed to that of the cold water zone as the "flood-front" progressed toward the wellbore. Following the influx of the cold oil into the cold water zone, similar changes in saturations were made in the preceding zones.

e) New Production Rate

From the temperature profile obtained at the previous time step, the oil and water viscosities were calculated at the average temperature of every element. The relative permeability to oil and the relative permeability to water were calculated for every element using the saturation distribution at the previous time step. The new rate was obtained from the equation:

$$W = \frac{0.00708\, h\Delta P}{\frac{1}{\lambda_{co}} \ln \frac{r_e}{R_{co}} + \frac{1}{\lambda_{cW}} \ln \frac{R_{co}}{R_H} + \frac{1}{\lambda_1} \ln \frac{R_1}{r_w} + \frac{1}{\lambda_2} \ln \frac{R_2}{R_1} + \ldots + \frac{1}{\lambda_m} \ln \frac{R_m}{R_{m-1}}} \quad (62)$$

where

$$R_{co} = \sqrt{R_{oi}^2 - \frac{5.61\, W_p}{\pi \phi h\, (1 - S_{or} - S_{wr})_{cW}}} \quad (63)$$

The cold water zone disappears when $R_{co} = R_H$. Equation 62 is still valid provided R_{co} is set equal to R_H. A general flow diagram for the calculations of back flow is given as follows:

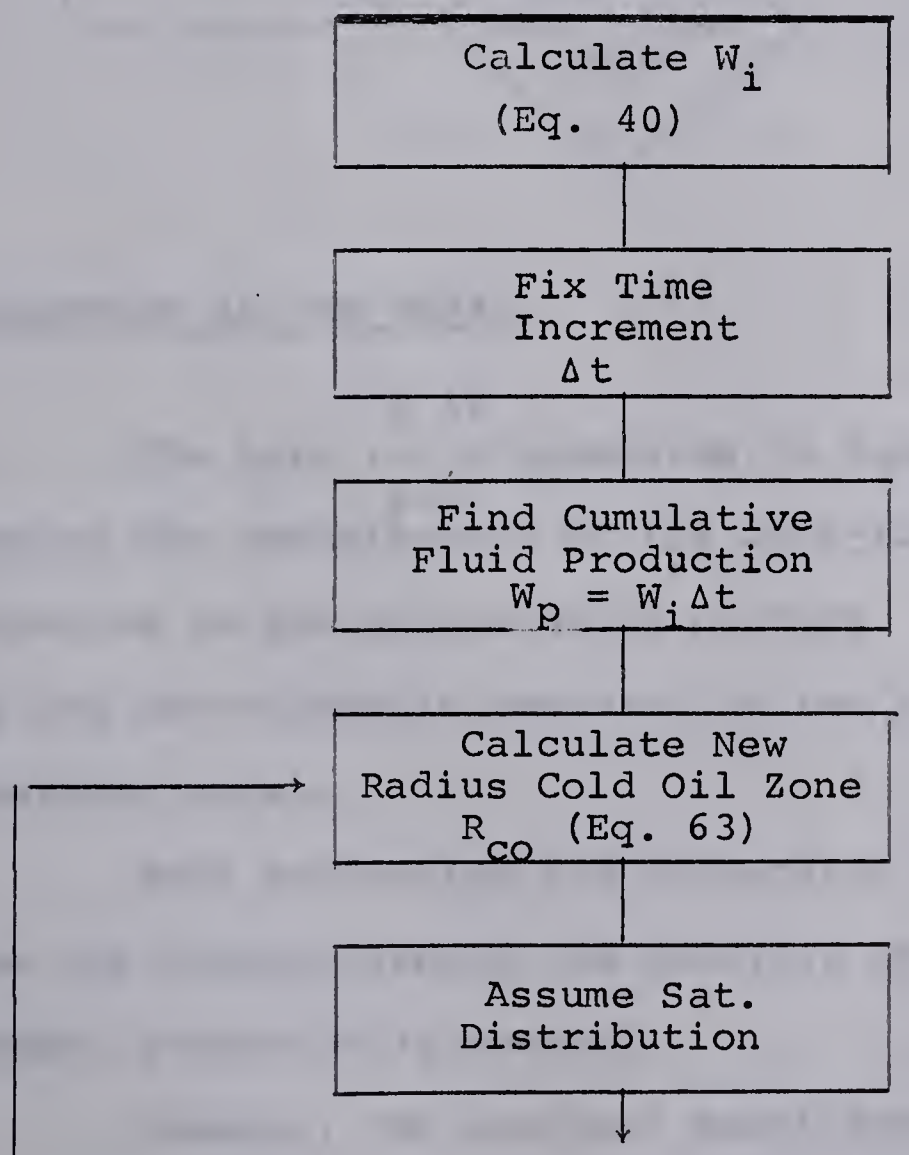

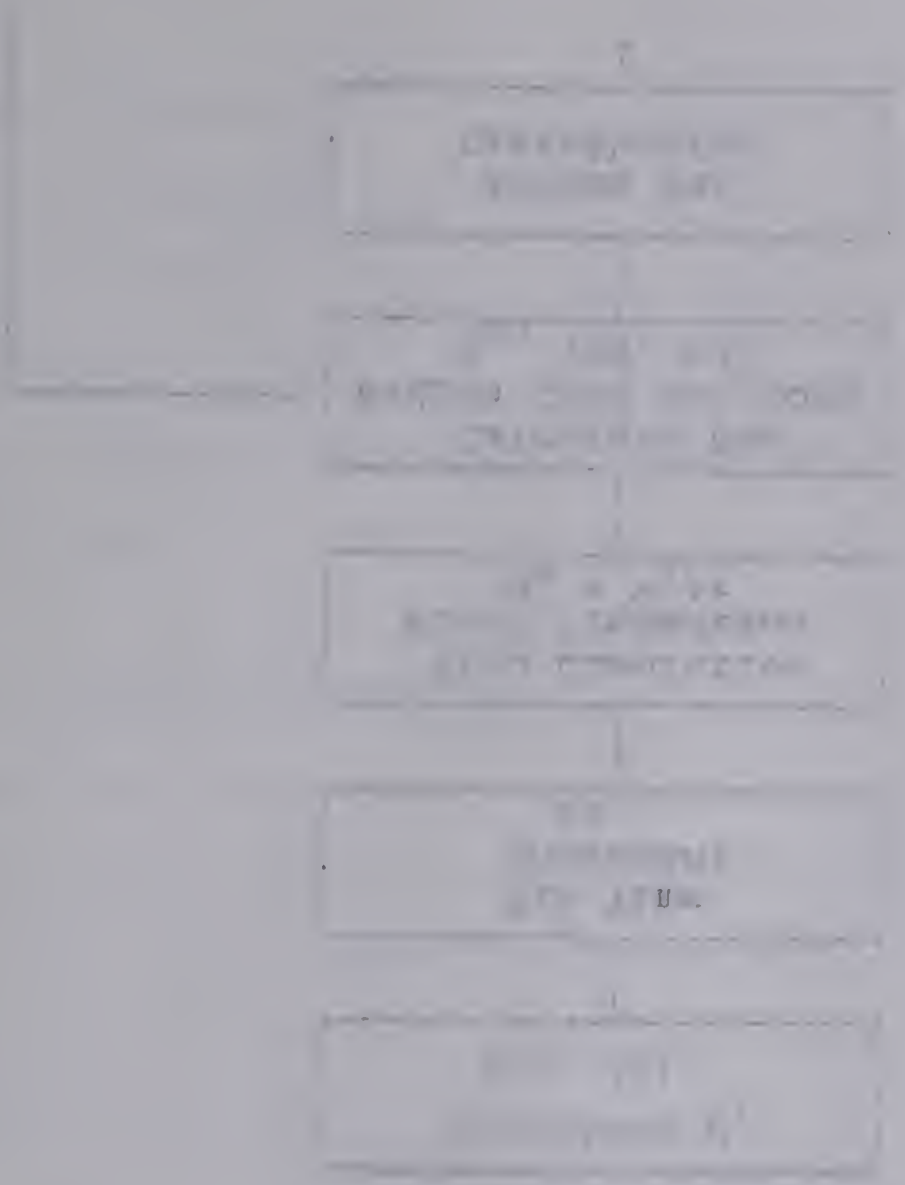

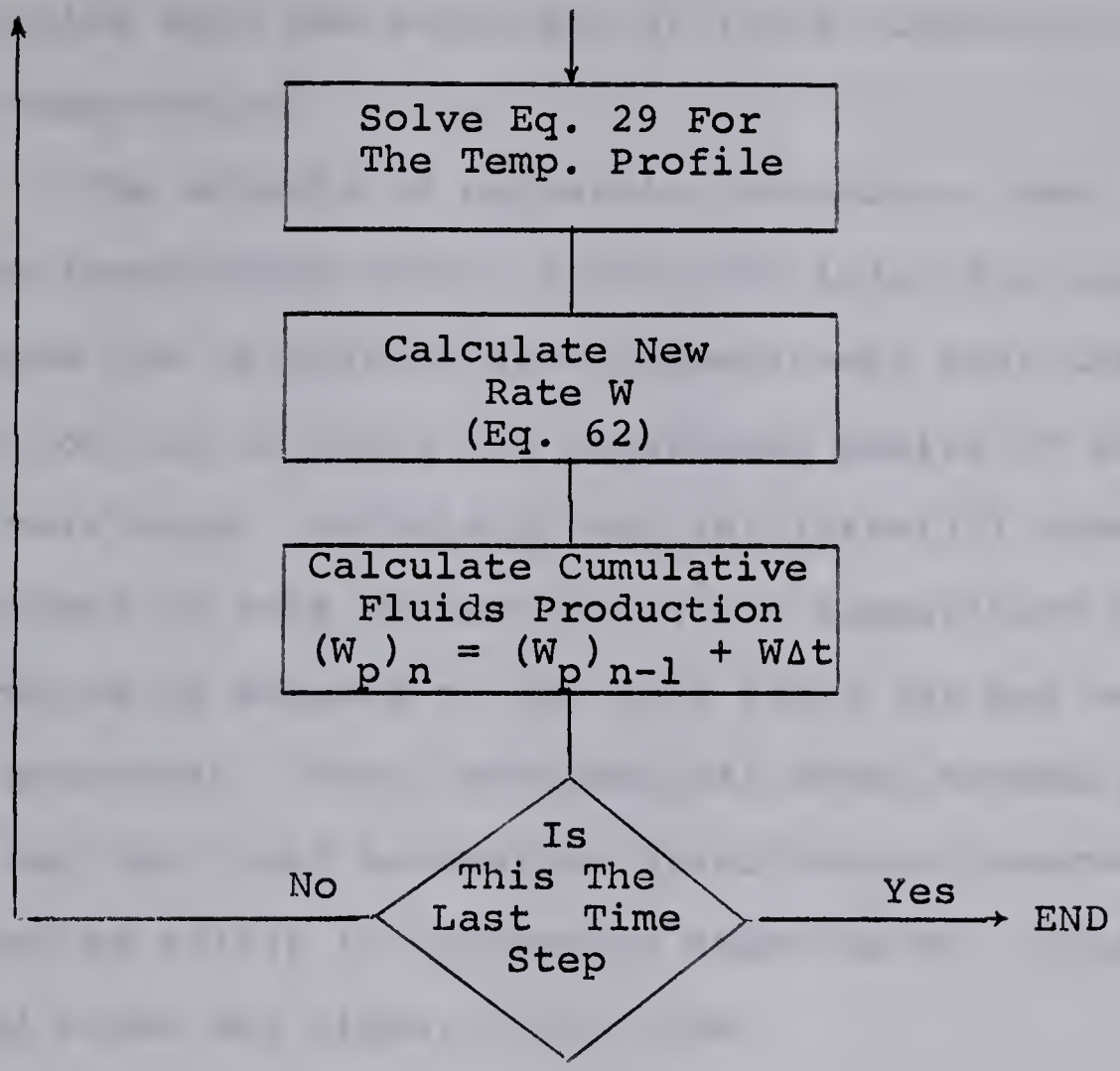

Discussion of the Model

The term $\left(-\frac{M}{r}\frac{\partial T}{\partial r}\right)$ appearing in Equation 29 takes into account the contribution of the bulk-flow heat transfer mechanism to the sand-cooling process. The term C accounts for the non-adiabatic behavior of the flat surfaces of the reservoir model.

Both conductive and convective heat transfer mechanisms are incorporatedin the analysis by using the effective thermal conductivity concept.

However, the proposed model does not consider multi-dimensional heat transfer and is limited to constant physical

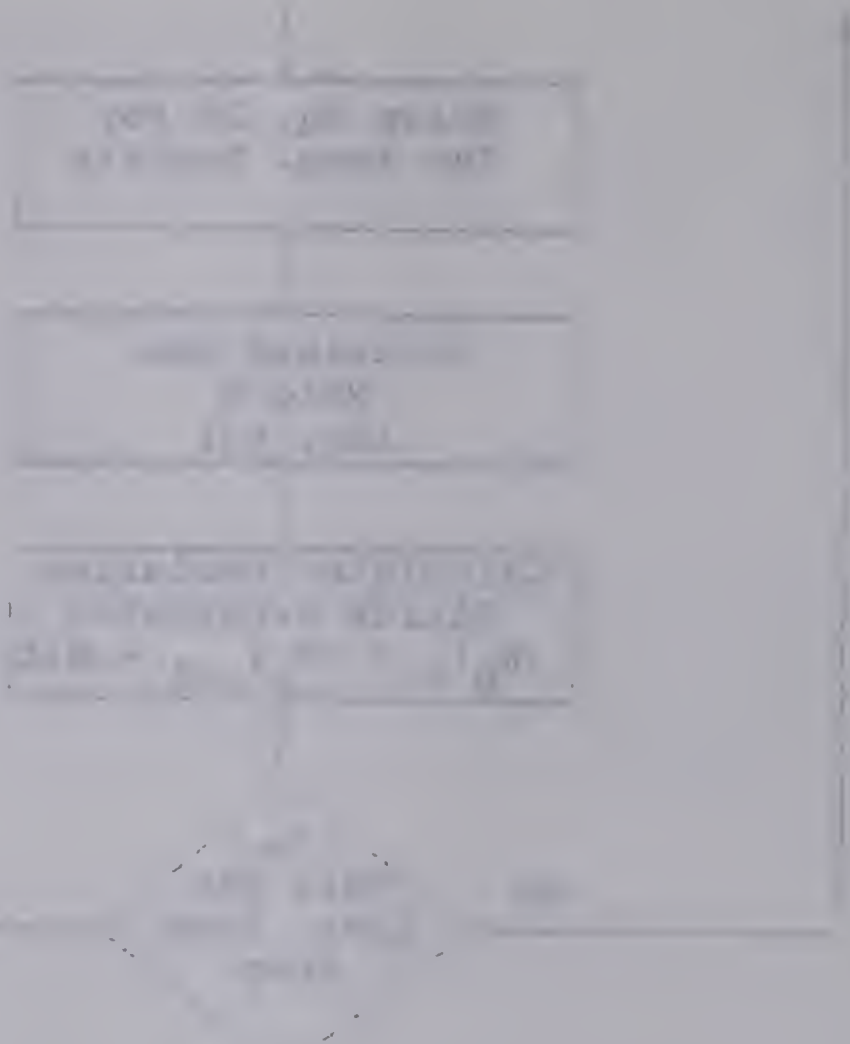

properties with the exception of fluid viscosity variation with temperature.

The effects of neglecting horizontal heat conduction in the impermeable strata during the injection period is to increase the calculated sand temperatures near the point of injection and to lower the calculated radius of the hot-reservoir zone. Avdonin(1) and Spillette(22) have compared the effect of this assumption on the temperature profile and the radius of advance of the heat front for hot water injection processes. Their mathematical model,however, does not consider the fluid saturation distribution observed by Willman et al(23) in laboratory experiments using sand-packed cores and linear fluid flow.

The assumption of zero thermal conductivity within the permeable sand, in the horizontal direction, during injection, will have effects similar to those just mentioned. The magnitude of these effects may be expected to be less pronounced.

The assumption that the sand and the fluid may be replaced by a hypothetical solid of thermal conductivity, k_e, may be considered as an accepted procedure to describe heat transfer effects in packed reactors. The calculation of this effective thermal conductivity for the combination of fluids encountered in oil reservoirs offers, however, some difficulties due to the lack of data and the choice of a proper technique for its calculation.

Those assumptions concerned with the saturation distribution both during injection and back production may affect the results seriously. This is the result of the important role which the composition of the fluids flowing play in the back-production calculations. A mathematical formulation to describe the saturation distribution and hence the composition of the fluid flowing with the initial temperature and saturation distributions of the present model would be complex. It was believed that this formulation was not worth attempting in the present case unless the heat transfer simplifications made in establishing the physical model are removed or proven to be valid.

EXAMPLE CALCULATIONS

To illustrate the use of the physical model for the calculation of back production, two example problems were run on a 7040 digital computer. The computing time for each example was approximately 15 minutes for a total production time of 600 days with time increments of 2 days.

The effective thermal conductivity for the oil-water-sand system was calculated using reference 5 as follows: Average readings for the silica-water and silica-ethyl alcohol were obtained from Figure 9 for v ~ 2 ft./hr. and averaged on a volume basis according to the equation

$$k_e = X_w k_{e_w} + X_o k_{e_o}$$

where

k_{e_w} = effective thermal conductivity, silica-water system

k_{e_o} = effective thermal conductivity, silica-ethyl alcohol system.

Thus, data for the silica-ethyl alcohol system were assumed to be applicable to the sand-oil system in the first approximation due to the lack of the proper data. The variation of k_e with the fluid composition, X, was accounted for in the calculations.

Example 1

The oil viscosity versus temperature curve for this example has been plotted in Figure 10, that corresponding to Example 2 appears in Figure 27. The viscosity readings at 90°F are 109 and 2300 cp respectively.

The choice of viscosities in this order of magnitude was made in order to compare the effect of viscosity on the back production rate.

The initial radii and oil saturation distribution of the back production period are shown in Figure 11, permeability data are plotted in Figure 9. Additional reservoir and fluid properties are

K	= 612 md	r_e	= 330 ft.
h	= 25 ft.	r_w	= 0.25 ft.
$P_e - P_w$	= 400 psi	T_{ST}	= 530°F
ϕ	= 0.266	T_i	= 95°F
S_{wc}	= 0.095	$\bar{T}$	= 312°F

Total injection time = 720 hr.

Steam injected = 21890 bbls (as condensate)

$$(\rho_w)_{\bar{T}} = 52.28 \text{ lbm/cu.ft.}$$

$$(\rho_o)_{\bar{T}} = (\rho_o)_{T_i} \left| 1 - 20 \left(\bar{T}/T_{ST}\right) \right|$$

$$= 58.45 \times 0.882$$

$$= 51.45 \text{ lbm/cu.ft.}$$

$$(\rho_r)_{\bar{T}} = 140 \text{ lbm/cu.ft.}$$

$$(C_{pw})_{\overline{T}} = 1.03 \text{ Btu/lbm°F}$$

$$(C_{po})_{\overline{T}} = 0.50 \text{ Btu/lbm°F}$$

$$(C_{pr})_{\overline{T}} = 0.23 \text{ Btu/lbm°F}$$

$$k_{OB} = 1.09 \text{ Btu/ft.°F hr}$$

$$k_{eo} = 1.20 \text{ Btu/ft.°F hr (from Ref. 5 for } v < 2 \text{ ft/hr.}$$

$$k_{ew} = 1.70 \text{ Btu/ft.°F hr. (from Reference 5)}$$

The oil viscosity versus temperature data were fitted by the following fifth degree polynomial

$$\mu_o = 10^{\beta}$$

where

$$\beta = -0.65019612 + 0.44799295 \times 10^3 \left(\frac{1}{T}\right) + 0.75749706 \times 10^3 \left(\frac{1}{T^2}\right) - 0.60803823 \times 10^7 \left(\frac{1}{T^3}\right) + 0.59698224 \times 10^9 \left(\frac{1}{T^4}\right) - 0.18164653 \times 10^{11} \left(\frac{1}{T^5}\right)$$

The water viscosity versus temperature were calculated from the equation(18).

$$\mu_w = \frac{100}{2.1482\left|(0.55556T - 26.213) + \sqrt{8078.4 + (0.55556T - 26.213)^2}\right| - 120}$$

The relative permeability data presented in Figure 10 were fitted by sixth degree polynomials. The equations are as follows:

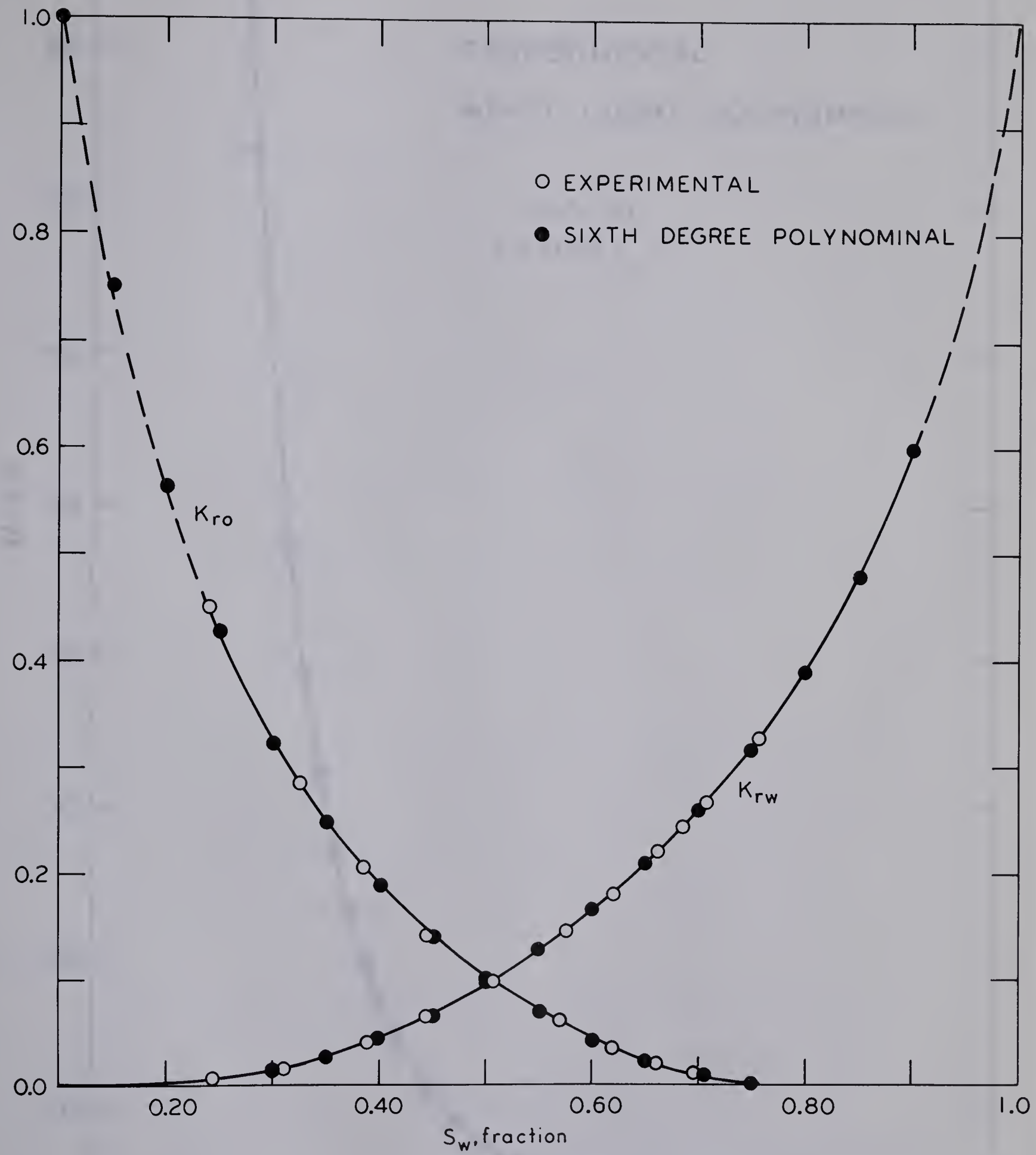

FIG. 9
EXAMPLE I.
RELATIVE PERMEABILITY VS. WATER SATURATION

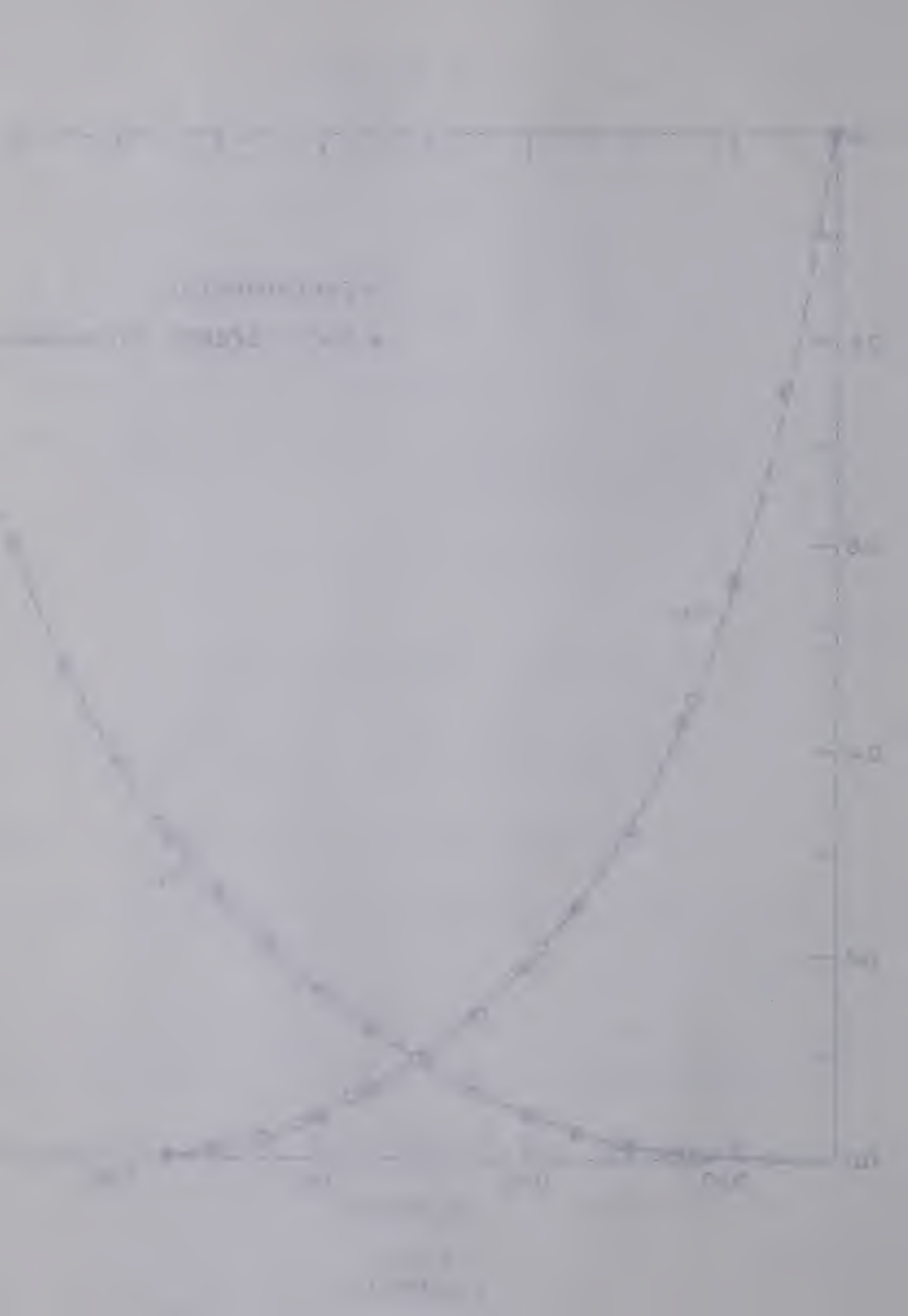

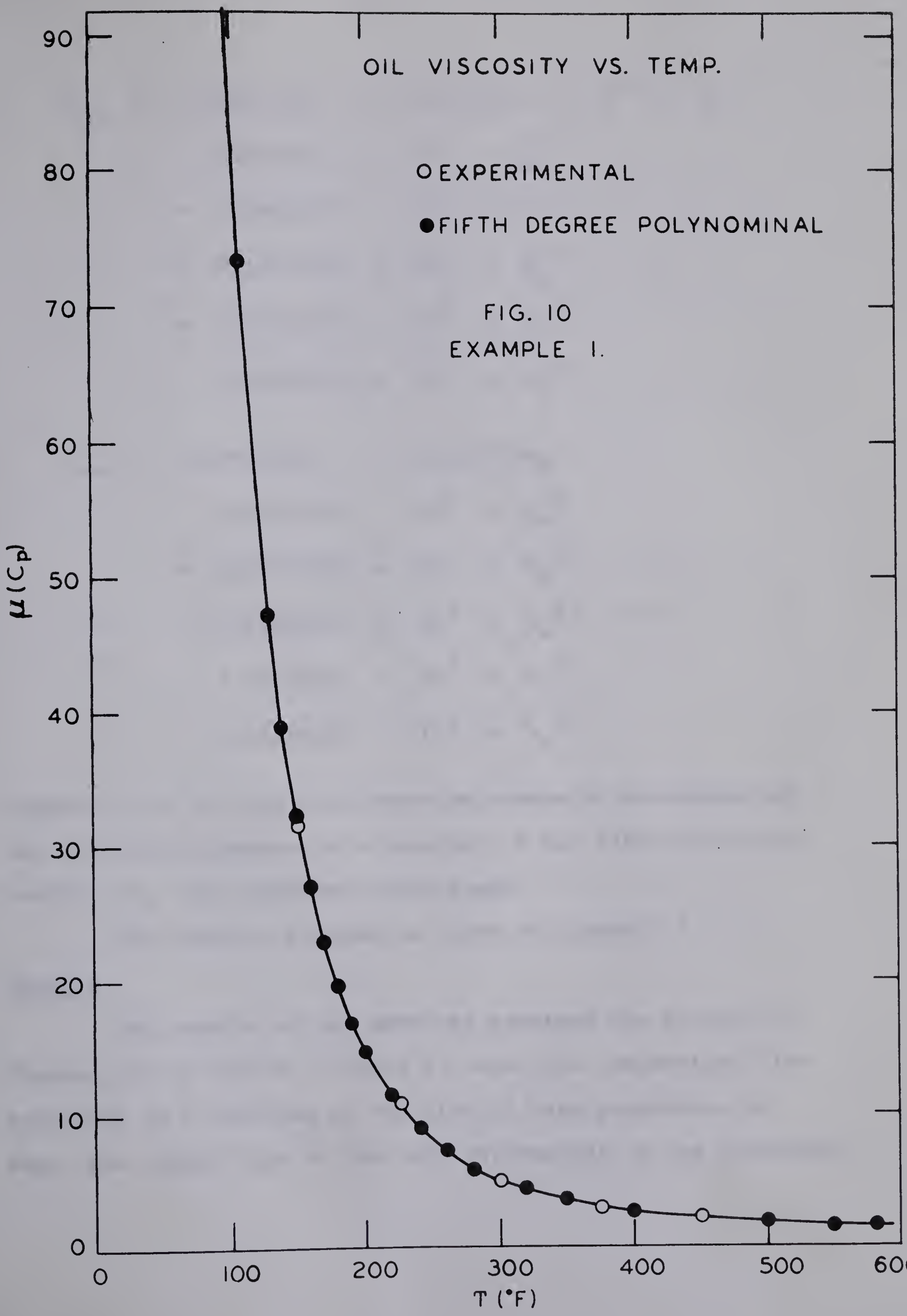

FIG. 10
EXAMPLE 1.

$$k_{ro} = -0.06920184 + 0.12099786 \times 10^{1} \times S_o - 0.86392291 \times 10^{1} \times S_o^{2} + 0.28682803 \times 10^{2} \times S_o^{3} - 0.43337840 \times 10^{2} \times S_o^{4} + 0.30396180 \times 10^{2} \times S_o^{5} - 0.64854211 \times 10^{1} \times S_o^{6}$$

$$k_{rw} = -0.04883480 + 0.78113385 S_w - 0.46846743 \times 10^{1} \times S_w^{2} + 0.12766994 \times 10^{2} \times S_w^{3} - 0.12893017 \times 10^{2} \times S_w^{4} + 0.35564310 \times 10^{1} \times S_w^{5} + 0.15006140 \times 10^{1} \times S_w^{6}$$

Figures 12 to 21 show the step-wise change in saturation of the reservoir elements as a function of the total fluid production, W_p, for subsequent time steps.

The computer program is given in Appendix 2.

Results

The results of the computer programs are plotted in Figures 22, 23 and 24. Figure 22 shows the temperature distribution as a function of the time of back production in days, the center line at the left corresponds to the production

well and the dashed line at the right to the external radius of the heated reservoir zone.

The results for the rate of back production as a function of time are given in Figure 23, where the two sets of points show the effect of changing the chosen Δt from 4 days to 2 days, on the rate of back production. The discussion of the above results appears after Example 2.

The results of Example 2 appear in the same order as Example 1.

Example 2

The initial radii and saturation distribution are represented schematically in Figure 25. The additional data used are

$K = 3000$ md
$h = 10$ ft.
$P_e - P_w = 1600$ psi
$\phi = 0.362$
$S_{wc} = 0.17$
$(C_{pw})_{\overline{T}} = 1.013$ Btu/lbm°F
$(C_{po})_{\overline{T}} = 0.50$ Btu/lbm°F
$T_{ST} = 445$°F
$T_i = 74$°F
Total injection time = 720 hr.
$(\rho_w)_{\overline{T}} = 60.13$ lbm/cu.ft.
$(\rho_o)_{\overline{T}} = 50.32$ lbm/cu.ft.
$k_{OB} = 1.5$ Btu/ft.°F hr.

$$\mu_o = 3.2048 \times 10^{11} T^{-4.26237} \qquad 90°F < T < 185°F$$

$$\mu_o = 0.95946 \times 10^{11} T^{-4.03010} \qquad T > 185°F$$

$$k_{ro} = 0.45844418 - 0.79728708 \times 10^{1} \times S_o + 0.50700872 \times 10^{2} \times S_o^{2} - 0.15004158 \times 10^{3} \times S_o^{3} + 0.23162574 \times 10^{3} \times S_o^{4} - 0.17147780 \times 10^{3} \times S_o^{5} + 0.47635128 \times 10^{2} \times S_o^{6}$$

$$k_{rw} = 0.20999427 \times 10 - 0.31857588 \times 10^{2} S_w + 0.18840244 \times 10^{3} S_w^{2} - 0.55419683 \times 10^{3} S_w^{3} + 0.85247842 \times 10^{3} S_w^{4} - 0.64546960 \times 10^{3} S_w^{5} + 0.18954912 \times 10^{3} S_w^{6}$$

$$0.25 < S_w < 1.0$$

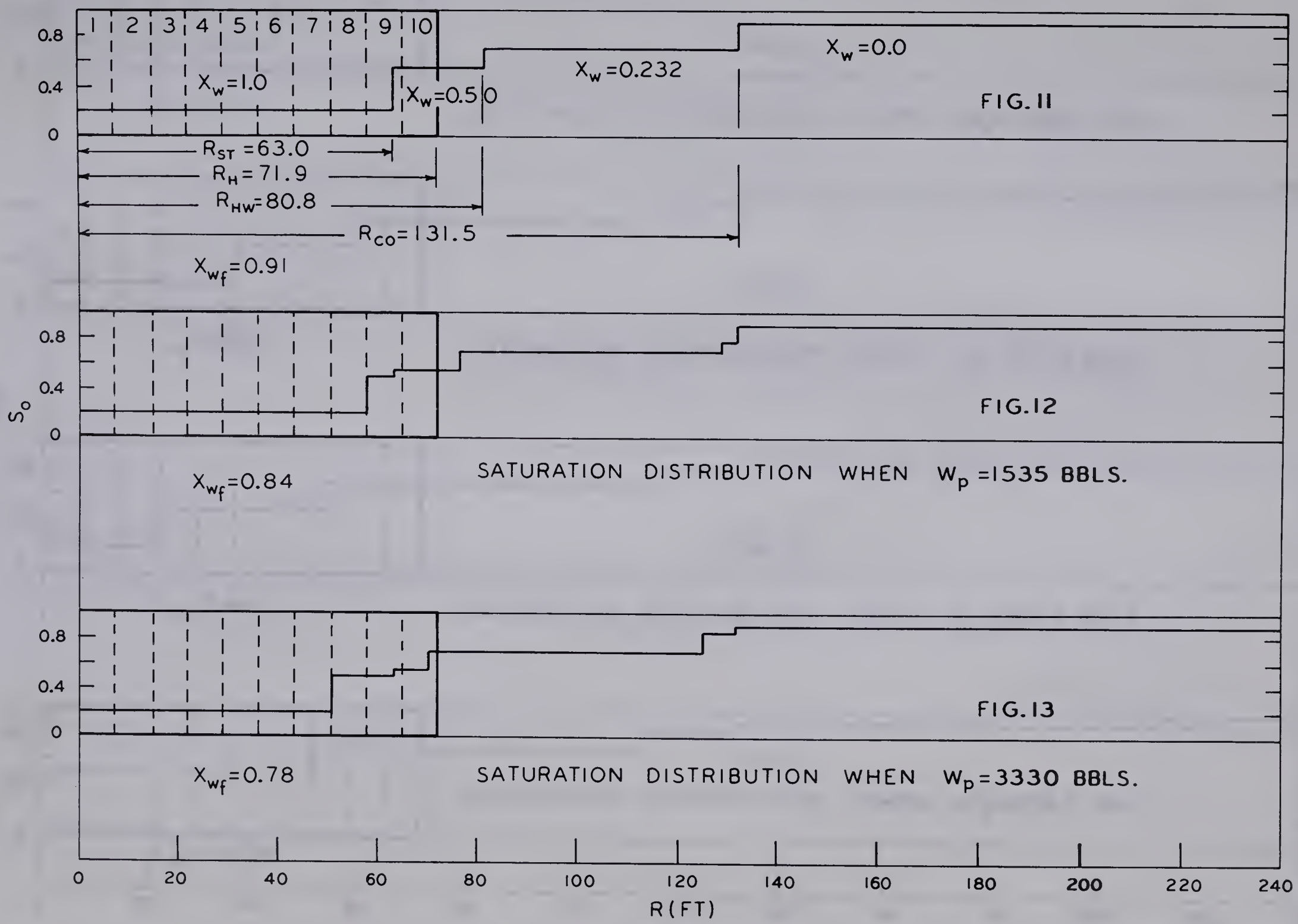

FIG. 11

FIG. 12

SATURATION DISTRIBUTION WHEN W_p=1535 BBLS.

FIG. 13

SATURATION DISTRIBUTION WHEN W_p=3330 BBLS.

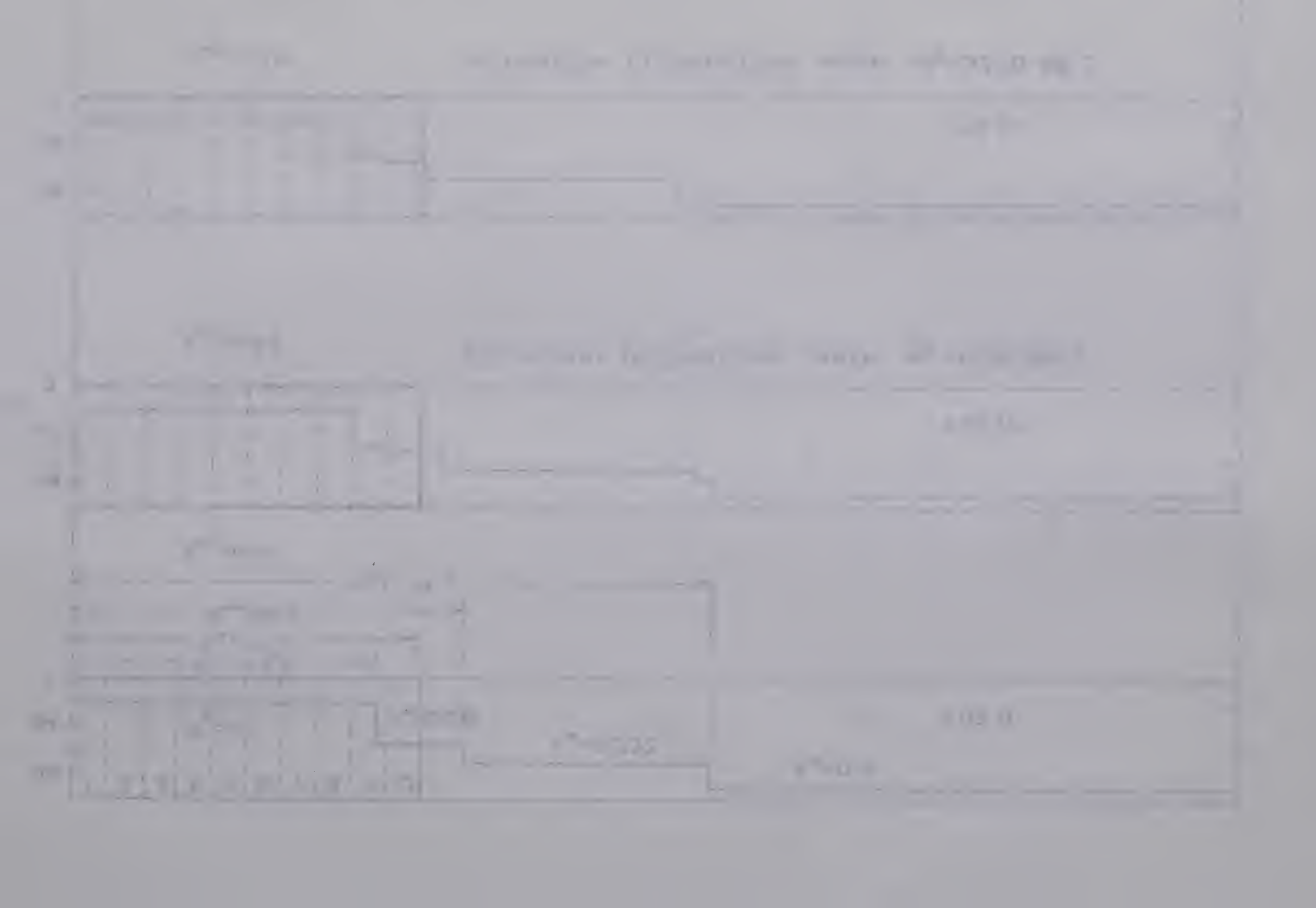

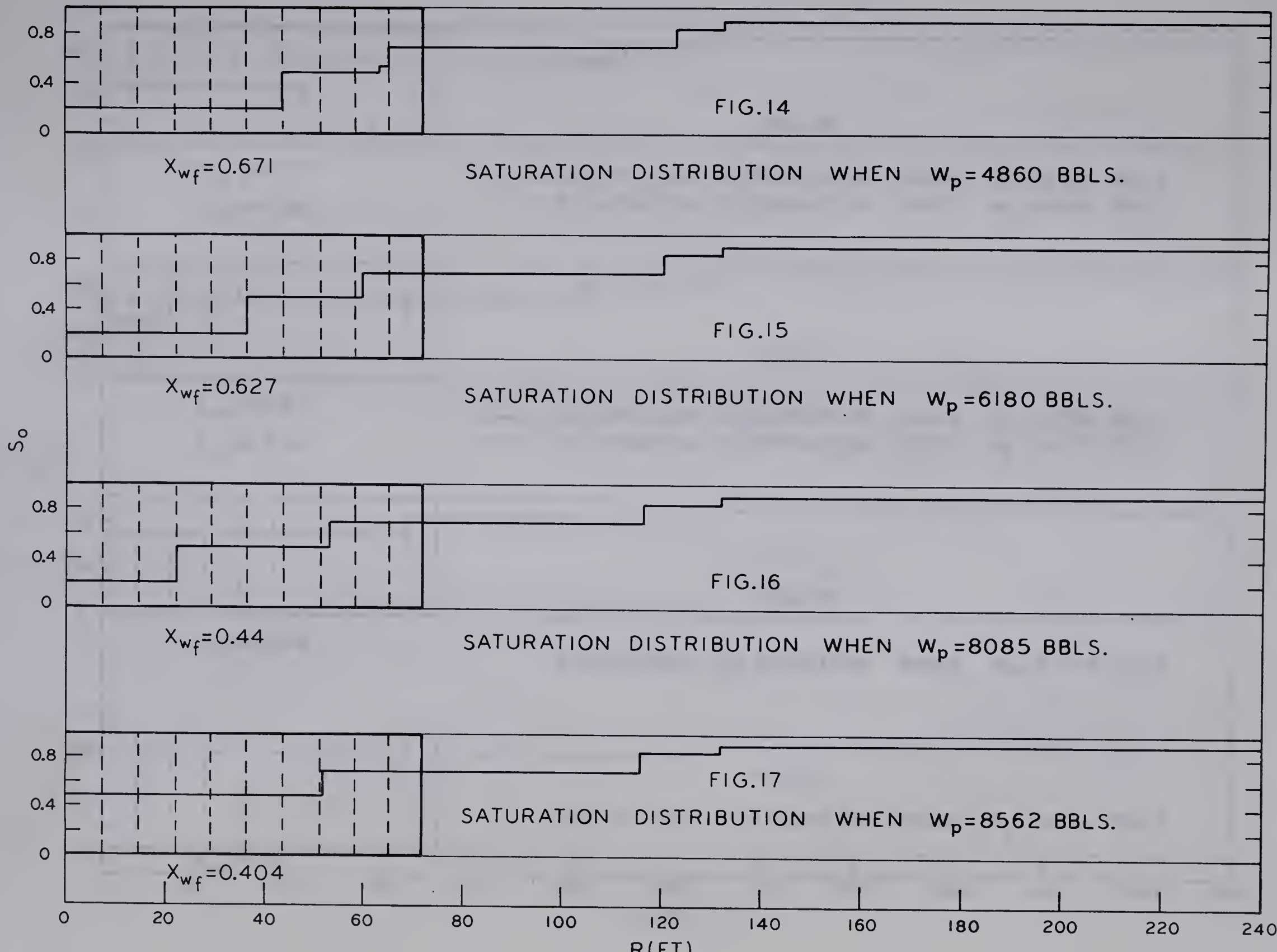
0.8
0.4
0
X_{wf}=0.671
FIG.14
SATURATION DISTRIBUTION WHEN W_p=4860 BBLS.
0.8
0.4
0
X_{wf}=0.627
FIG.15
SATURATION DISTRIBUTION WHEN W_p=6180 BBLS.
S_o
0.8
0.4
0
X_{wf}=0.44
FIG.16
SATURATION DISTRIBUTION WHEN W_p=8085 BBLS.
0.8
0.4
0
X_{wf}=0.404
FIG.17
SATURATION DISTRIBUTION WHEN W_p=8562 BBLS.
0
20
40
60
80
100
120
140
160
180
200
220
240
R(FT)

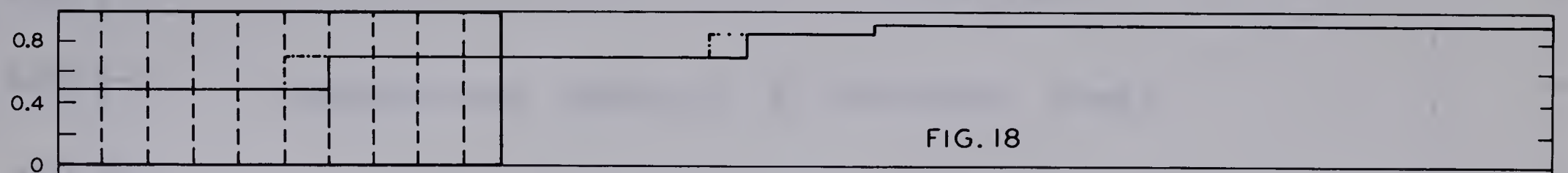

FIG. 18

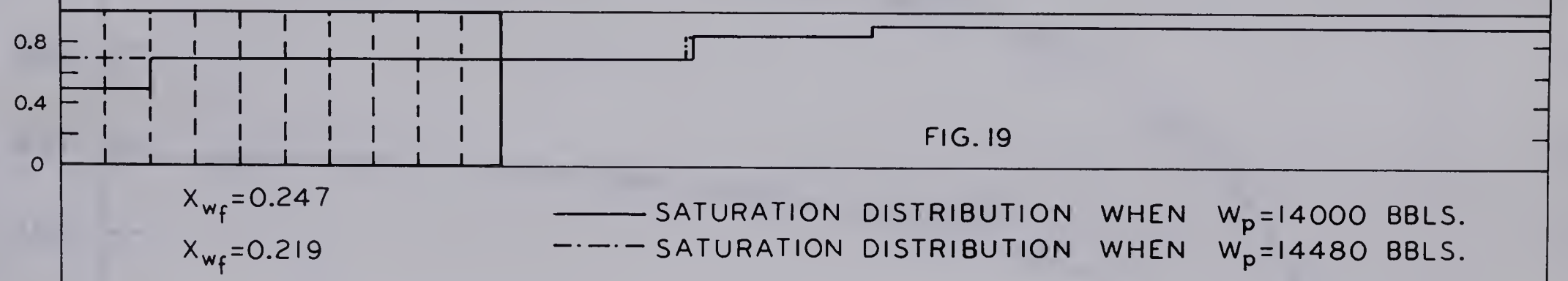

FIG. 19

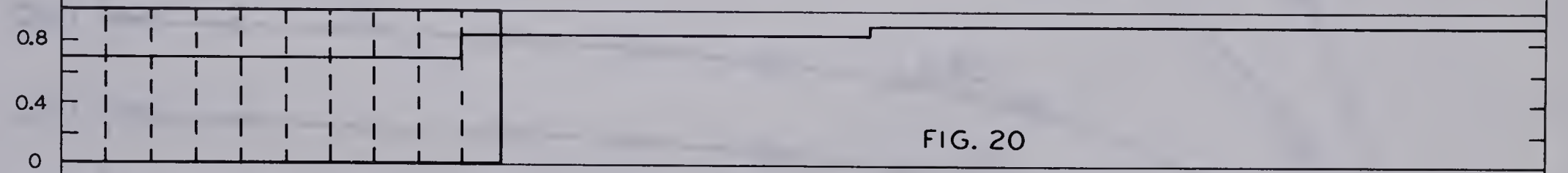

FIG. 20

FIG. 21

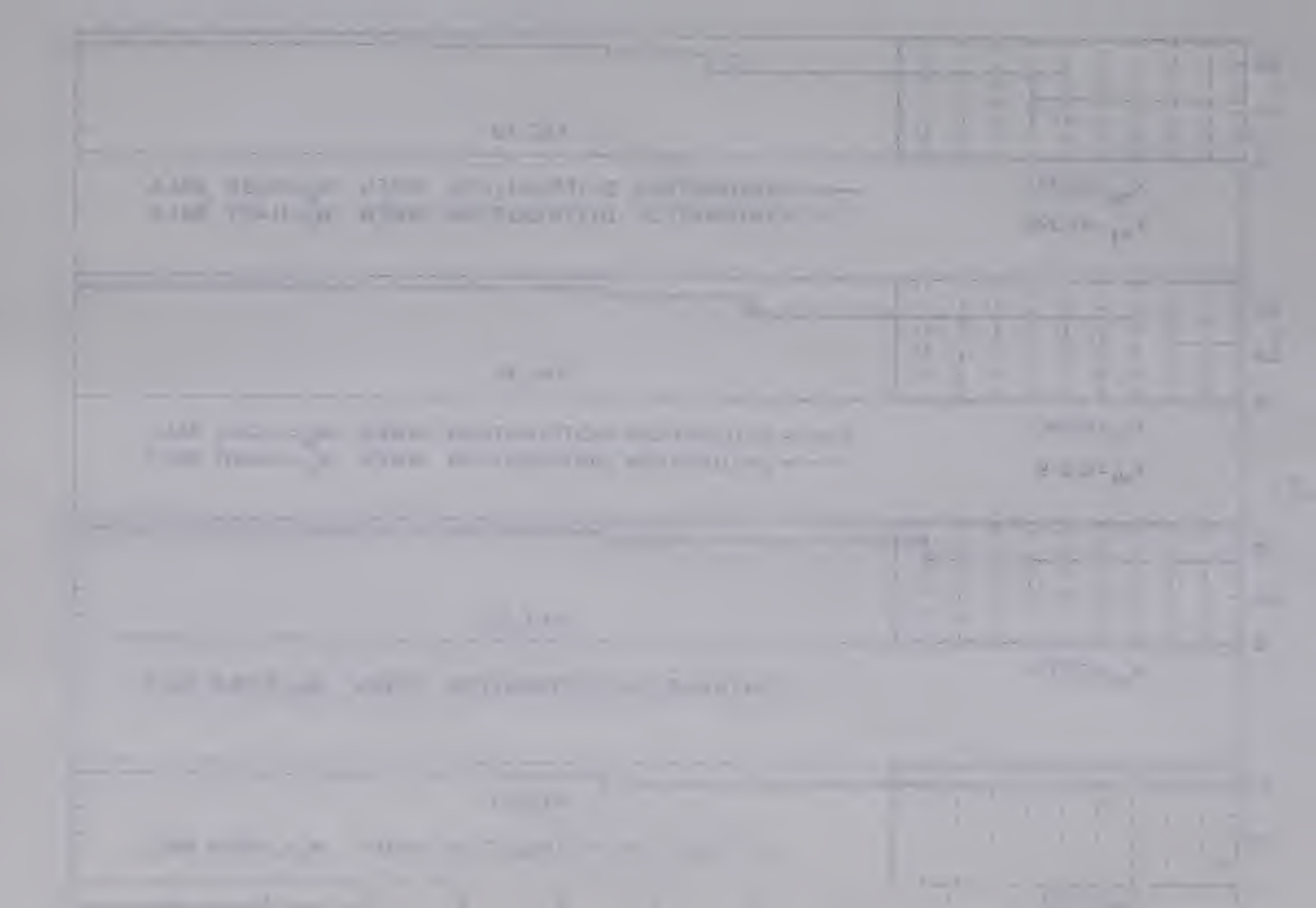

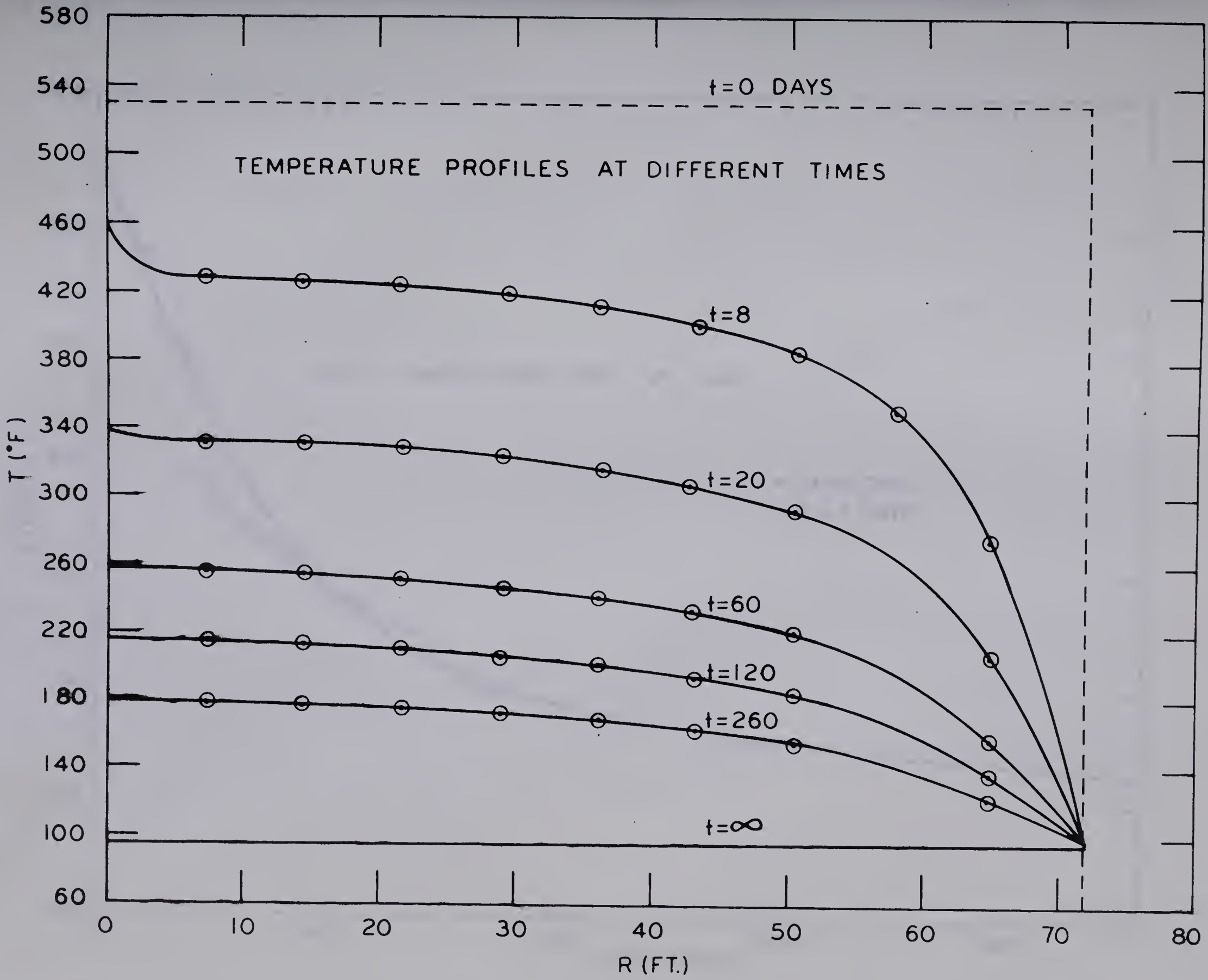
TEMPERATURE PROFILES AT DIFFERENT TIMES
t=0 DAYS
t=8
t=20
t=60
t=120
t=260
t=∞
T (°F)
R (FT.)
580
540
500
460
420
380
340
300
260
220
180
140
100
60
0
10
20
30
40
50
60
70
80

FIG.22

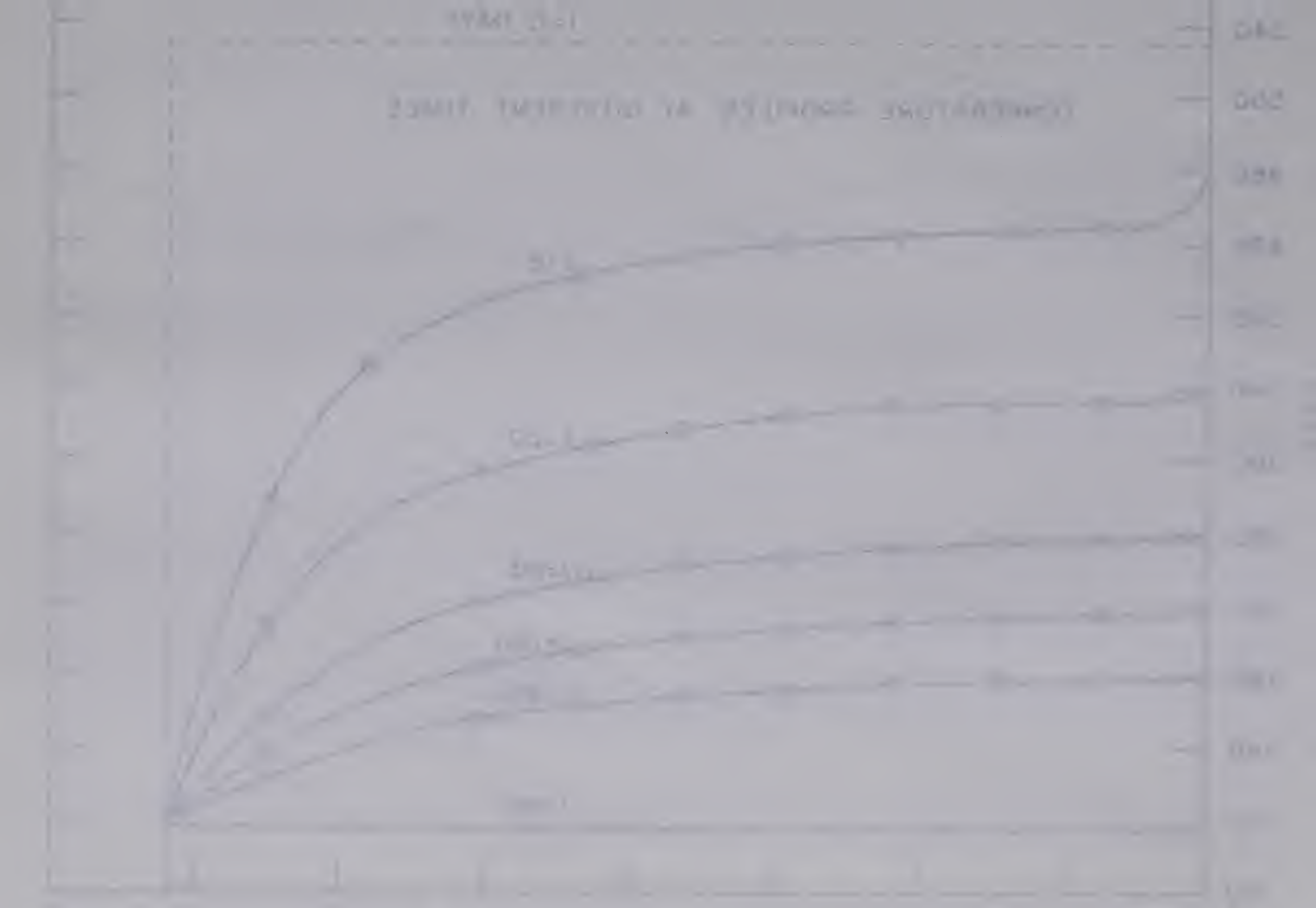

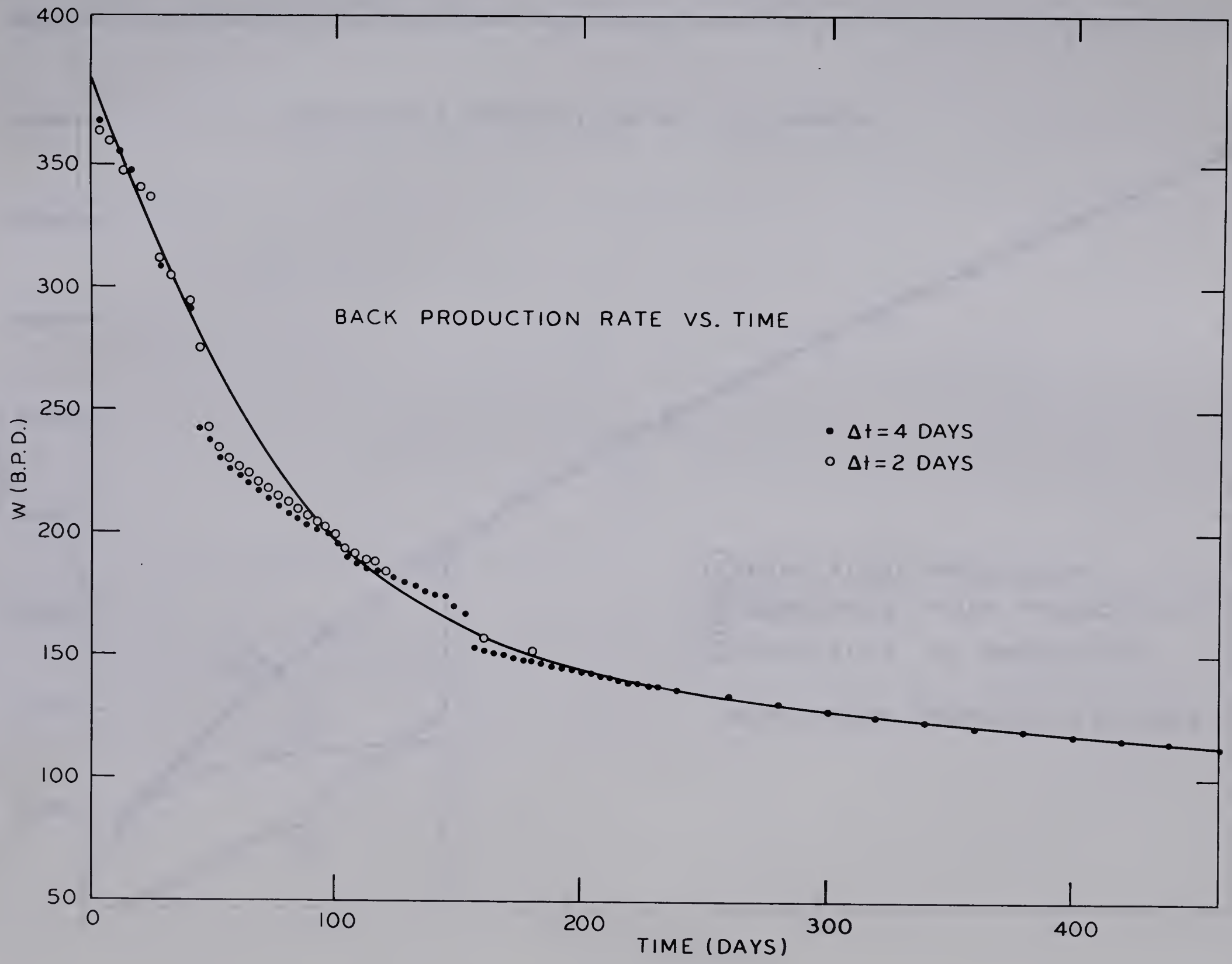
BACK PRODUCTION RATE VS. TIME
W (B.P.D.)
TIME (DAYS)
• Δt = 4 DAYS
o Δt = 2 DAYS
400
350
300
250
200
150
100
50
0
100
200
300
400

FIG. 23

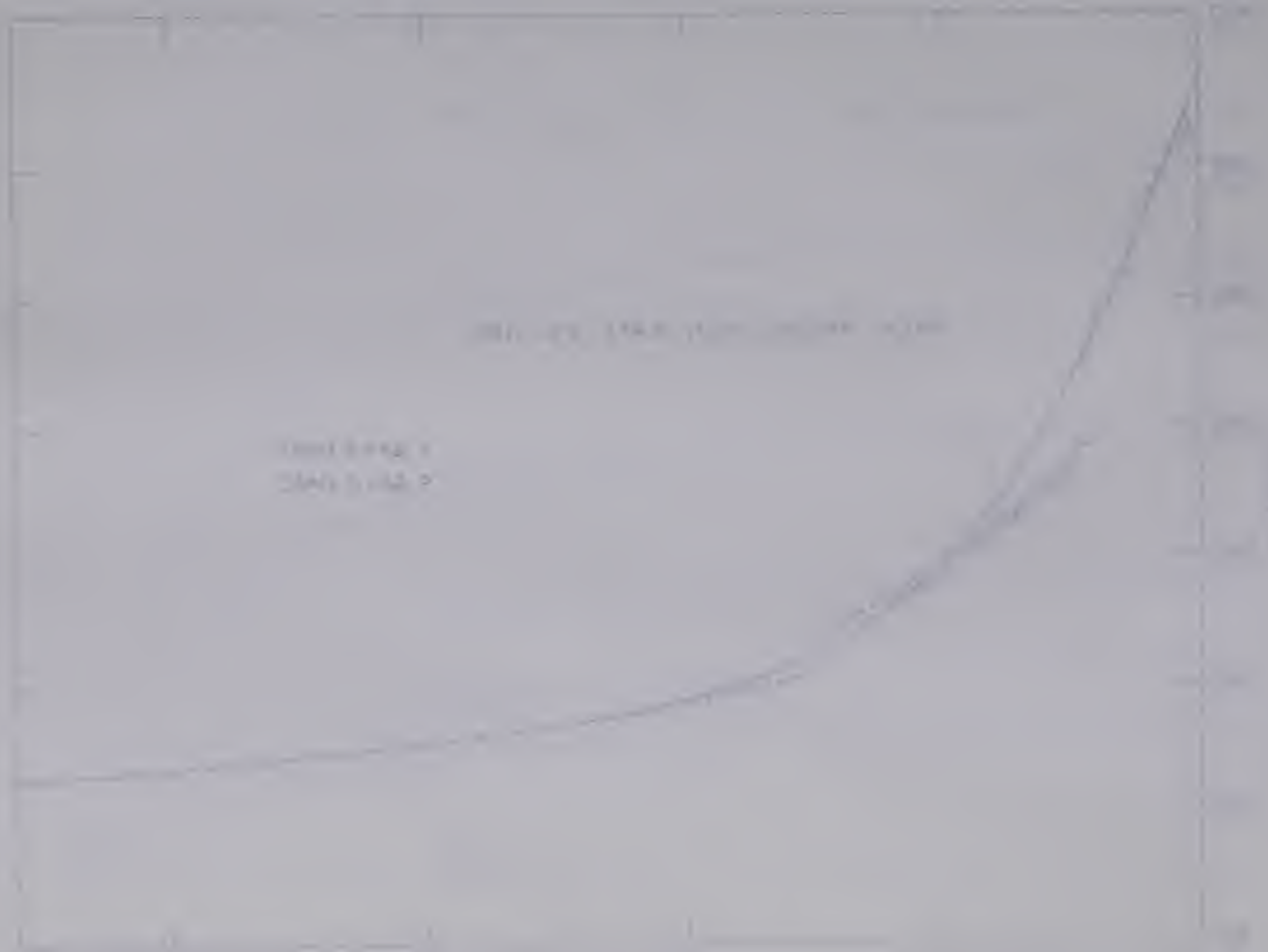

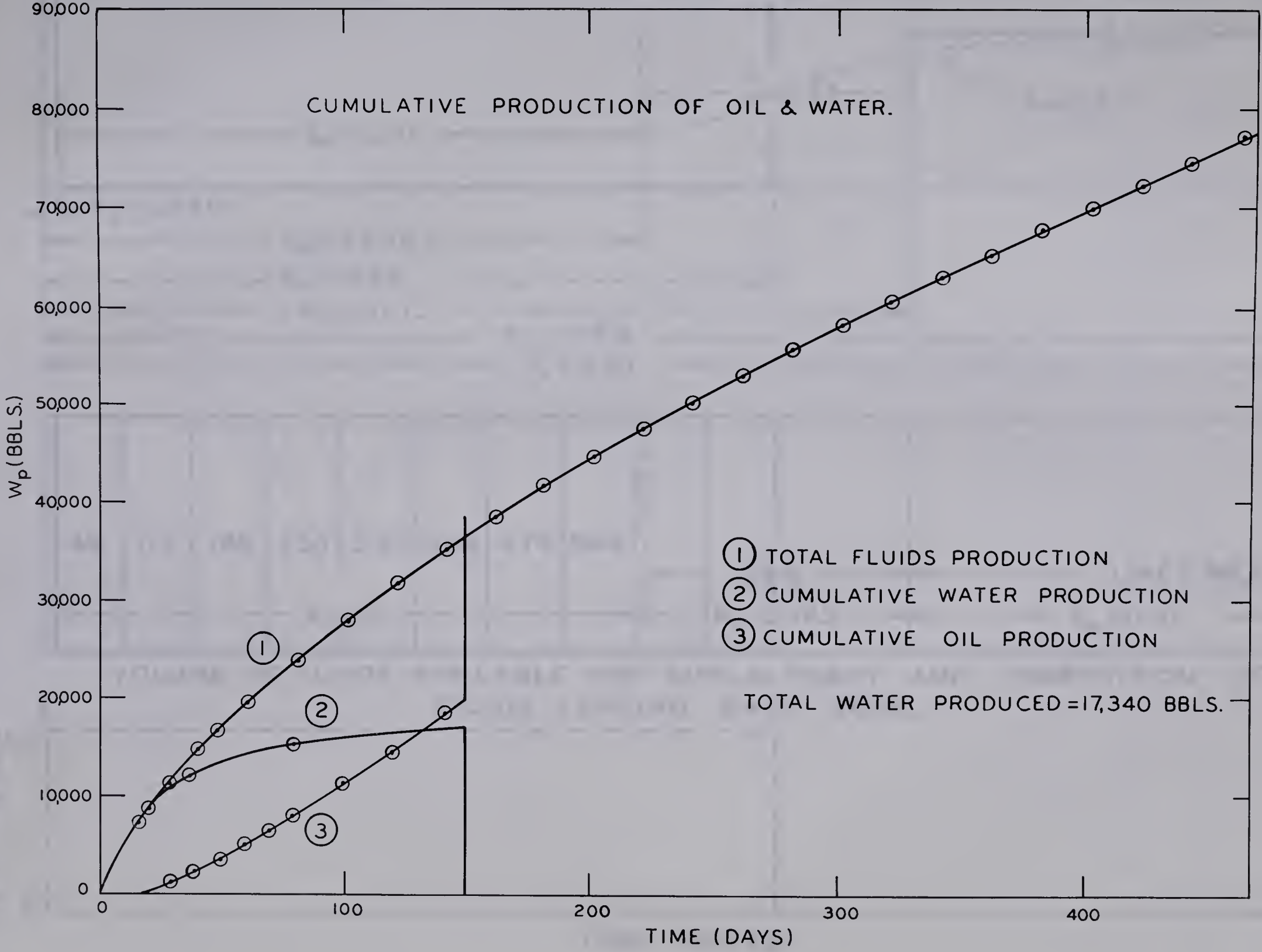
CUMULATIVE PRODUCTION OF OIL & WATER.
W_p (BBLS.)
90,000
80,000
70,000
60,000
50,000
40,000
30,000
20,000
10,000
0
0
100
200
300
400
TIME (DAYS)
1
2
3
① TOTAL FLUIDS PRODUCTION
② CUMULATIVE WATER PRODUCTION
③ CUMULATIVE OIL PRODUCTION
TOTAL WATER PRODUCED = 17,340 BBLS.

FIG.24

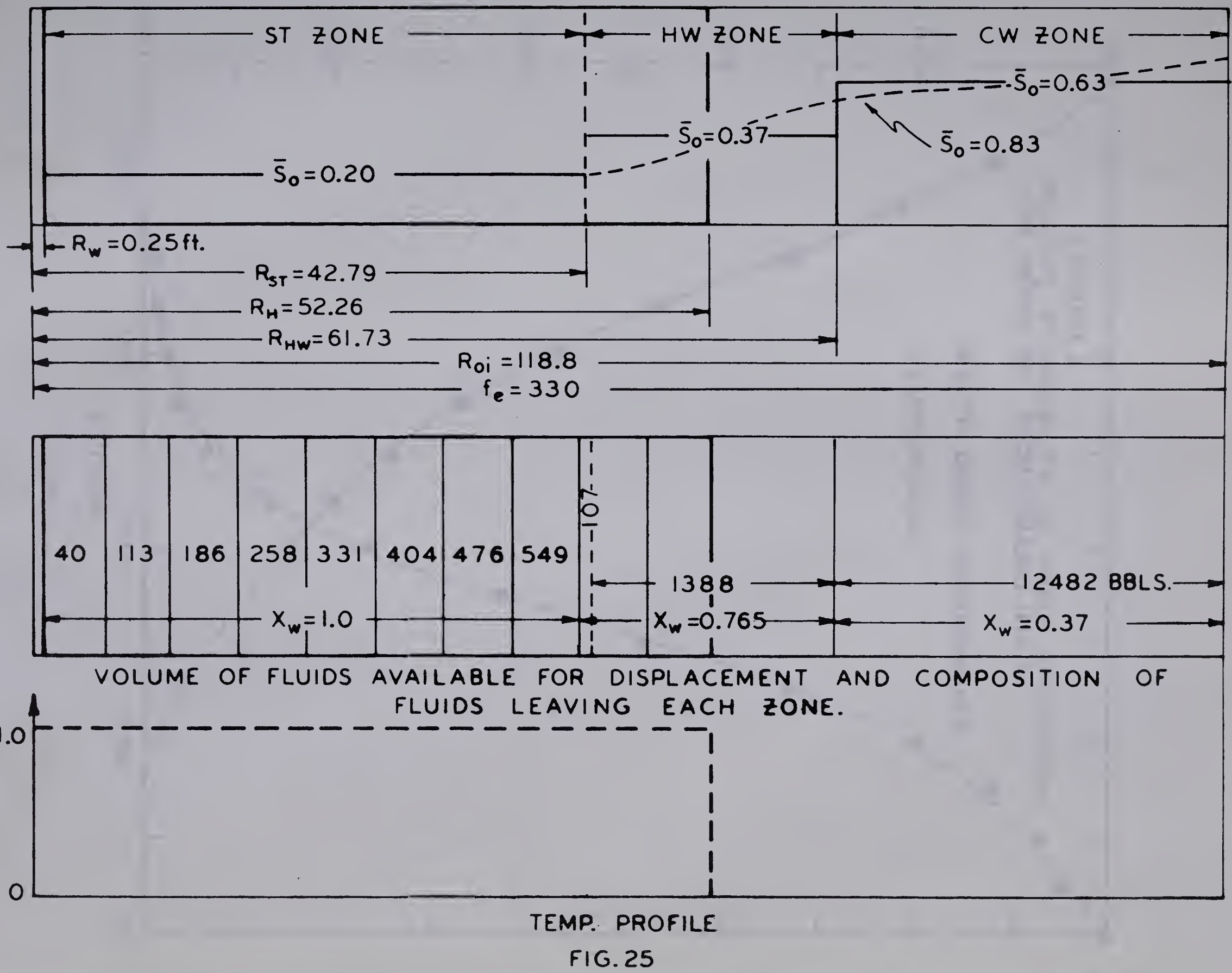
ST ZONE
HW ZONE
CW ZONE
$\bar{S}_o$=0.63
$\bar{S}_o$=0.37
$\bar{S}_o$=0.83
$\bar{S}_o$=0.20
R_w=0.25ft.
R_{ST}=42.79
R_H=52.26
R_{HW}=61.73
R_{oi}=118.8
f_e=330
40
113
186
258
331
404
476
549
107
1388
12482 BBLS.
X_w=1.0
X_w=0.765
X_w=0.37
VOLUME OF FLUIDS AVAILABLE FOR DISPLACEMENT AND COMPOSITION OF FLUIDS LEAVING EACH ZONE.
TEMP. PROFILE
1.0
0
TEMP. PROFILE

FIG. 25

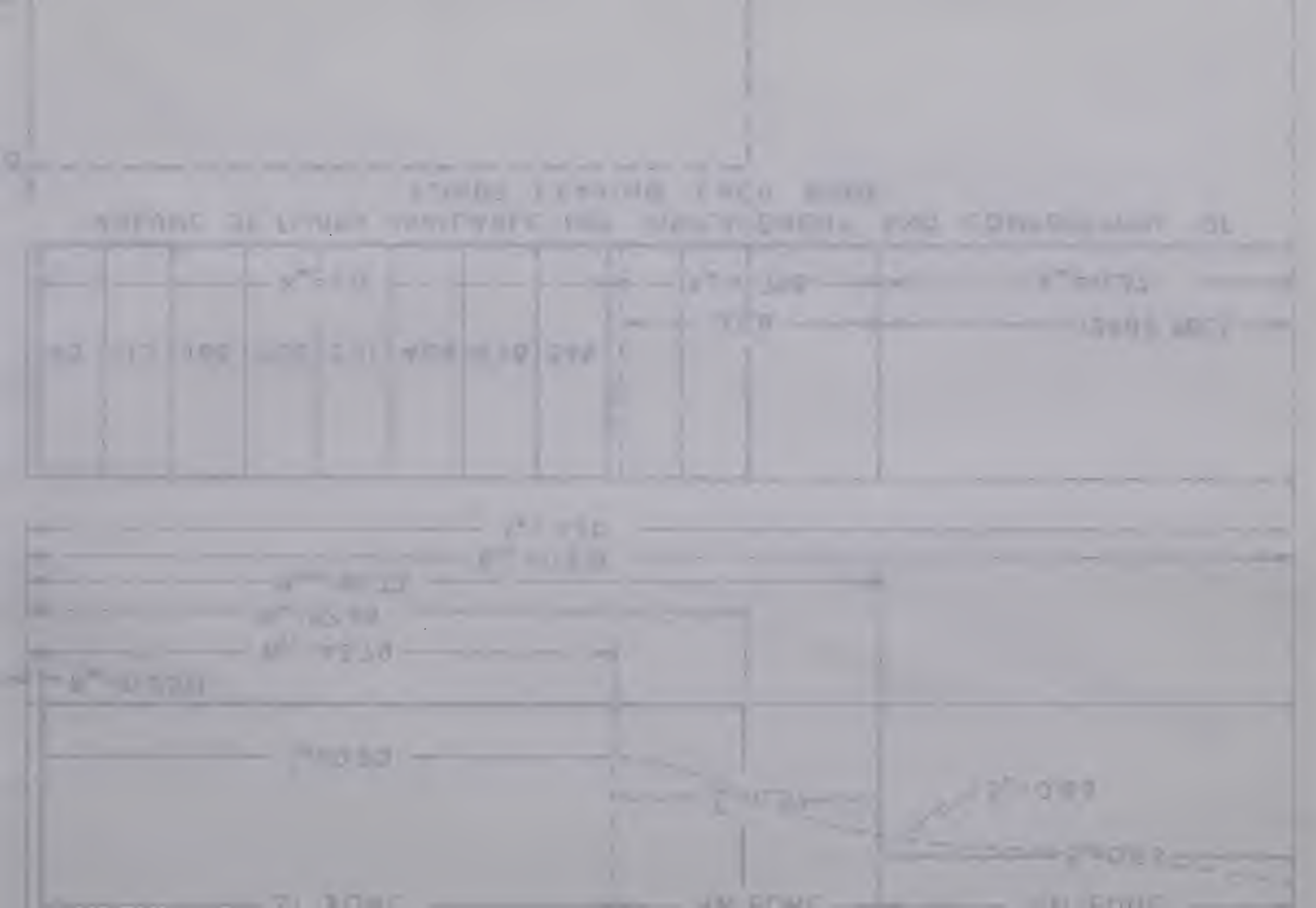

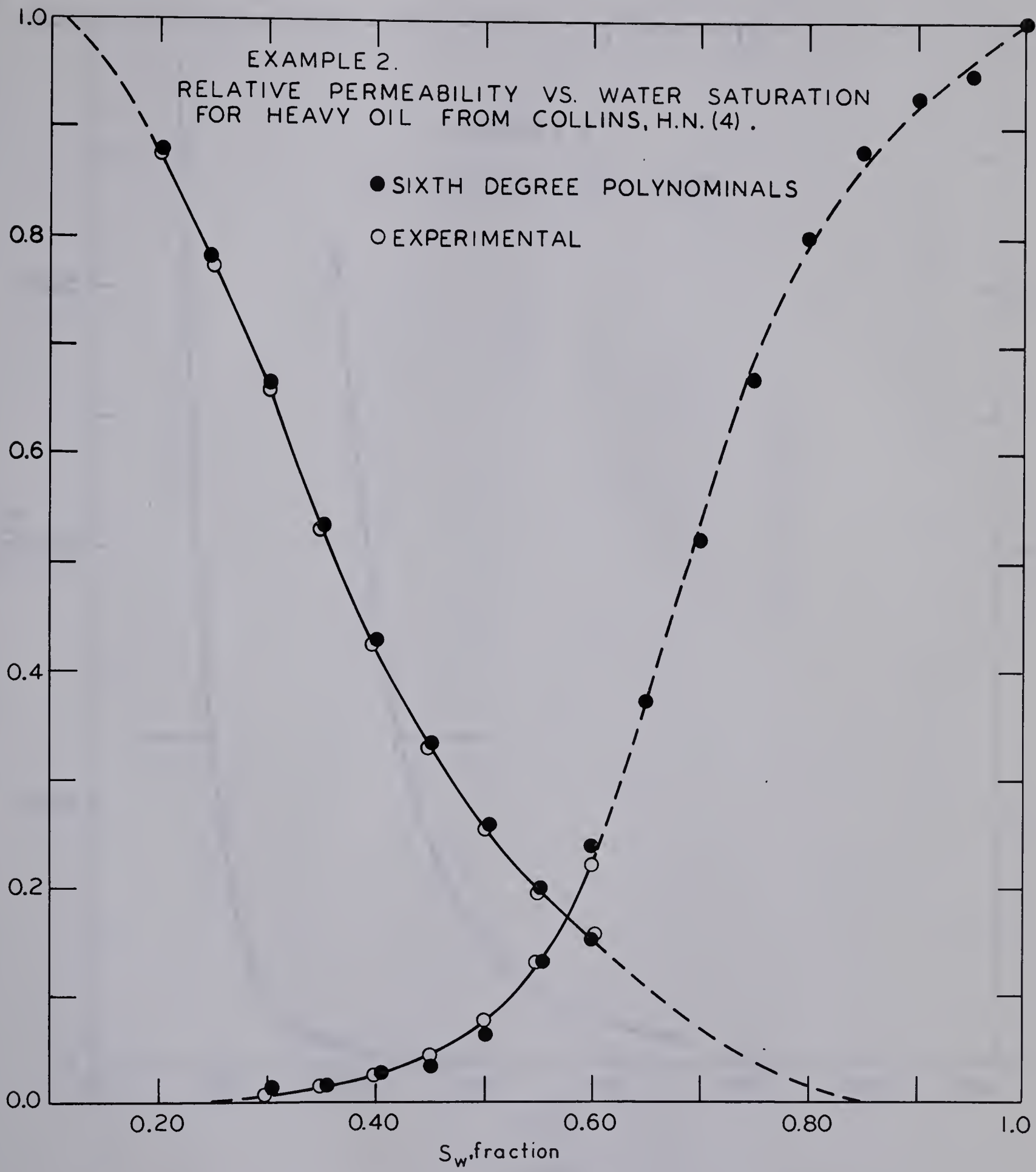
EXAMPLE 2.
RELATIVE PERMEABILITY VS. WATER SATURATION
FOR HEAVY OIL FROM COLLINS, H.N. (4).
● SIXTH DEGREE POLYNOMINALS
○ EXPERIMENTAL
1.0
0.8
0.6
0.4
0.2
0.0
0.20
0.40
0.60
0.80
1.0
S_w, fraction

FIG. 26

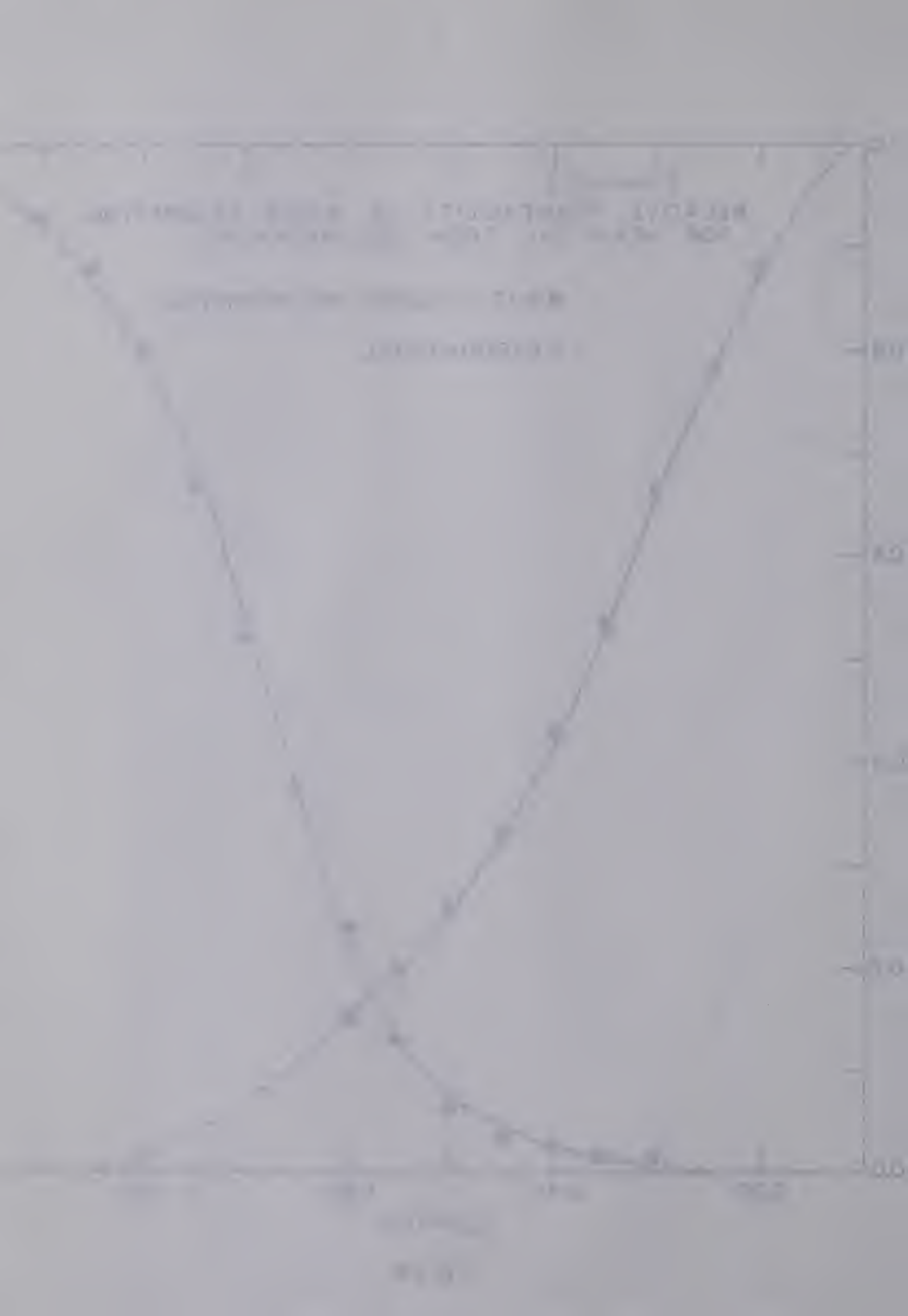

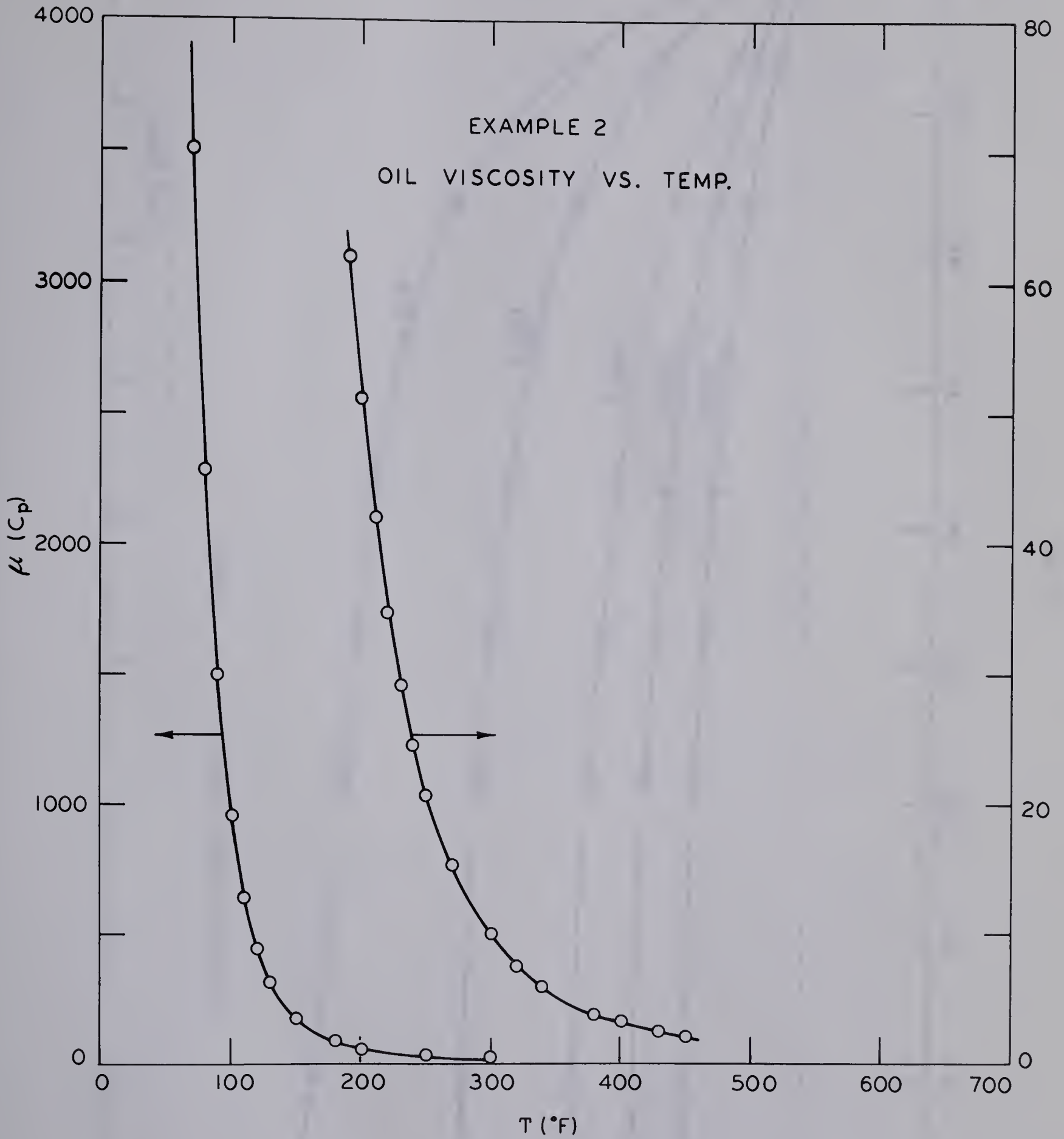
EXAMPLE 2
OIL VISCOSITY VS. TEMP.
μ (cp)
4000
3000
2000
1000
0
80
60
40
20
0
0
100
200
300
400
500
600
700
T (°F)

FIG. 27

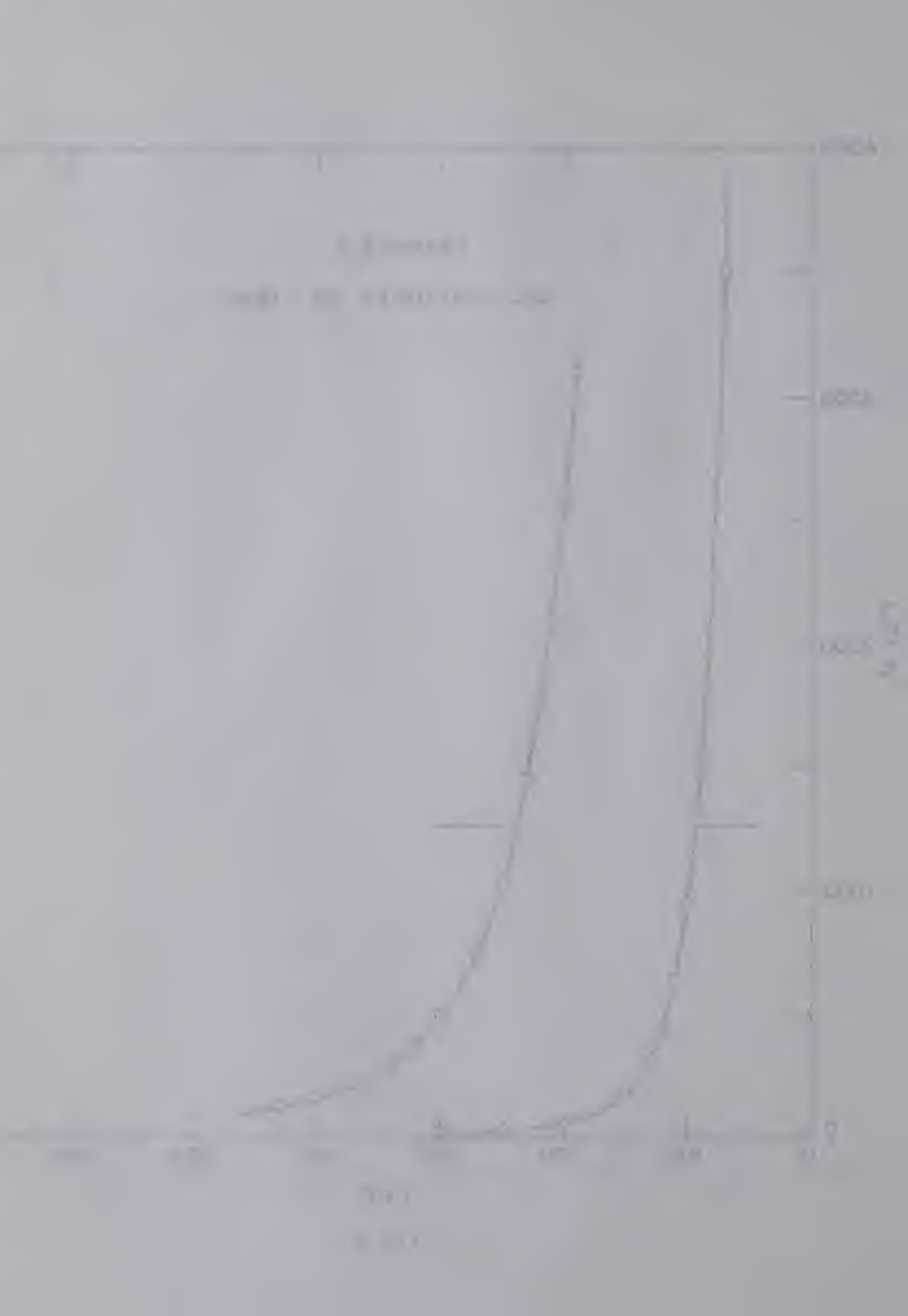

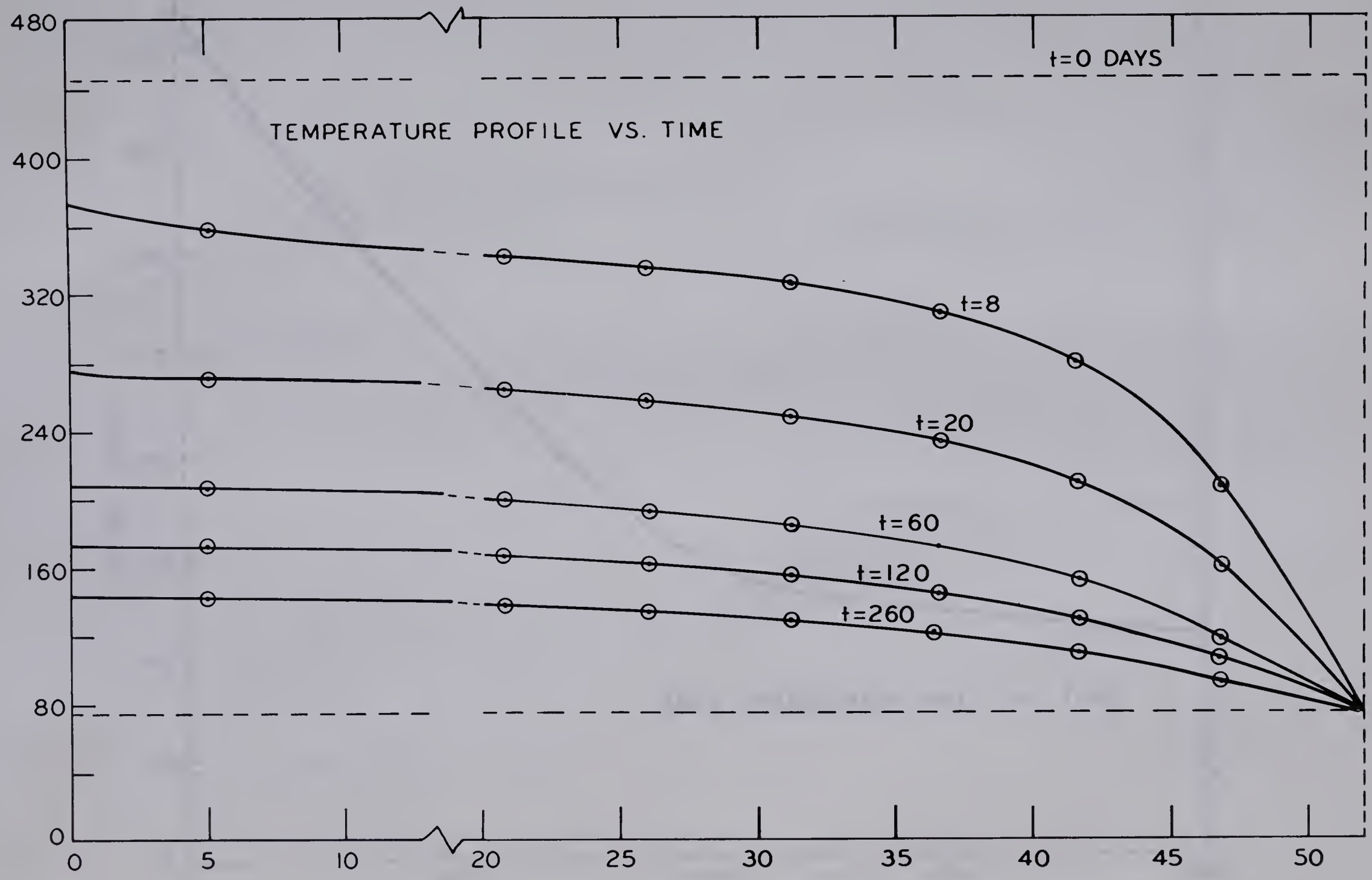
480
400
320
240
160
80
0
0
5
10
20
25
30
35
40
45
50
t=0 DAYS
TEMPERATURE PROFILE VS. TIME
t=8
t=20
t=60
t=120
t=260

FIG.28

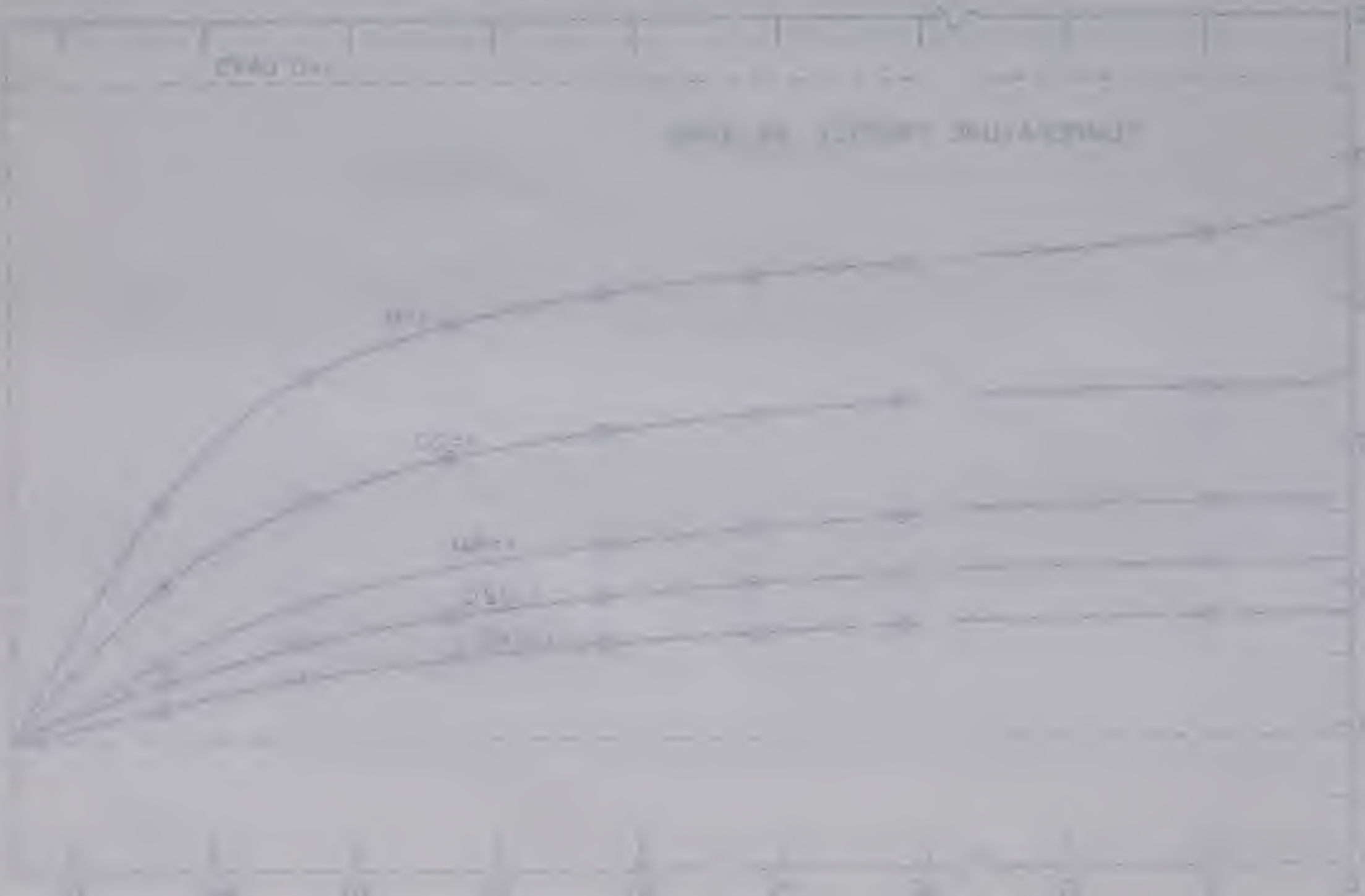

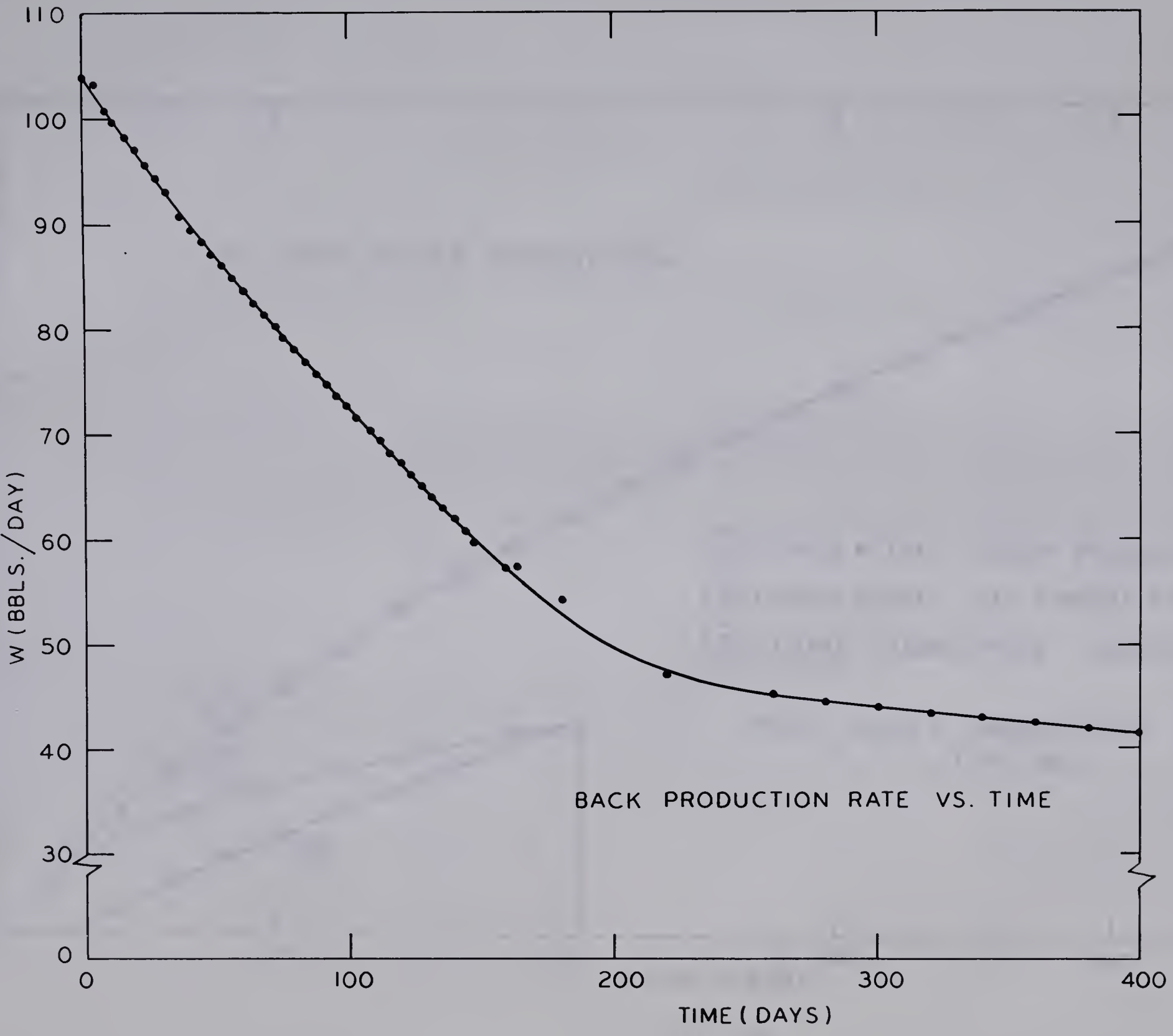
110
100
90
80
70
60
50
40
30
0
W (BBLS./DAY)
0
100
200
300
400
TIME (DAYS)
BACK PRODUCTION RATE VS. TIME

FIG. 29

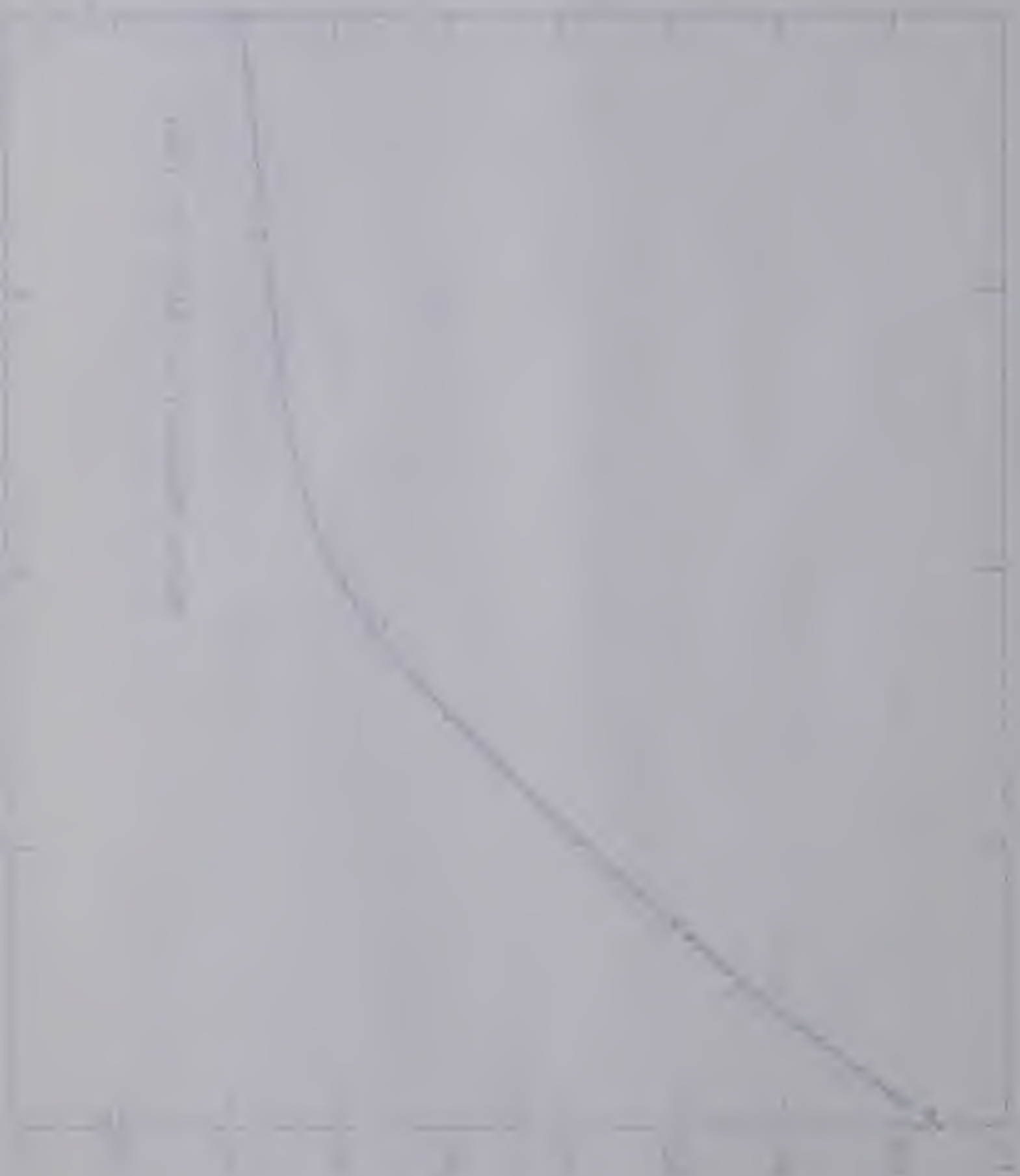

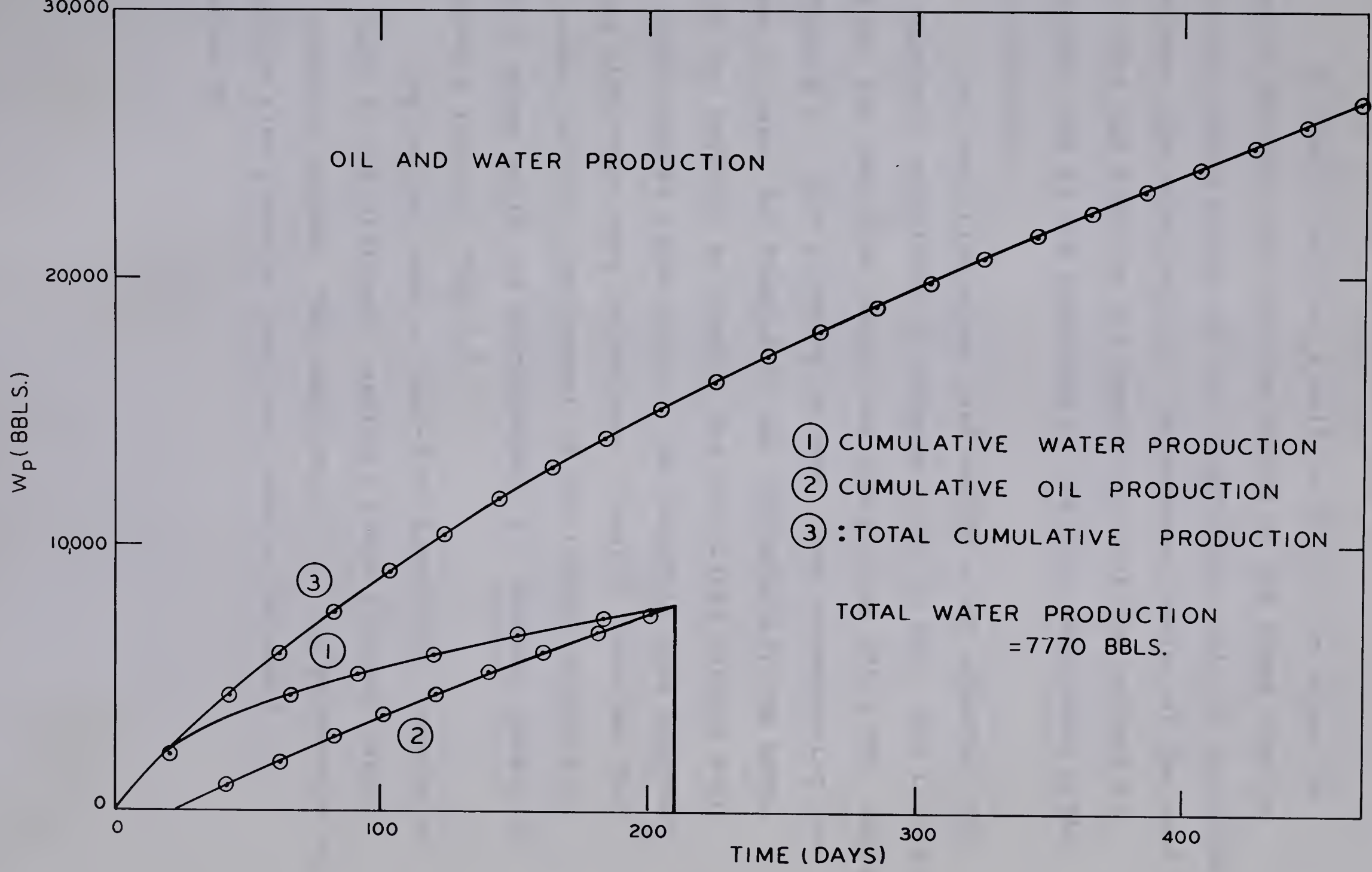
OIL AND WATER PRODUCTION
30,000
20,000
10,000
0
W_p (BBLS.)
0
100
200
300
400
TIME (DAYS)
① CUMULATIVE WATER PRODUCTION
② CUMULATIVE OIL PRODUCTION
③ : TOTAL CUMULATIVE PRODUCTION
TOTAL WATER PRODUCTION
= 7770 BBLS.
1
2
3

FIG. 30

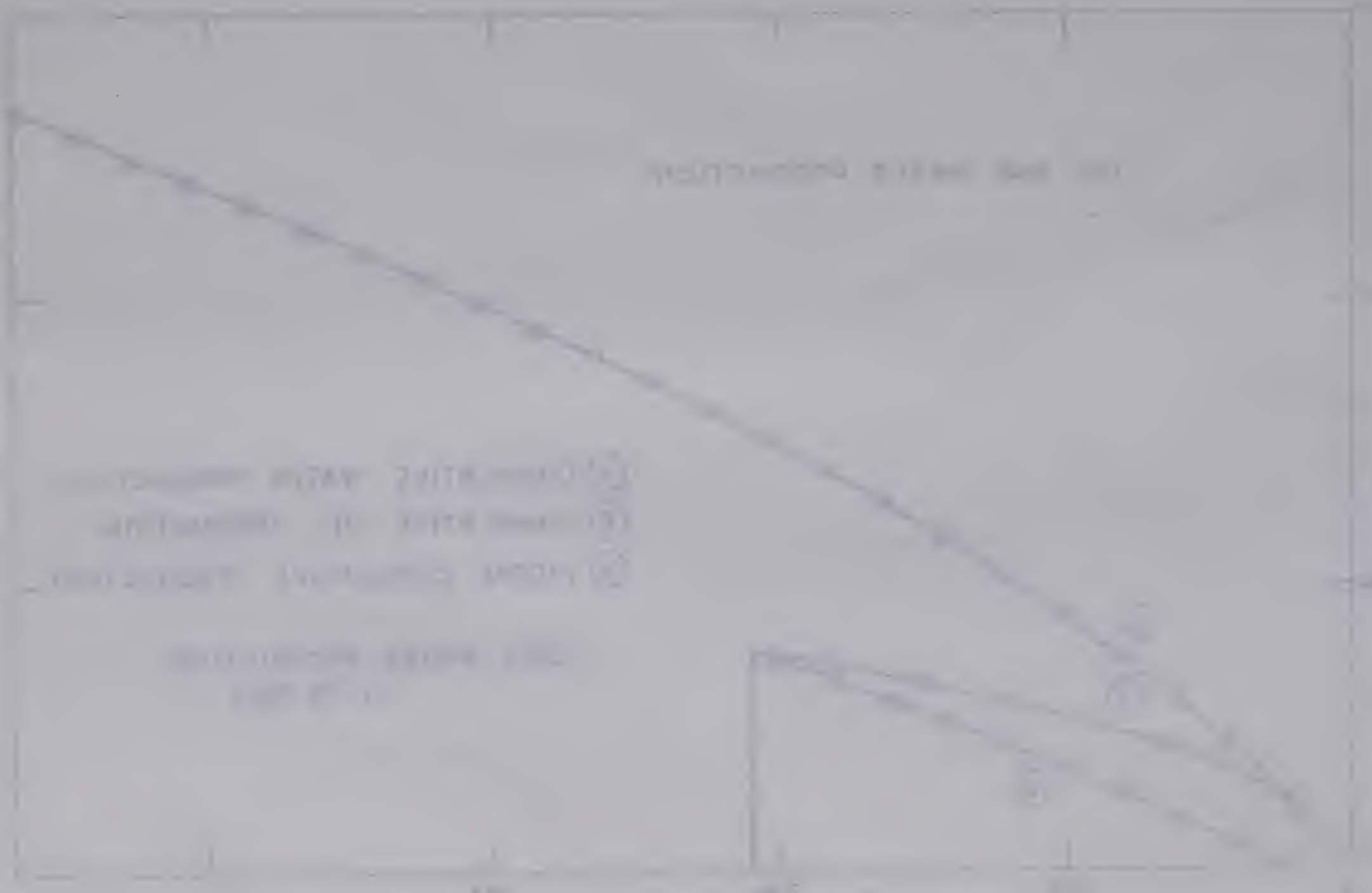

DISCUSSION OF RESULTS

In field practice, a well is shut-in to allow the steam to condense and the pore volume of the steam zone to fill with liquid before the back production cycle is initiated. Therefore, the calculation of the external radius of the cold water zone was based on the assumption that the content of the steam zone at the beginning of the back production cycle was condensate.

The total production rate before steam injection for the reservoir conditions of Example 1 was 55 BPD. The initial rate for the back-flow period was found to be 384.3 BPD, which represents a 7-fold increase in rate. The corresponding increase in rate, for Example 2, was approximately the same. It was not possible to compare the calculated results with any field results since most of the reservoir data reported in the literature were incomplete. Long(12) reported that the lowest ratio of improvement of the initial production rate of seven wells was approximately 10, whereas, Boberg(2) reported a ratio of only 2.5.

The initial rate of back-flow essentially depends on the radii of the different reservoir zones attained during the injection period. The position of the cold water-cold oil interface also plays an important role as indicated by Equation 45.

The calculation procedure of the back production rate does not account for any beneficial effects of heating on damaged wellbores(2). In addition, the assumptions of constant sandface pressure and radially-uniform injection of fluids into the reservoir were made.

The scatter of points in Figure 23 is the result of the large changes in the oil saturation of some elements assumed in the numerical calculation. In this example the oil mobility is more dependent on the relative oil permeability than in Example 2. To illustrate the nature of this dependence, consider the decrease in rate when t = 24 days. The change in oil saturation of Element 7 from 0.49 to 0.69 (see Appendix 2) corresponds to a change in the resistance of this element to fluid flow from 0.003 to 0.015. This sudden increase in resistance causes the sharp decrease in rate, observed in Figure 23.

Two distinct regions of different slope may be clearly distinguished in Figure 23. The division between these regions occurs at approximately t = 150 days. In the left-hand region, the back-flow rate decreases drastically with time, while the decrease in the right-hand region is much less pronounced. An examination of Figure 24 reveals that t = 150 days corresponds to the time when the production of water stops. A possible explanation of this discontinuity in the back production rate versus time curve is the change in the

cooling rate of the reservoir due to the change in saturation from water to oil. Since specific heat of oil is approximately one-half of that of water, the thermal energy transferred to the oil is reduced to one-half of the previous value.

A change in the size of the time step from 4 to 2 days produced the following maximum variation of results:

a) Temperature 3%

b) Back-flow rate 3%

c) Total fluids production 2%

where the results for Δt = 2 days were used as the basis of comparison. For back production times less than 12 days, however, a temperature variation of 29% was encountered at grid points near to the external boundary of the model.

It was also observed that the calculated temperature of the first grid point from the center, independent of the size of the time step, was always lower than the corresponding temperature of the next grid point during the first three or four time steps (see Appendix 2).

A smoother profile would be obtained by incorporating the term C into equation 53.

The back production rate curve for Example 2 did not exhibit the scatter of points encountered in the same curve for Example 1. The reason for this behavior may be explained by comparing the oil mobilities as follows:

Example 1 $k = 612$

$\mu_o = 109 \quad (90°F)$

$$\lambda_o = \frac{k_{ro}k}{\mu_o} = \frac{612}{109}(k_{ro}) \approx 5.61\, k_{ro}$$

Example 2 $k = 3000$

$\mu_o = 2300 \quad (°F)$

$$\lambda_o = \frac{k_{ro}k}{\mu_o} = \frac{3000}{2300}(k_{ro}) \approx 1.30\, k_{ro}$$

Thus, a given change in oil saturation changes the oil mobility of Example 1 approximately 4.3 times the corresponding change in Example 2. This means that the error introduced in Example 1, due to the step function approximations of the S_o versus time curve, will be reflected on the rate versus time curve as a sharper decrease in rate than the corresponding decrease in rate for the same approximations in Example 2.

CONCLUSIONS

The examples show that the saturation conditions of the reservoir at the end of the injection period essentially control the cooling rate of the sand during the earlier part of the back flow. During this part of the cycle, a rapid decrease of the back production rate with time has been observed in field operations(2) as well as in this study.

Relatively large step-wise approximations for the oil saturation in the reservoir elements will produce smooth rate-time curves for those cases where the ratio (k/μ_o) is close to unity. The size of these approximations becomes critical for very favorable mobilities.

RECOMMENDATIONS

Work in the following areas is necessary prior to drawing detailed conclusions on the proposed model for evaluating the "Push-Pull" method of steam injection as well as on the method itself.

1. The mathematical treatment of the injection period should be revised and two-dimensional heat transfer accounted for.
2. A mathematical approach to describe the displacement of oil from the sand in the presence of thermal effects should be developed.
3. A method for predicting the effective thermal conductivity of oil-water-sand and oil-water-natural gas-sand systems is needed to describe the thermal behavior of the reservoir.

NOMENCLATURE

A	=	area, ft^2
dA	=	differential area, ft^2
C_p	=	combined specific heat of sand and fluids at constant pressure, $C_p = C_{pr}(1 - \phi) + C_{pf}\phi$, Btu/lbm°F
C_{pf}	=	combined specific heat of oil and water on volume-fraction basis, $C_{pf} = X_w C_{pw} + X_o C_{po}$, Btu/lbm°F
C_{pi}	=	specific heat of i^{th} substance
h	=	permeable sand thickness, ft.
ha	=	convective heat transfer coefficient, based on a unit volume of bulk porous media, Btu/hr.ft^3°F
H_L	=	rate of heat loss, Btu/hr.
H_f	=	rate of heat injection at sandface, Btu/hr.
k	=	thermal conductivity, Btu/hr.ft.°F
K	=	absolute permeability, md
M'	=	combined heat capacity of sand, oil and water as defined by Equation 4, Btu/ft^3°F
N	=	number of time increments used up to a fixed production time t
P	=	pressure, psia
ΔP	=	pressure difference between the outer and inner radius of reservoir, psi
q	=	heat flow rate, Btu/hr.
$\dot{q}$	=	heat flow rate through element of area dA of flat surfaces of cylindrical model, $\dot{q} = q_T dA$, Btu/hr.
q_T	=	total heat flux through flat surfaces of cylindrical model, Btu/hr.ft^2
r	=	r-direction coordinate, ft.
r_e	=	outer-well radius, ft.

r_w = wellbore radius, ft.

R_H = "effective radius" as defined in Reference 1

$R_1 R_2 \ldots R_m$ = radii of elements 1, 2, ... m, ft.

S = fluid saturation, fraction

t = back production time, $t = N\Delta t$, hr.

t_I = combined injection and soaking time, hr.

t_j = combined injection and soaking time for the j^{th} reservoir element, hr.

T = temperature, °F

$\bar{T}$ = average temperature, °F

T_s = surface temperature of flat surfaces of the model, °F

v = fluid velocity based on "effective" flow area (A_{eff} = cross-sectional area/ϕ), ft/hr.

V_F = velocity of "square" heat front, ft/hr.

W = back production rate of combined oil and water, res. bbls/day

W_p = cumulative fluids production, res. bbls.

x = x-direction coordinate, ft.

X = volumetric fraction of oil or water flowing, fraction

X_F = x-coordinate of "square" heat front, ft.

Y = dimensionless distance, $Y = (ha/k_w\phi)^{1/2}x$

Z = Z-direction coordinate, ft.

Z' = integration variable

Greek Letters

α = thermal diffusivity, $= k/\rho C_p$, $ft^2/hr.$

Δ = forward difference

η = dimensionless time, $= (ha/k_w\phi)^{1/2}vt$

λ = mobility of fluids, $\lambda_{co} = (K_{ro}K/\mu_o)_{co} + (K_{rw}K/\mu_w)_{co}$, md/C_p

μ = fluid viscosity, centipoise

ν = dimensionless group, $\nu = (2k_{OB}/M'h\sqrt{\alpha_{OB}})t^{1/2}$

ξ = integration variable

ρ = combined density of sand and fluids, $\rho = \rho_r(1 - \phi) + \rho_f\phi$, lbm/ft^3

ρ_f = combined density of fluids, $\rho_f = X_w\rho_w = X_o\rho_o$, lbm/ft^3

ρ_i = density of i^{th} substance

$\tau_1, \tau_2 \ldots$ = cumulative back production time, $\tau_i = i\Delta t$, hr.

ϕ = effective porosity, fraction

Subscripts

C = connate saturation

CO = cold oil zone of reservoir

CW = cold water zone of reservoir

e = effective

f = fluid

HW1 = hot water zone assumed at initial reservoir temperature

HW2 = hot water zone assumed at steam temperature

i = initial

j = j^{th} grid intersection in r-direction

n = time increment level

o = oil

oi = initial conditions of oil zone

OB = overburden

r = rock, relative or residual

ST = steam

W = water

LIST OF REFERENCES

1. Avdonin, N.A.: "On the Different Methods of Calculating the Temperature Fields of a Stratum During Thermal Injection", Neft'i Gaz, Vol. 7, No. 8, 1964, p. 39.

2. Boberg, T.C.: "What's the Score on Thermal Recovery and Thermal Stimulation", The Oil and Gas Journal, August 23, 1965, p. 78.

3. Carslaw, H.S. and Jaeger, J.C.: "Conduction of Heat in Solids", Clarendon Press, Oxford, 2nd Ed., 1959, p. 59, 63.

4. Collins, H.N.: "High Viscosity Crude Oil Displacement in a Long Unconsolidated Sand Pack Using a Native Brine", Masters Thesis, University of Alberta, April, 1964.

5. Green, D.W. and Perry, R.H.: "Heat Transfer with a Flowing Fluid Through Porous Media", Chem. Eng. Prog. Symp. Series, Heat Transfer, Buffalo, 1961, p. 61.

6. Hadidi, T.A.R., Ph.D. Thesis, Pennsylvania State University, 1955.

7. Hausen, H.Z., Math. Mech., Vol. 9, 1929, p. 173.

8. Jenkins, R. and Aronofsky, J.S.: "Analysis of Heat Transfer Processes in Porous Media - New Concepts in Reservoir Heat Engineering", Proc. 18th Tech. Conf. on Petr. Prod., Penn. State Univ, 1954, p. 69.

9. Klinkenberg, A.: "Numerical Evaluation of Equations Describing Transient Heat and Mass Transfer in Packed Solids", Ind. Eng. Chem., Vol. 40, 1948, p. 1992.

10. Kunii, D. and Smith, J.M.: "Heat Transfer Characteristics of Porous Rocks", AIChE Journal, Vol. 7, 1961, p. 29.

11. Lauwerier, H.A.: "The Transport of Heat in an Oil Layer Caused by the Injection of Hot Fluid", Appl. Sci. Res., Sec. A, Vol. 5, 1955, p. 145.

12. Long, R.J.: "Steam for Secondary Recovery - Kern Field California", Preprint, Rocky Mountain Regional Meeting, Billings, Montana, June 10-11, 1965.

13. Malofeev, G.E.: "Experimental Study of Formation Heating When Injecting Hot Water", Neft'i Gaz, Vol. 1, No. 12, 1958, p. 77.

14. Malofeev, G.E.: "Simulation of the Formation-Heating Process During the Injection of Hot Fluid", Nefti'i Gaz, Vol. 2, No. 9, 1959, p. 49.

15. Majofeev, G.E.: "Calculation of the Temperature Distribution in a Formation When Pumping Hot Fluid into a Well", Neft'i Gaz, Vol. 3, No. 7, 1960, p. 59.

16. Marx, J.W. and Langenheim, R.H.: "Reservoir Heating by Hot Fluid Injection", Trans. AIME, Vol. 216, 1959, p. 312.

17. Peaceman, W.D. and Rachford, H.H.,Jr.: "The Numerical Solution of Parabolic and Elliptic Differential Equations", J. Soc. Indust. Appl. Math., Vol. 3, 1955, p. 28.

18. Perry, J.H. Ed.: "Chemical Engineers' Handbook", McGraw-Hill Book Co., Inc., 3rd Ed., 1950, p. 374.

19. Preston, F.W. and Hasen, R.D.: "Further Studies on Heat Transfer in Unconsolidated Sands During Water Injection", Producers Monthly, Vol. 18, No. 4, Feb. 1954, p. 24.

20. Rubinshtein, L.I.: "The Total Heat Losses in Injection of a Hot Liquid into a Stratum", Neft'i Gaz, Vol. 2, No. 9, 1959, p. 41.

21. Schumann, T.E.W., J. Franklin Inst., Vol. 208, 1929, p. 405.

22. Spillette, A.G.: "Heat Transfer During Hot Fluid Injection into an Oil Reservoir", Preprint 16th Annual Meeting Can. Inst. of Mining and Metallurgy, May 4th, 1965, Calgary.

23. Willman, B.T., Valleroy, V.V., Runberg, G.W., Cornelius, A.J. and Powers, L.W.: "Laboratory Studies of Oil Recovery by Steam Injection", Trans. AIME, Vol. 222, 1961, p. 681.

A P P E N D I X I

Overburden and Underburden Temperatures Versus Back Production Time

Define

$$\theta = T - T_i$$

$$\theta_o = T_{ST} - T_i$$

$$\theta_{Z=0} = \theta_s = \theta_s(t)$$

P.D.E. and B.C.

$$\frac{\partial^2 \theta}{\partial Z^2} = \frac{1}{K_o} \frac{\partial \theta}{\partial t} \qquad (A)$$

$$\text{I.C.} \quad t = 0 \quad \theta = \theta_o \operatorname{erfc} \frac{Z}{2\sqrt{\alpha_{OB} t_j}}$$

$$\text{B.C.} \quad t > 0 \quad \theta_s = \theta_s(t) \quad \text{at} \quad Z = 0$$

$$\theta = 0 \quad \text{at} \quad Z = \infty$$

Putting $\theta = U + V$

Equation A can be written as two P.D.E.

$$\frac{\partial^2 U}{\partial Z^2} = \frac{1}{\alpha_{OB}} \frac{\partial U}{\partial t} \qquad (B)$$

$$\text{I.C.} \quad t = 0 \quad U = \theta_o \operatorname{erfc} \frac{Z}{2\sqrt{\alpha_{OB} t_j}}$$

$$\text{B.C.} \quad t > 0 \quad U = 0 \quad \text{at} \quad Z = 0$$

$$U = 0 \quad \text{at} \quad Z = \infty$$

and

$$\frac{\partial^2 V}{\partial Z^2} = \frac{1}{\alpha_{OB}} \frac{\partial V}{\partial t} \qquad (C)$$

I.C. $t = 0$ $V = 0$

B.C. $t > 0$ $V = \theta_s(t)$ at $Z = 0$

$V = 0$ at $Z = \infty$

The solution of Equation B is

$$U = \frac{1}{2\sqrt{\pi \alpha_{OB} t}} \int_0^\infty f(Z') \left\{ e^{-\frac{(Z - Z')^2}{4\alpha_{OB} t}} - e^{-\frac{(Z + Z')^2}{4\alpha_{OB} t}} \right\} dZ' \qquad (D)$$

where

$$f(Z') = \theta_o \operatorname{erfc} \frac{Z'}{2\sqrt{\alpha_{OB} t_j}}$$

The solution of the Equation C is (Duhamel's theorem)

$$V = \frac{Z}{2\sqrt{\pi \alpha_{OB}}} \int_0^t \theta_s(\lambda) \frac{e^{-\frac{Z^2}{4\alpha_{OB}(t-\lambda)}}}{(t - \lambda)^{3/2}} d\lambda$$

Putting $\xi^2 = \dfrac{Z^2}{4\alpha_{OB}(t - \lambda)}$, the above equation may be written as

$$V(Z,t) = \frac{2}{\sqrt{\pi}} \int_{\frac{Z}{2\sqrt{\alpha_{OB} t}}}^\infty \theta_s\left(t - \frac{Z^2}{4\alpha_{OB}\xi^2}\right) e^{-\xi^2} d\xi \qquad (E)$$

The solution for θ becomes

$$\theta = U + V = \frac{1}{2\sqrt{\pi \alpha_{OB} t}} \int_0^\infty \theta_o \operatorname{erfc} \frac{Z'}{2\sqrt{\alpha_{OB} t_j}} \left\{ e^{-\frac{(Z-Z')^2}{4\alpha_{OB} t}} \right.$$

$$- e^{-\frac{(Z+Z')^2}{4\alpha_{OB}t}} \Big\} dZ' + \frac{2}{\sqrt{\pi}} \int_{\frac{Z}{2\sqrt{\alpha_{OB}t}}}^{\infty} \theta_s\left(t - \frac{Z^2}{4\alpha_{OB}\xi^2}\right) e^{-\xi^2} d\xi$$

$$\left.\frac{\partial \theta}{\partial Z}\right|_{Z=0} = \left.\frac{\partial U}{\partial Z}\right|_{Z=0} + \left.\frac{\partial U}{\partial Z}\right|_{Z=0}$$

From D

$$\left.\frac{\partial U}{\partial Z}\right|_{Z=0} = \frac{\theta_o}{2\sqrt{\pi\alpha_{OB}t}} \left[\int_o^{\infty} \left(\operatorname{erfc} \frac{Z'}{2\sqrt{\alpha_{OB}t_j}}\right) \frac{Z'}{2\alpha_{OB}t} e^{-\frac{Z'^2}{4\alpha_{OB}t}} dZ' \right.$$

$$\left. + \int_o^{\infty} \left(\operatorname{erfc} \frac{Z'}{2\sqrt{\alpha_{OB}t_j}}\right) \frac{Z'}{2\alpha_{OB}t} e^{-\frac{Z'^2}{4\alpha_{OB}t}} dZ' \right]$$

The above expression can be simplified and integrated by parts to give

$$\left.\frac{\partial U}{\partial Z}\right|_{Z=0} = \frac{\theta_o}{\sqrt{\pi\alpha_{OB}}} \left(\frac{1}{\sqrt{t}} - \frac{1}{\sqrt{t + t_j}}\right) \qquad (F)$$

Consider $\theta_s(t)$ as a step function;

$$\theta_s(t) = \theta^{(1)} = \text{constant} \qquad 0 \leq t \leq \tau_1$$

$$\theta_s(t) = \theta^{(2)} = \text{constant} \qquad \tau_1 \leq t \leq \tau_2$$

$$\theta_s(t) = \theta^{(3)} = \text{constant} \qquad \tau_2 \leq t \leq \tau_3$$

etc.

Equation E can be integrated now to give

$$V(Z,t) = \theta^{(1)} \operatorname{erfc} \frac{Z}{2\sqrt{\alpha_{OB} t}} + (\theta^{(2)} - \theta^{(1)}) \operatorname{erfc} \frac{Z}{2\sqrt{\alpha_{OB}(t-\tau_1)}}$$

$$+ (\theta^{(3)} - \theta^{(2)}) \operatorname{erfc} \frac{Z}{2\sqrt{\alpha_{OB}(t-\tau_2)}} + \ldots$$

Then,

$$\left.\frac{\partial V}{\partial Z}\right|_{Z=0} = - \frac{\theta^{(1)}}{\sqrt{\pi \alpha_{OB} t}} - \frac{\theta^{(2)} - \theta^{(1)}}{\sqrt{\pi \alpha_{OB}(t-\tau_1)}} - \frac{\theta^{(3)} - \theta^{(2)}}{\sqrt{\pi \alpha_{OB}(t-\tau_2)}} - \ldots$$

$$\left.\frac{\partial \theta}{\partial Z}\right|_{Z=0} = \frac{\theta_o}{\sqrt{\pi \alpha_{OB}}} \left(\frac{1}{\sqrt{t}} - \frac{1}{\sqrt{t + t_j}}\right) + \left\{ - \frac{(1)}{\sqrt{\pi \alpha_{OB} t}} \right.$$

$$\left. + \frac{\theta^{(1)} - \theta^{(2)}}{\sqrt{\pi \alpha_{OB}(t - \tau_1)}} + \frac{\theta^{(2)} - \theta^{(3)}}{\sqrt{\pi \alpha_{OB}(t - \tau_2)}} + \ldots \right\}$$

The total heat flux is given by

$$q_T = \frac{2k_{OB}}{\sqrt{\pi \alpha_{OB}}} \left\{ \theta_o \left(\frac{1}{\sqrt{t}} - \frac{1}{\sqrt{t + t_j}}\right) - \frac{\theta^{(1)}}{\sqrt{t}} \right.$$

$$\left. + \frac{\theta^{(1)} - \theta^{(2)}}{\sqrt{t - \tau_1}} + \frac{\theta^{(2)} - \theta^{(3)}}{\sqrt{t - \tau_2}} + \ldots \right\}$$

or

$$q_T = \frac{2k_{OB}}{\sqrt{\pi \alpha_{OB}}} \left\{ (T_{ST} - T_i) \left(\frac{1}{\sqrt{t}} - \frac{1}{\sqrt{t + t_j}}\right) \right.$$

$$- \frac{T^{(1)} - T_i}{\sqrt{t}} + \frac{T^{(1)} - T^{(2)}}{\sqrt{t - \tau_1}} + \ldots \} \qquad (39)$$

The term C in Equation 29 for a cylindrical element P may be written as:

$$C_N = C_{LHS} \left[(T_{ST} - T_i) \left(\frac{1}{\sqrt{N}} - \frac{\Delta t}{\sqrt{N\Delta t + t_j}} \right) + \frac{T_i}{\sqrt{N}} \right]$$

$$+ C_{LHS} \left[\frac{\sqrt{N} - \sqrt{N-1}}{\sqrt{N(N-1)}} \right] T_P^{\Delta t}$$

$$+ C_{LHS} \left[\frac{\sqrt{N-1} - \sqrt{N-2}}{\sqrt{(N-1)(N-2)}} \right] T_P^{2\Delta t}$$

$$+ C_{LHS} \left[\frac{\sqrt{N-2} - \sqrt{N-3}}{\sqrt{(N-2)(N-3)}} \right] T_P^{3\Delta t}$$

$$+ \ldots\ldots\ldots\ldots\ldots$$

$$+ C_{LHS} \left[\frac{\sqrt{N - (N-2)} - \sqrt{N - (N-1)}}{\sqrt{[N - (N-2)][N - (N-1)]}} \right] T_P^{(N-1)\Delta t}$$

$$- C_{LHS} T_P^{N\Delta t} \qquad (G)$$

where

$$t = N\Delta t$$

$$C_{LHS} = \frac{\beta}{h\rho_N C_{PN}}$$

$$\beta = \frac{2k_{OB}}{\sqrt{\pi \alpha_{OB}}} \cdot \frac{1}{\sqrt{\Delta t}}$$

and N denotes the number of time increments chosen for a back production time, t.

Calculations for the First Time Increment

In the following illustration a time increment of 4 days was used. No appreciable change in the results was found when this time increment was halved.

a) Initial rate of back production

$$\lambda = \frac{k_{ro}k}{\mu_o} + \frac{k_{rw}k}{\mu_w} \qquad (44)$$

1) cold oil zone

$S_o = 0.905$, $k_{ro} = 1.0$ (Figure 9)

$S_w = 0.095$, $k_{rw} = 0.0$

$T = 95°F$ $\mu_o = 100\ C_p$ (Figure 10)

$$\lambda_{co} = \frac{1 \times 612}{100} = 6.12$$

2) cold water zone

$S_o = 0.69$, $k_{ro} = 0.306$ (Figure 9)

$S_w = 0.31$, $k_{rw} = 0.014$

$T = 95°F$ $\mu_w = 0.7225$ $\mu_o = 100$

$$\lambda_{cw} = \frac{0.306 \times 612}{100} + \frac{0.014 \times 612}{0.7225} = 14.392$$

$$W_i = \frac{0.00708 \times 25 \times 400}{\frac{1}{6.12} \ln \frac{330}{131.5} + \frac{1}{14.392} \ln \frac{131.5}{80.8}}$$

$$= 384.3 \text{ BPD} \qquad (45)$$

Irreducible oil and water saturations (from relative permeability curves):

$$S_{or} = 0.26$$

$$S_{wr} = 0.18 \qquad \text{(Figure 19)}$$

The hot cylinder was divided in ten equal Δr elements. The volume of oil and water in excess fo the above irreducible saturations were calculated for every element, these volumes are shown in Table 1. The composition of the mixture of oil and water flowing initially in every zone, calculated according to Equation 46 are also shown in Table 1.

b) Composition of fluids flowing in the hot portion of the reservoir.

Using Table 2 and Figure 11,

$$X_w \simeq 1.0 \times \frac{9638}{11678} + 0.5 \frac{2040}{11678} = 0.913$$

$$\frac{}{} + \frac{}{} = \frac{}{}$$

$$\frac{}{} = \frac{}{} \cdot \frac{}{} \cdot \frac{}{}$$

$$= \frac{}{}$$

$$= \frac{}{}$$

$$= \frac{}{}$$

Table 1

Element or Zone	Volume of Displaceable Liquids	Total Volume of Displaceable Liquids	Composition (X_w)
1	120	120	1.0
2	357	477	1.0
3	596	1073	1.0
4	837	1910	1.0
5	1072	2982	1.0
6	1320	4302	1.0
7	1545	5847	1.0
8	1776	7623	1.0
9	2015	9638	1.0
10	2040	11678	0.5
Hot water zone 1	2800	14478	0.5
Cold water	22460	36938	0.23
Cold oil	221750	258688	0.0

Table 2

Element	Injection Time (hr)	C term
1	720	assumed negligible
2	710	$C_2 = 0.336292 - 0.000904T_2$ (1)
3	690	$C_3 = 0.334623 - 0.000904T_3$ (1)
4	660	$C_4 = 0.331998 - 0.000904T_4$ (1)
5	620	$C_5 = 0.328243 - 0.000904T_5$ (1)
6	560	$C_6 = 0.321980 - 0.000904T_6$ (1)
7	485	$C_7 = 0.312825 - 0.000904T_7$ (1)
8	400	$C_8 = 0.300033 - 0.000904T_8$ (1)
9	285	$C_9 = 0.276317 - 0.000904T_9$ (1)
10	145	$C_{10} = 0.226922 - 0.000904T_{10}$ (1)

c) Calculation of the temperature profile

1) Computation of M

$$\rho_f = X_w\rho_w + X_o\rho_o = 0.913 \times 52.28 + 0.087 \times 51.45$$
$$= 52.208$$

$$C_{pf} = X_wC_{pw} + X_oC_{po} = 0.913 \times 1.03 + 0.087 \times 0.50$$
$$= 0.9839$$

$$\rho C_p = \rho_r C_{pr}(1 - \phi) + \rho_f C_{pf}\phi$$
$$= 140 \times 0.23\ (1 - 0.266) + 52.208 \times 0.9839 \times 0.266$$
$$= 37.298$$

$$M = \frac{0.03720 \times 384.3 \times 52.208 \times 0.9839}{25 \times 37.298}$$
$$= 0.7875$$

2) Calculation of C

The hot reservoir and the adjacent strata were divided in ten equal Δr increments. The injection time for every element was calculated a explained earlier using Equation 1 of Reference 23. The term C for the first time increment, obtained by combining Equations 31 and 39,is given by

$$C = \frac{q_T}{h\rho C_p} = \frac{2k_{OB}}{h\rho C_p\sqrt{\pi\alpha_{OB}}}\left[(T_{ST} - T_i)\left(\frac{1}{\sqrt{\Delta t}} - \frac{1}{\sqrt{\Delta t + t_j}}\right)\right.$$
$$\left. - \frac{T^{(1)} - T_i}{\sqrt{\Delta t}}\right]$$

Table 2 shows the injection time for every element and the corresponding equation for the C term. Equations 53 to 57 (the latter written for j = 3 to j = 10) with the C term replaced by the above expressions, gave a system of simultaneous algebraic equations. The system of equations may be written in the compact matrix notation as

$$AT = r$$

A check of the solution was made by multiplying the found T-vector by the original matrix and subtracting the new independent vector, r', from the original r. The maximum deviation was found to be less than 0.0001%.

d) New saturation distribution

1) Fluids production

$$W_p = W_i \Delta t = 384.31 \times 4 = 1537.24 \text{ bbls}$$

2) New radius of the cold oil zone

$$R_{co} = \sqrt{131.5^2 - \frac{5.61 \times 1537.24}{\pi \times 0.266 \times 25(1 - 0.26 - 0.18)}}$$

$$= 128.7 \text{ ft.}$$

3) The above production equals the volume of the displaceable liquids from the section of element 9 located inside the steam zone. The saturation of this element should be changed to (Equation 61):

$$S_o = 0.20 + (1 - 0.26)0.5 = 0.47$$

The saturation in the other part of the hot cylinder remains unchanged for the second time increment.

e) New production rate

Following the method outlined in the preceding pages, the new production rate to use in the second time increment for the calculation of the temperature profile was found to be

$$W = 359.90 \text{ BPD}$$

Second Time Step

A new value for M is computed, now, using the new rate and calculating a new composition for the fluids flowing from the new saturation distribution. New values for C should be calculated according to the equation

$$C = \frac{q_T}{h\rho C_p} = \frac{2k_{OB}}{h\rho C_p \sqrt{\pi \alpha_{OB}}} \left[(T_{ST} - T_i) \left(\frac{1}{\sqrt{2\Delta t}} - \frac{1}{\sqrt{2\Delta t + t_j}} \right) \right.$$

$$\left. - \frac{T^{(1)} - T_i}{\sqrt{2\Delta t}} + \frac{T^{(1)} - T^{(2)}}{\sqrt{2\Delta t - \Delta t}} \right]$$

where $T^{(2)}$ is the unknown temperature. The value for $T^{(1)}$ is obtained from the previous temperature profile. Equation 29 is replaced for the finite differences approximations and the new system of algebraic equations solved for the new T-vector. The rate at the end of the second time increment is found using the new temperature profile and the new saturation distribution.

APPENDIX II

THE COMPUTER PROGRAM

Nomenclature of Computer Input

BCO = λ_{co} = mobility of fluid in cold oil zone, md/Cp

BCW = λ_{cw} = mobility of fluid in cold water zone, md/Cp

CONOB = k_{OB} = overburden thermal conductivity, Btu/ft.hr.°F

CWO = k_{ew} = effective thermal conductivity sand-water system, Btu/ft.hr.°F

CPO = C_{po} = specific heat of oil at constant pressure and average temperature, Btu/lbm°F

CPROCK = C_{pr} = specific heat of sand, Btu/lbm°F

CPW = C_{pw} = specific heat of water at constant pressure and average temperature, Btu/lbm°F

DSCO = ΔS_{co} = $1 - S_{or} - S_{wr}$ = total saturation change in cold oil zone, fraction

DSHW = ΔS_{HW} = $1 - S_{or} - S_{wr}$ = total saturation change in cold water zone, fraction

DIFOB = α_{OB} = overburden diffusivity, $ft^2/hr.$

DPR = ΔP = pressure drop, psi

H = h = permeable sand thickness, ft.

PERM = K = absolute permeability, md

POR = ϕ = porosity, fraction

RH = R_H = "effective radius", ft.

RHW = R_{HW} = radius of cold water zone, ft.

ROI = R_{oi} = initial radius of cold oil zone, ft.

ROO = ρ_o = oil density at average temperature, lbm/ft^3

ROROCK = ρ_r = sand density, lbm/ft^3

ROW = ρ_w = water density at average temperature, lbm/ft^3

RST = R_{ST} = steam zone radius, ft.

SO = S_o = oil saturation, fraction

SOR = S_{or} = residual oil saturation, fraction

SW = S_w = water saturation, fraction

SWC = S_{wc} = connate water saturation, fraction

TI = T_i = initial reservoir temperature, °F

TIMEIN = t_I = combined time of injection and soaking, hr.

TST = T_{ST} = steam temperature, °F

XW = X_w = volumetric fraction of water flowing

XO = X_o = volumetric fraction of oil flowing

Nomenclature of Computer Output

TEMPERATURE PROFILE = temperature at each grid point to count from the wellbore, °F

SOLUTION ERROR = relative error (percent) made in the solution of the matrix for grid point in question

ELEMENT BY ELEMENT RESISTANCE = value of the term $(1/\lambda)\ \ln\ (R_m/R_{m-1})$ for every element, Cp/md

```
PLE NO 1                                FORTRAN SOURCE LIST
      SOURCE STATEMENT

 $IBFTC DECKA   NOLIST,NODECK
  100 FORMAT (4F10.3/3F10.3/3F10.3/3F10.3/4F10.3/2F10.3/5F10.3)
  101 FORMAT (1H 13F10.6)
  102 FORMAT (14X,6F10.3/14X,6F10.3/14X,6F10.3/14X,6F10.3/14X,3F10.3)
  103 FORMAT (8F10.2)
  104 FORMAT (10F8.3)
  105 FORMAT (1H 8F15.3)
  106 FORMAT (2F10.3)
  107 FORMAT (10F8.1)
  108 FORMAT(1HL13X,29HINITIAL BACK PRODUCTION RATE=,F15.2,4H BPD)
  109 FORMAT(14X,32HINCREMENTAL AND TOTAL PRODUCTION,2F10.1)
  110 FORMAT(14X,23HSATURATION DISTRIBUTION/14X,10F6.3)
 1111 FORMAT(1HL13X,15HRESERVOIR AFTER,F10.1,5H DAYS)
  602 FORMAT(14X,19HORIGINAL SATURATION/14X,10F6.3)
  603 FORMAT (14X,23HTOTAL TIME OF INJECTION/14X,10F6.1)
      COMMON M,CLHS,     DTIME,R,PERM,RH,BCO,BCW,H,DPR,DELTAR,TI,RR1,
     1 X(10),Y(10),B(10),SO(10),T(15,150),W(150),NTIME,IXY,GIXY,HIXY
      DIMENSION C1(10),C2(10),C12(10),CCP(10,150),C(10,150),DC(10,150),
     1 PPP(10,150),TIMEIN(10),RTOTME(10),CP(10),CRHS(10),XC1(10),XC2(10)
      READ (5,100) RST,ROI,RHW,RH,SOR,DSHW,DSCO,ROW,ROO,ROROCK,
     1 CPW,CPO,CPROCK,DIFOB,CONOB,TST,TI,XW,XO,DPR,POR,H,BCO,BCW
      READ (5,103) PERM,SWC
      READ (5,104) (SO(I),I=1,10)
      READ (5,106) CWO,COO
      READ(5,107) (TIMEIN(J),J=1,10)
      READ (5,106) DTIME
      WRITE(6,102) RST,ROI,RHW,RH,SOR,DSHW,DSCO,ROW,ROO,ROROCK,CPW,CPO,
     1 CPROCK,DIFOB,CONOB,TST,TI,XW,XO,DPR,POR,H,BCO,BCW,CWO,COO,PERM
      WRITE (6,602) (SO(I),I=1,10)
      WRITE (6,603) (TIMEIN(J),J=1,10)
      VOLHZ=(3.1416*RST**2*POR*H*(1.-SOR-SWC)/5.61)
      CPF=XW*CPW+XO*CPO
      ROF=XW*ROW+XO*ROO
      ROCEPE=ROROCK*CPROCK*(1.-POR)+ROF*CPF*POR
      PR=(5.61*WP)/(3.1416*POR*H*DSCO)
      R=SQRT(ROI**2-PR)
      IF (R.LE.RH) R=RH
      WW=(0.00708*H*DPR)/((1./BCO)*ALOG(330./R)+(1./BCW)*ALOG(R/RHW))
      RR1=0.25
      TIME=DTIME
      DEN=SQRT(3.1416*DIFOB)
    4 RTIME=1./SQRT(TIME)
      CPT=2.*(CONOB/DEN)*RTIME
      DO 50 I=1,10
      RTOTME(I)=1./SQRT(TIME+TIMEIN(I))
      CP(I)=2.*(CONOB/DEN)*((TST-TI)*(RTIME-RTOTME(I))+TI*RTIME)
   50 CRHS(I)=CP(I)/(H*ROCEPE)
      IF (TIME.EQ.2.*DTIME) GO TO 5
      CLHS=CPT/(H*ROCEPE)
      WRITE (6,108)WW
      WI=WW
      WP=WI*DTIME/24.
    9 WF=(0.03720*WW)/(H*POR)
      M=10
      XM=M
```

```
BPIC USERS    NOLIST,NODECK
100 FORMAT (4F10.5/F10.3,4E10.3/E10.3,2E10.3/F10.3/F10.4/5F10.3)
101 FORMAT (1H 8E16.8)
102 FORMAT (1H1,5X,4HTIME,7X,2HRC,8X,4HCONC,7X,3HCRHS,7X,4HCRF1,7X,2HW)
103 FORMAT (5E16.8)
104 FORMAT (10F8.3)
105 FORMAT (1H 3E15.5)
106 FORMAT (1H 7E12.4)
107 FORMAT (10F8.3)
108 FORMAT(1H1,13X,27HCHEMICAL BACK PRODUCTION RATE=,E15.5,4H MP
109 FORMAT(1H0,32HTOTAL AMMONIA AND TOTAL PRODUCTION,2F15.5)
110 FORMAT(1H0,28HCONCENTRATION DISTRIBUTION/1H0,10F8.3)
111 FORMAT(1H0,3X,10HREFERENCE TIME,14X,3H BCS)
200 FORMAT(1H0,15HSTIRRING CONDITION/1H0,10F8.3)
201 FORMAT (1H0,21HINITIAL TIME OF BACK-PRODUCTION,1PE6.4)
   COMMON W,CTRIS   DTIME,W,PHRS,RHO,SCN,RCW,H,DPR,DELTAR,T
  1 (10),CR(10),CRI(10),SO(10),X(10),SC(10),W1(10),RTIME,TI(10),STIR,
  1 CONC,CP(10),CP1(10),CRF1(10),CRF2(10),CRHS(10),CRHT(10),DC(1
  1 FRF(10),(10),TIME(10),ATOMB(10),CP1(10),CRHS(10),CRT(10)
   READ (5,100) RST,ROT,RHO,PH,SCN,CONC,RSCO,DPR,RHC,RMOCX,
  1 DP1,CMO,CRHCX,DTFOB,CONDB,ZST,TI,RR,RC,DPR,POR,H,RCD,REW
   READ (5,103) RCHM,DHC
   READ (5,104) (SO(I),I=1,10)
   READ (5,104) SYN,COC
   READ(5,107) (TIME(I),I=1,10)
   READ (5,103) DCHB
   WRITE(6,102) RST,ROT,RHO,PH,SCN,DPR,DPR,WIN,RSCO,RMOCX,C
  1 CRHCX,DTFOB,CONDB,ZST,TI,X,RC,RR,RCM,H,RCD,RCW,CMO,COD
   WRITE (6,200) (SO(I),I=1,10)
   WRITE (6,201) (TIME(I),I=1,10)
   VCH=(3.14*RHO**2*PH**(1.-COR-COM)/3.6)
   CRF=XX*CP*EXCHO
   SCF=XX*RON*D*DEC
   RDCPRHNOWDCX=CFRDCX*(1.-FCR)+RDRHCPF*WDR
   PR=(3.14*RP)/(1.414*CX*P*RSCO)
   K=SQRT(RCI**2-R*)
   IF (R.LE.RHY C=RH
   WW=(0.007004*H*DPR)/((1./RCO)*ALOG(SD.VR)+(1./RCW)*ALOG(R/
   RRE=0.25
   TIME=DTIME
   DEN=SQRT(3.14*AM*DIFOB)
 4 RTIME=1./SQRT(TIME)
   CRF=2.*(CONCB/DEN)*RTIME
   DO 90 I=1,10
   RTOTME(I)=1./SQRT(TIME*(TIME(I)))
   CRF1(I)=2.*(CONDB/DEN)*((X-1)*TIME-RTDTME(I)*(TI*DTIME)
90 CRHS(I)=CRF1(I)/H*RDCEPC)
   IF (TIME.LE.2.*DTIME) GO TO 5
   CLHS=CRF/(H*RDCEPS)
   WRITE (6,103)WW
   WI=W
```

```
LE NO 1                                    FORTRAN SOURCE LIST DECKA
      SOURCE STATEMENT

      CONO=XW*CWO+XO*COO
      DIAO=CONO/ROCEPE
      XMM=WF*ROF*CPF*POR/ROCEPE
      DELTAR=RH/XM
      Y(1)=(2.*DIAO+XMM)/(DELTAR**2)
      X(1)=Y(1)+1./DTIME
      L=M-1
      XL=L
      DO 1 N=1,L
      XN=N
      RR=XN*DELTAR
      X(N+1)=DIAO/(DELTAR**2)
      Y(N+1)=(DIAO+XMM)/(6.*XN*DELTAR**2)
    1 CONTINUE
      IF (WW.NE.WI) GO TO 10
      OWF=(0.03720*WI)/(H*POR)
      OXMM=OWF*ROF*CPF*POR/ROCEPE
      OCON=CONO
      ODIA=DIAO
      OXM=ODIA/(DELTAR**2)
      OYM=(ODIA+OXMM)/(6.*XL*DELTAR**2)
      B(1)=-TST*1./DTIME
      DO 2 J=2,L
      B(J)=-2.*TST/DTIME-CRHS(J)
    2 CONTINUE
      B(M)=(2.*OYM+OXM-(2./DTIME))*TST-(OXM+2.*OYM)*(TST+TI)/2.-(X(M)+2.
     1*Y(M))*TI-CRHS(M)
      NTIME=1
      IXY=1
      GIXY=0.
      HIXY=0.
      RIXY=DTIME/24.
      WRITE (6,1111) RIXY
      CALL TEMP
      CALL RATE
      WP=WP+(WI+W(1))*DTIME/24./2.
      WW=W(IXY)
   11 ROF=XW*ROW+XO*ROO
      CPF=XW*CPW+XO*CPO
      ROCEPE=ROROCK*CPROCK*(1.-POR)+ROF*CPF*POR
      PR=(5.61*WP)/(3.1416*POR*H*DSCO)
      ENDCW=ROI**2-PR
      IF(ENDCW.LT.0.)GO TO 143
      R=SQRT(ENDCW)
      IF(R.GT.RH)GO TO 44
  143 R=RH
   44 IF (WW.LT.W(1)) GO TO 12
      DO 3 J=2,M
      XC1(J)=CP(J)-CPT*T(J,NTIME)
      C1(J)=XC1(J)/ROCEPE
    3 CONTINUE
      TIME=2.*DTIME
      GO TO 4
    5 DO 6 J=2,M
      XC2(J)=CP(J)+CPT*(SQRT(2.)-1.)*T(J,NTIME)/SQRT(2.)
```

```
LE NO 1                                    FORTRAN SOURCE LIST DECKA
      SOURCE STATEMENT

    6 C2(J)=XC2(J)/ROCEPE
      DO 7 J=2,M
      C12(J)=C1(J)+C2(J)
    7 CONTINUE
      CLHS=CPT/ROCEPE
      B(1)=-Y(1)*T(2,NTIME)+(Y(1)-1./DTIME)*T(1,NTIME)
      B(2)=-(X(2)-2.*Y(2))*T(1,NTIME)-(2./DTIME-2.*X(2)-3.*Y(2))*
     1 T(2,NTIME)-(X(2)+6.*Y(2))*T(3,NTIME)+Y(2)*T(4,NTIME)-C12(2)
      DO 8 J=3,M
      B(J)=-Y(J)*T(J-2,NTIME)-(X(J)-6.*Y(J))*T(J-1,NTIME)-(2./DTIME-
     1 2.*X(J)+3.*Y(J))*T(J,NTIME)-(X(J)+2.*Y(J))*T(J+1,NTIME)-C12(J)
    8 CONTINUE
      GO TO 9
   10 B(M)=B(M)-(X(M)+2.*Y(M))*T(M+1,NTIME)
      NTIME=NTIME+1
      IXY=IXY+1
      FIXY=IXY
      RIXY=DTIME*FIXY/24.
      IF (HIXY.EQ.GIXY) WRITE (6,1111)RIXY
      IF (IXY.EQ.150) GO TO 32
      CALL TEMP
      IF (T(7,NTIME).LE.TI) GO TO 32
      IF (ABS(T(8,NTIME)-TI).LE.2.) GO TO 39
      IF (ABS(T(9,NTIME)-TI).LE.2.) GO TO 40
      IF (ABS(T(10,NTIME)-TI).LE.2.) GO TO 41
   43 CALL RATE
      DWP=(W(NTIME-1)+W(NTIME))*DTIME/(2.*24.)
      WP=WP+DWP
      IF (HIXY.EQ.GIXY) WRITE (6,109)DWP,WP
      IF ((WP.GE.1535.).AND.(WP.LT.3311.)) GO TO 77
      IF ((WP.GE.3311.).AND.(WP.LT.4856.)) GO TO 33
      IF ((WP.GE.4856.).AND.(WP.LT.6176.)) GO TO 24
      IF ((WP.GE.6176.).AND.(WP.LT.8085.)) GO TO 28
      IF ((WP.GE.8085.).AND.(WP.LT.8562.)) GO TO 29
      IF ((WP.GE.8562.).AND.(WP.LT.9158.))SO(3)=.49
      IF ((WP.GE.9158.).AND.(WP.LT.9515.)) SO(2)=.49
      IF ((WP.GE.9515.).AND.(WP.LT.10177.)) GO TO 30
      IF ((WP.GE.10177.).AND.(WP.LT.11497.)) GO TO 34
      IF ((WP.GE.11497.).AND.(WP.LT.12569.)) GO TO 35
      IF ((WP.GE.12569.).AND.(WP.LT.14002.)) GO TO 36
      IF ((WP.GE.14002.).AND.(WP.LT.14479.)) GO TO 205
      IF ((WP.GE.14479.).AND.(WP.LT.14836.)) SO(2)=.69
      IF ((WP.GE.14836.).AND.(WP.LT.16337.)) GO TO 206
      IF ((WP.GE.16337.).AND.(WP.LT.27316.)) GO TO 207
      IF ((WP.GE.27316.).AND.(WP.LT.31107.)) GO TO 114
      IF ((WP.GE.31107.).AND.(WP.LT.33972.)) GO TO 300
      IF ((WP.GE.33972.).AND.(WP.LT.35881.)) GO TO 302
      IF ((WP.GE.35881.).AND.(WP.LT.36884.)) GO TO 304
      IF (WP.GE.36834.) GO TO  307
   27 WW=W(IXY)
      XO=1.-XW
      IF (HIXY.EQ.GIXY) WRITE (6,110) (SO(I),I=1,M)
      GO TO 11
   12 CLHS=CPT/ROCEPE
      LL=NTIME+1
```

```
LE NO 1                                  FORTRAN SOURCE LIST DECKA
      SOURCE STATEMENT

      DO 22 JJ=NTIME,LL
      XJJ=JJ
      DO 21 J=2,M
      CCP(J,JJ)=CLHS*((TST-TI)*(1./SQRT(XJJ)-SQRT(DTIME)/SQRT(XJJ*DTIME+
     1 TIMEIN(J)))+TI/SQRT(XJJ))
      CC=0.
      DO 18 N=2,NTIME
      K=LL-N
      XNN=N
      CC=CC+CLHS*(SQRT(XNN)-SQRT(XNN-1.))*T(J,K)/SQRT(XNN*(XNN-1.))
   18 CONTINUE
   21 C(J,JJ)=CCP(J,JJ)+CC
   22 CONTINUE
      DO 23 I=2,M
      PPP(I,NTIME)=C(I,NTIME)-CLHS*T(I,NTIME)
   23 DC(I,NTIME)=PPP(I,NTIME)+C(I,LL)
   25 B(1)=-Y(1)*T(2,NTIME)+(Y(1)-1./DTIME)*T(1,NTIME)
      B(2)=-(X(2)-2.*Y(2))*T(1,NTIME)-(2./DTIME-2.*X(2)-3.*Y(2))*
     1 T(2,NTIME)-(X(2)+6.*Y(2))*T(3,NTIME)+Y(2)*T(4,NTIME)-DC(2,NTIME)
      DO 26 J=3,M
      B(J)=-Y(J)*T(J-2,NTIME)-(X(J)-6.*Y(J))*T(J-1,NTIME)-(2./DTIME-
     1 2.*X(J)+3.*Y(J))*T(J,NTIME)-(X(J)+2.*Y(J))*T(J+1,NTIME)-
     2 DC(J,NTIME)
   26 CONTINUE
      GO TO 9
   77 SO(9)=.49
      XW=.841
      GO TO 27
   33 SO(8)=.49
      SO(9)=.49
      XW=.78
      GO TO 27
   24 DO 79 I=7,9
   79 SO(I)=.49
      SO(10)=.69
      XW=.671
      GO TO 27
   28 DO 80 I=6,8
   80 SO(I)=.49
      SO(9)=.69
      XW=.627
      GO TO 27
   29 DO 81 I=4,7
   81 SO(I)=.49
      DO 82 I=8,10
   82 SO(I)=.69
      XW=.44
      GO TO 27
   30 DO 83 I=1,7
   83 SO(I)=.49
      DO 84 I=8,10
   84 SO(I)=.69
      XW=.404
      GO TO 27
   34 DO 112 I=1,6
```

'LE NO 1 FORTRAN SOURCE LIST DECKA

```
      SOURCE STATEMENT

  112 SO(I)=.49
      DO 113 I=7,10
  113 SO(I)=.69
      XW=.371
      GO TO 27
   35 DO 115 I=1,5
  115 SO(I)=.49
      DO 116 I=6,10
  116 SO(I)=.69
      XW=.326
      GO TO 27
   36 DO 117 I=1,4
  117 SO(I)=.49
      DO 118 I=5,10
  118 SO(I)=.69
      XW=.293
      GO TO 27
  205 DO 120 I=3,10
  120 SO(I)=.69
      XW=.247
      GO TO 27
  206 DO 122 I=1,10
  122 SO(I)=.69
      XW=.219
      GO TO 27
  207 SO(10)=.82
      XW=.209
      GO TO 27
  114 DO 119 I=8,10
  119 SO(I)=.82
      XW=.116
      GO TO 27
  300 DO 301 I=6,10
  301 SO(I)=.82
      XW=.065
      GO TO 27
  302 DO 303 I=4,10
  303 SO(I)=.82
      XW=.021
      GO TO 27
  304 DO 305 I=2,10
  305 SO(I)=.82
      XW=0.0
      GO TO 27
  307 DO 308 I=1,10
  308 SO(I)=.82
      XW=0.0
      GO TO 27
   39 DO 201 I=8,10
  201 T(I,NTIME)=TI
      M=7
      GO TO 43
   40 DO 202 I=9,10
  202 T(I,NTIME)=TI
      M=8
```

```
LE NO 1                                  FORTRAN SOURCE LIST DECKA
     SOURCE STATEMENT

        GO TO 43
    41  T(10,NTIME)=TI
        M=9
        GO TO 43
    32  CALL EXIT
        END
```

```
LE NO 1                                  FORTRAN SOURCE LIST
      SOURCE STATEMENT

$IBFTC SOLUT   NOLIST,NODECK
       SUBROUTINE TEMP
  199 FORMAT (1H 13F10.6)
  200 FORMAT (14X,19HTEMPERATURE PROFILE/14X,11F6.1)
  201 FORMAT (14X,14HSOLUTION ERROR/14X,10F6.3)
       COMMON M,CLHS,     DTIME,R,PERM,RH,BCO,BCW,H,DPR,DELTAR,TI,RR1,
      1 X(10),Y(10),B(10),SO(10),T(15,150),W(150),NTIME,IXY
       DIMENSION ERROR(10)
       DOUBLE PRECISION A(10,10),AA(10,10),BB(10),XQT(10),TE(11,150),
      1 DIF(10),PCENT(10),AL(10,10),AM(10,10),AU(10,10),AV(10,10),XIS,
      2 VALUE,ZX,ZXX,ZV,ZW,ZQ,ZR,BOB
       DO 10 J=1,10
       DO 10 I=1,10
   10 A(I,J)=0.
       A(1,1)=-X(1)
       A(2,1)=X(2)-2.*Y(2)
       A(3,1)=Y(3)
       A(1,2)=Y(1)
       A(2,2)=-2./DTIME-2.*X(2)-3.*Y(2)-CLHS
       A(3,2)=X(3)-6.*Y(3)
       A(4,2)=Y(4)
       A(2,3)=X(2)+6.*Y(2)
       A(3,3)=-2./DTIME-2.*X(3)+3.*Y(3)-CLHS
       A(4,3)=X(4)-6.*Y(4)
       A(5,3)=Y(5)
       A(2,4)=-Y(2)
       A(3,4)=X(3)+2.*Y(3)
       A(4,4)=-2./DTIME-2.*X(4)+3.*Y(4)-CLHS
       A(5,4)=X(5)-6.*Y(5)
       A(6,4)=Y(6)
       LL=M-3
       DO 5 I=4,LL
       A(I,I+1)=X(I)+2.*Y(I)
       A(I+1,I+1)=-2./DTIME-2.*X(I+1)+3.*Y(I+1)-CLHS
       A(I+2,I+1)=X(I+2)-6.*Y(I+2)
       A(I+3,I+1)=Y(I+3)
    5 CONTINUE
       A(M-2,M-1)=X(M-2)+2.*Y(M-2)
       A(M-1,M-1)=-2./DTIME-2.*X(M-1)+3.*Y(M-1)-CLHS
       A(M,M-1)=X(M)-6.*Y(M)
       A(M-1,M)=X(M-1)+2.*Y(M-1)
       A(M,M)=-2./DTIME-2.*X(M)+3.*Y(M)-CLHS
       DO 7 J=1,M
       DO 7 I=1,M
    7 AA(I,J)=A(I,J)
       DO 8 I=1,M
    8 BB(I)=B(I)
       DO 13 I=1,M
   13 XQT(I)=B(I)
C      CALCULATION OF L AND U
       DO 105 K=2,M
       KK=K-1
       DO 104 J=1,KK
       AL(J,K)=0.0
       AM(J,K)=0.0
```

```
'LE NO 1                                    FORTRAN SOURCE LIST SOLUT
      SOURCE STATEMENT

      AU(K,J)=0.0
  104 AV(K,J)=0.0
  105 CONTINUE
      IF(A(1,1).EQ.0.) GO TO 150
  106 XIS=ABS(A(1,1))
      AL(1,1)=SQRT(XIS)
      AU(1,1)=A(1,1)/AL(1,1)
      DO 107 J=2,M
      AU(1,J)=A(1,J)/AL(1,1)
  107 AL(J,1)=A(J,1)/AU(1,1)
      DO 115 K=2,M
      KK=K-1
      VALUE=0.0
      DO 108 J=1,KK
  108 VALUE=VALUE+AL(K,J)*AU(J,K)
      ZX=A(K,K)-VALUE
      IF(ZX.EQ.0.) GO TO 150
  109 ZXX=ABS(ZX)
      AL(K,K)=SQRT(ZXX)
      AU(K,K)=ZX/AL(K,K)
      KP=K+1
      KK=K-1
      IF(KP.GT.M ) GO TO 115
      DO 112 I=KP,M
      ZV=0.0
      ZW=0.0
      DO 110 LP=1,KK
      ZV=ZV+AL(K,LP)*AU(LP,I)
  110 ZW=ZW+AL(I,LP)*AU(LP,K)
      AU(K,I)=(A(K,I)-ZV)/AL(K,K)
  112 AL(I,K)=(A(I,K)-ZW)/AU(K,K)
  115 CONTINUE
C     L AND U ARE CALCULATED
C     PROCEEDING TO CALCULATE L-INVERSE AND U-INVERSE
      DO 119 K=1,M
      AM(K,K)=1.0/AL(K,K)
  119 AV(K,K)=1.0/AU(K,K)
      DO 125 K=2,M
      KK=K-1
      DO 122 J=1,KK
      ZQ=0.0
      DO 120 L=J,KK
  120 ZQ=ZQ+AL(K,L)*AM(L,J)
  122 AM(K,J)=-ZQ/AL(K,K)
  125 CONTINUE
      IJN=M+1
      DO 135 KL=1,IJN
      K=IJN-KL
      IF(K.LE.1) GO TO 136
  126 DO 130 JK=1,K
      J=K-JK
      IF(J.LT.1) GO TO 135
  127 ZR=0.0
      JP=J+1
      DO 128 L=JP,K
```

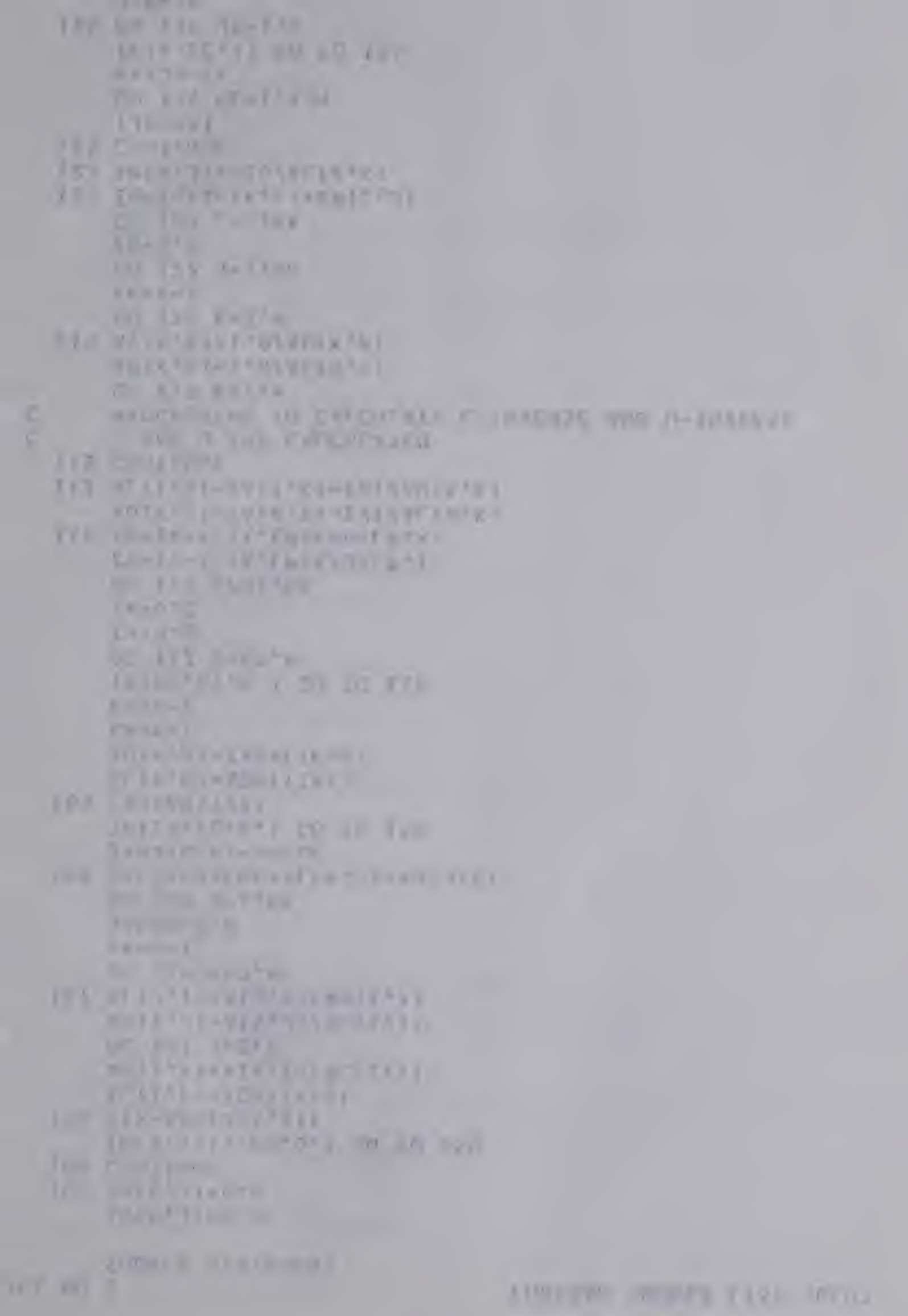

```
PLE NO 1                                    FORTRAN SOURCE LIST SOLUT
      SOURCE STATEMENT

  128 ZR=ZR+AU(J,L)*AV(L,K)
  130 AV(J,K)=-ZR/AU(J,J)
  135 CONTINUE
C     PROCEEDING TO CALCULATE G-INVERSE=U-INVERSE*L-INVERSE
  136 DO 140 K=1,M
      DO 140 J=1,M
      A(J,K)=0.0
      DO 137 L=1,M
  137 A(J,K)=A(J,K)+AV(J,L)*AM(L,K)
  140 CONTINUE
      GO TO 152
  150 WRITE(6,151)
  151 FORMAT(1H ,29H THE METHOD IS NOT APPLICABLE)
  152 CONTINUE
      DO 153 I=1,M
      TE(I,NTIME)=0.
      DO 153 J=1,M
  153 TE(I,NTIME)=TE(I,NTIME)+A(I,J)*XQT(J)
      DO 14 I=1,IJN
   14 T(I,NTIME)=SNGL(TE(I,NTIME))
      T(M+1,NTIME)=TI
      WRITE (6,200) (T(I,NTIME),I=1,IJN)
      DO 9 J=1,M
      BOB=0.
      DO 12 I=1,M
   12 BOB=BOB+AA(J,I)*TE(I,NTIME)
      DIF(J)=BB(J)-BOB
      PCENT(J)=DIF(J)*100./BB(J)
    9 CONTINUE
      DO 15 J=1,M
   15 ERROR(J)=SNGL(PCENT(J))
      WRITE (6,201) (ERROR(J),J=1,M)
  202 RETURN
      END
```

```
LE NO 1                                  FORTRAN SOURCE LIST
      SOURCE STATEMENT

$IBFTC NINAL   NOLIST,NODECK
      SUBROUTINE RATE
  200 FORMAT (1H 13F10.6)
 5000 FORMAT (1X,13F6.1/5F6.1)
 5001 FORMAT (2X,18F4.2)
 5002 FORMAT (1X,7F10.3)
 5003 FORMAT (1X,1F5.3,12F6.2/5F6.2)
 5004 FORMAT(14X,4HRATE,F10.1)
 5005 FORMAT(14X,29HELEMENT BY ELEMENT RESISTANCE/14X,10F6.3)
      COMMON M,CLHS,     DTIME,R,PERM,RH,BCO,BCW,H,DPR,DELTAR,TI,RR1,
     1 X(10),Y(10),B(10),SO(10),T(15,150),W(150),NTIME,IXY,GIXY,HIXY
      DIMENSION TA(20),SW(20),VISCO1(20),VISW(20),BCHW(20),BBC(20)
      PWMAX=(1./BCO)*ALOG(330./R)+(1./BCW)*ALOG(R/RH)
      XM=M
      T(M+1,NTIME)=TI
      DO 1 J=1,M
      IJ=M+1-J
      SW(IJ)=1.-SO(IJ)
      XKRO=-0.69201835E-01+0.12099786E+01*SO(IJ)-0.86392291E+01*SO(IJ)**
     1 2+0.28682803E+02*SO(IJ)**3-0.43337840E+02*SO(IJ)**4+0.30396180E+
     2 02*SO(IJ)**5-0.64854211E+01*SO(IJ)**6
      XKRW=-0.48834803E-01+0.78113385E+00*SW(IJ)-0.46846743E+01*SW(IJ)**
     1 2+0.12766994E+02*SW(IJ)**3-0.12893017E+02*SW(IJ)**4+0.35564310E+
     2 01*SW(IJ)**5+0.15006140E+01*SW(IJ)**6
      TA(IJ)=(T(IJ+1,NTIME)+T(IJ,NTIME))/2.
      POLYVO=-0.65019612E+00+0.44799295E+03*1./TA(IJ)+0.75749706E+03*
     1 1./TA(IJ)**2-0.60803823E+07*1./TA(IJ)**3+0.59698224E+09*1./TA(IJ)
     2 **4-0.18164653E+11*1./TA(IJ)**5
      VISCO1(IJ)=EXP(2.30258509*POLYVO)
  503 XMOBO=XKRO*PERM/VISCO1(IJ)
      VISWA=.55556*TA(IJ)-26.2128
      VISWB=VISWA**2
      VISWC=8078.4+VISWB
      VISWD=VISWA+SQRT(VISWC)
      DENVIS=2.1482*VISWD-120.
      VISW(IJ)=100./DENVIS
      XMOBW=XKRW*PERM/VISW(IJ)
      BCHW(IJ)=XMOBO+XMOBW
      BBC(IJ)=1./BCHW(IJ)
      IF (BBC(IJ).LE.0.001)GO TO 504
    1 CONTINUE
  504 IX=IJ-1
      IF (IX.EQ.0 ) GO TO 506
      DO 77 K=1,IX
   77 BBC(K)=0.
  506 WA=PWMAX+BBC(1)*ALOG(DELTAR/RR1)
      WC=0.
      DO 66 N=2,M
      XN=N
      WB=BBC(N)*ALOG(XN/(XN-1.))
      WC=WC+WB
   66 CONTINUE
      WD=WA+WC
      W(IXY) =(.00708*H*DPR)/WD
      IF (HIXY.NE.GIXY) GO TO 50
```

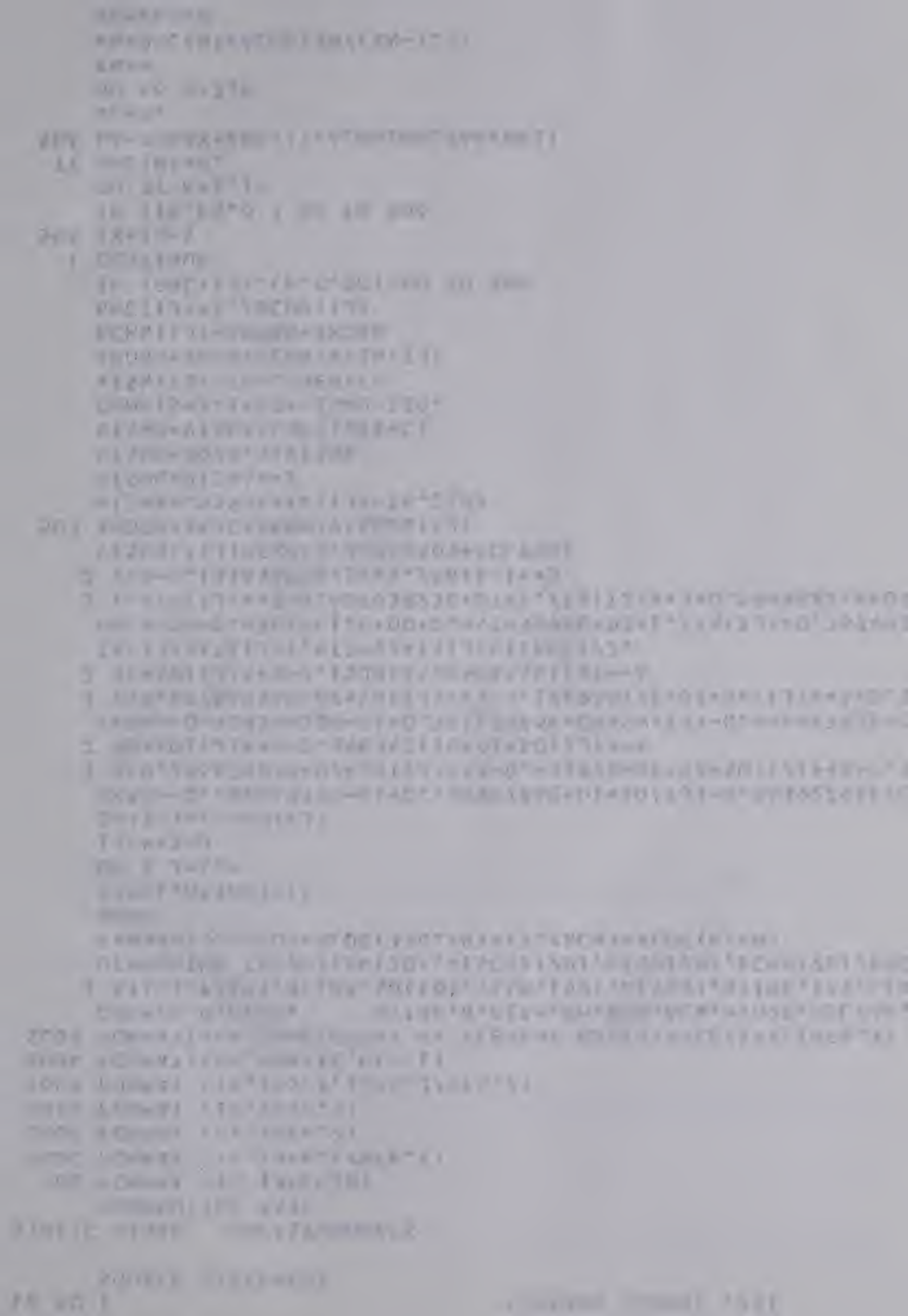

```
PLE NO 1                                   FORTRAN SOURCE LIST NINAL
      SOURCE STATEMENT

      WRITE (6,5004) W(IXY)
      WRITE (6,5005) (BBC(IJ),IJ=1,M)
   50 RETURN
      END
```

```
150052 EXAMPLE NO 1                                IBLDR -- JOB   LEAL

CT PROGRAM IS BEING ENTERED INTO STORAGE.
          63.000   131.500    80.750    71.900     0.260     0.560
           0.645    52.280    51.450   140.000     1.030     0.500
           0.230     0.031     1.090   530.000    95.000     0.913
           0.087   400.000     0.266    25.000     6.120    14.392
           1.700     1.200   612.000
     ORIGINAL SATURATION
      0.200 0.200 0.200 0.200 0.200 0.200 0.200 0.200 0.200 0.540
     TOTAL TIME OF INJECTION
      720.0 710.0 690.0 660.0 620.0 560.0 485.0 400.0 285.0 145.0

     INITIAL BACK PRODUCTION RATE=          384.31 BPD

     RESERVOIR AFTER        4.0 DAYS
     TEMPERATURE PROFILE
      526.6 524.5 524.8 524.4 524.3 524.1 523.7 522.9 519.3 478.6  95.0
     SOLUTION ERROR
     -0.000 0.000 0.000 0.000 0.000 0.000 0.000-0.000 0.000-0.000
     RATE      367.3
     ELEMENT BY ELEMENT RESISTANCE
      0.000 0.000 0.000 0.000 0.000 0.000 0.000 0.000 0.000 0.004

     RESERVOIR AFTER        8.0 DAYS
     TEMPERATURE PROFILE
      462.9 424.3 427.2 421.7 417.6 410.1 399.4 384.0 353.4 275.1  95.0
     SOLUTION ERROR
     -0.000 0.000 0.000 0.000 0.000 0.000 0.000 0.000 0.000 0.000
     RATE      359.9
     ELEMENT BY ELEMENT RESISTANCE
      0.000 0.000 0.000 0.000 0.000 0.000 0.000 0.000 0.001 0.007
     INCREMENTAL AND TOTAL PRODUCTION    1454.3     4494.7
     SATURATION DISTRIBUTION
      0.200 0.200 0.200 0.200 0.200 0.200 0.200 0.490 0.490 0.540

     RESERVOIR AFTER       12.0 DAYS
     TEMPERATURE PROFILE
      381.1 366.5 370.6 363.9 361.2 354.8 346.2 333.5 308.6 249.4  95.0
     SOLUTION ERROR
      0.000-0.000 0.000 0.000 0.000 0.000 0.000 0.000-0.000 0.000
     RATE      355.2
     ELEMENT BY ELEMENT RESISTANCE
      0.000 0.000 0.000 0.000 0.000 0.000 0.001 0.003 0.003 0.008
     INCREMENTAL AND TOTAL PRODUCTION    1430.1     5924.9
     SATURATION DISTRIBUTION
      0.200 0.200 0.200 0.200 0.200 0.200 0.490 0.490 0.490 0.690
```

```
RESERVOIR AFTER       16.0 DAYS
TEMPERATURE PROFILE
 354.1 350.2 350.4 344.4 341.4 334.1 324.5 310.5 283.9 224.0  95.0
SOLUTION ERROR
 0.000-0.000 0.000 0.000 0.000 0.000 0.000 0.000 0.000 0.000
RATE      346.6
ELEMENT BY ELEMENT RESISTANCE
 0.000 0.000 0.000 0.000 0.000 0.001 0.003 0.003 0.004 0.032
INCREMENTAL AND TOTAL PRODUCTION     1403.6     7328.5
SATURATION DISTRIBUTION
 0.200 0.200 0.200 0.200 0.200 0.490 0.490 0.490 0.690 0.690


RESERVOIR AFTER       20.0 DAYS
TEMPERATURE PROFILE
 338.9 331.6 331.7 326.2 323.0 315.6 306.0 292.0 265.7 209.6  95.0
SOLUTION ERROR
-0.000-0.000 0.000 0.000 0.000 0.000 0.000 0.000 0.000 0.000
RATE      339.5
ELEMENT BY ELEMENT RESISTANCE
 0.000 0.000 0.000 0.000 0.001 0.003 0.003 0.003 0.017 0.034
INCREMENTAL AND TOTAL PRODUCTION     1372.3     8700.8
SATURATION DISTRIBUTION
 0.200 0.200 0.490 0.200 0.200 0.490 0.490 0.490 0.690 0.690


RESERVOIR AFTER       24.0 DAYS
TEMPERATURE PROFILE
 323.1 318.5 318.3 312.8 309.5 302.0 292.3 278.2 252.1 198.2  95.0
SOLUTION ERROR
 0.000-0.000 0.000 0.000 0.000 0.000 0.000 0.000 0.000 0.000
RATE      335.6
ELEMENT BY ELEMENT RESISTANCE
 0.000 0.000 0.000 0.000 0.001 0.003 0.003 0.003 0.018 0.037
INCREMENTAL AND TOTAL PRODUCTION     1350.3    10051.1
SATURATION DISTRIBUTION
 0.490 0.490 0.490 0.490 0.490 0.490 0.490 0.690 0.690 0.690


RESERVOIR AFTER       28.0 DAYS
TEMPERATURE PROFILE
 311.6 307.0 306.5 301.3 297.9 290.4 280.7 266.7 241.2 189.9  95.0
SOLUTION ERROR
-0.000-0.000 0.000 0.000 0.000 0.000 0.000 0.000 0.000-0.000
RATE      309.8
ELEMENT BY ELEMENT RESISTANCE
 0.003 0.003 0.003 0.003 0.003 0.003 0.003 0.015 0.020 0.038
INCREMENTAL AND TOTAL PRODUCTION     1290.8    11341.8
SATURATION DISTRIBUTION
 0.490 0.490 0.490 0.490 0.490 0.490 0.690 0.690 0.690 0.690
```

```
RESERVOIR AFTER       60.0 DAYS
TEMPERATURE PROFILE
 257.7 254.8 253.8 249.6 246.1 239.3 230.6 218.2 196.7 157.6  95.0
SOLUTION ERROR
-0.000 0.000 0.000 0.000 0.000 0.000 0.000 0.000 0.000 0.000
RATE      223.3
ELEMENT BY ELEMENT RESISTANCE
 0.015 0.015 0.015 0.015 0.016 0.017 0.018 0.021 0.027 0.105
INCREMENTAL AND TOTAL PRODUCTION      899.9   19725.7
SATURATION DISTRIBUTION
 0.690 0.690 0.690 0.690 0.690 0.690 0.690 0.690 0.690 0.820


RESERVOIR AFTER       64.0 DAYS
TEMPERATURE PROFILE
 253.5 250.8 249.6 245.6 242.1 235.4 226.8 214.6 193.4 155.4  95.0
SOLUTION ERROR
 0.000 0.000 0.000 0.000 0.000 0.000 0.000 0.000 0.000 0.000
RATE      220.1
ELEMENT BY ELEMENT RESISTANCE
 0.015 0.015 0.015 0.016 0.017 0.017 0.019 0.022 0.028 0.108
INCREMENTAL AND TOTAL PRODUCTION      886.8   20612.5
SATURATION DISTRIBUTION
 0.690 0.690 0.690 0.690 0.690 0.690 0.690 0.690 0.690 0.820


RESERVOIR AFTER       68.0 DAYS
TEMPERATURE PROFILE
 249.5 247.0 245.8 241.8 238.4 231.8 223.3 211.2 190.5 153.3  95.0
SOLUTION ERROR
-0.000-0.000 0.000 0.000 0.000 0.000 0.000 0.000 0.000 0.000
RATE      217.0
ELEMENT BY ELEMENT RESISTANCE
 0.015 0.016 0.016 0.016 0.017 0.018 0.019 0.022 0.029 0.110
INCREMENTAL AND TOTAL PRODUCTION      874.2   21486.7
SATURATION DISTRIBUTION
 0.690 0.690 0.690 0.690 0.690 0.690 0.690 0.690 0.690 0.820


RESERVOIR AFTER       72.0 DAYS
TEMPERATURE PROFILE
 245.8 243.4 242.3 238.4 235.0 228.5 220.1 208.2 187.8 151.5  95.0
SOLUTION ERROR
-0.000-0.000 0.000 0.000 0.000 0.000 0.000 0.000 0.000 0.000
RATE      214.1
ELEMENT BY ELEMENT RESISTANCE
 0.016 0.016 0.016 0.017 0.017 0.018 0.020 0.023 0.029 0.112
INCREMENTAL AND TOTAL PRODUCTION      862.1   22348.9
SATURATION DISTRIBUTION
 0.690 0.690 0.690 0.690 0.690 0.690 0.690 0.690 0.690 0.820
```

```
RESERVOIR AFTER       80.0 DAYS
TEMPERATURE PROFILE
 239.2 237.1 235.9 232.1 228.8 222.5 214.3 202.7 182.9 148.1  95.0
SOLUTION ERROR
 0.000 0.000 0.000 0.000 0.000 0.000-0.000 0.000 0.000 0.000
RATE      208.4
ELEMENT BY ELEMENT RESISTANCE
 0.017 0.017 0.017 0.018 0.018 0.019 0.021 0.024 0.030 0.115
INCREMENTAL AND TOTAL PRODUCTION      839.2   24038.6
SATURATION DISTRIBUTION
 0.690 0.690 0.690 0.690 0.690 0.690 0.690 0.690 0.690 0.820


RESERVOIR AFTER       84.0 DAYS
TEMPERATURE PROFILE
 236.2 234.2 233.0 229.3 226.0 219.7 211.7 200.2 180.7 146.6  95.0
SOLUTION ERROR
-0.000-0.000 0.000 0.000 0.000 0.000 0.000 0.000 0.000 0.000
RATE      205.7
ELEMENT BY ELEMENT RESISTANCE
 0.017 0.017 0.017 0.018 0.019 0.020 0.021 0.024 0.031 0.117
INCREMENTAL AND TOTAL PRODUCTION      828.2   24866.8
SATURATION DISTRIBUTION
 0.690 0.690 0.690 0.690 0.690 0.690 0.690 0.690 0.690 0.820


RESERVOIR AFTER       88.0 DAYS
TEMPERATURE PROFILE
 233.4 231.5 230.3 226.6 223.3 217.2 209.2 197.9 178.7 145.3  95.0
SOLUTION ERROR
 0.000-0.000 0.000 0.000 0.000 0.000 0.000 0.000 0.000 0.000
RATE      203.1
ELEMENT BY ELEMENT RESISTANCE
 0.017 0.018 0.018 0.018 0.019 0.020 0.022 0.025 0.031 0.119
INCREMENTAL AND TOTAL PRODUCTION      817.6   25684.4
SATURATION DISTRIBUTION
 0.690 0.690 0.690 0.690 0.690 0.690 0.690 0.690 0.690 0.820


RESERVOIR AFTER       92.0 DAYS
TEMPERATURE PROFILE
 230.7 228.9 227.7 224.1 220.9 214.8 206.9 195.7 176.8 144.0  95.0
SOLUTION ERROR
-0.000-0.000 0.000 0.000 0.000 0.000 0.000 0.000 0.000 0.000
RATE      200.5
ELEMENT BY ELEMENT RESISTANCE
 0.018 0.018 0.018 0.019 0.019 0.020 0.022 0.025 0.032 0.120
INCREMENTAL AND TOTAL PRODUCTION      807.1   26491.5
SATURATION DISTRIBUTION
 0.690 0.690 0.690 0.690 0.690 0.690 0.690 0.690 0.690 0.820
```

```
RESERVOIR AFTER      572.0 DAYS
TEMPERATURE PROFILE
 152.1 151.8 151.0 149.5 147.6 144.5 140.4 134.5 125.3 111.6  95.0
SOLUTION ERROR
-0.000 0.000 0.000 0.000 0.000 0.000 0.000 0.000 0.000 0.000
RATE      106.9
ELEMENT BY ELEMENT RESISTANCE
 0.068 0.068 0.070 0.072 0.075 0.079 0.086 0.099 0.122 0.168
INCREMENTAL AND TOTAL PRODUCTION      428.0   89665.2
SATURATION DISTRIBUTION
 0.820 0.820 0.820 0.820 0.820 0.820 0.820 0.820 0.820 0.820


RESERVOIR AFTER      576.0 DAYS
TEMPERATURE PROFILE
 151.9 151.6 150.8 149.3 147.4 144.4 140.3 134.4 125.2 111.6  95.0
SOLUTION ERROR
 0.000-0.000 0.000 0.000 0.000 0.000 0.000 0.000 0.000 0.000
RATE      106.7
ELEMENT BY ELEMENT RESISTANCE
 0.068 0.069 0.070 0.072 0.075 0.079 0.087 0.099 0.123 0.168
INCREMENTAL AND TOTAL PRODUCTION      427.2   90092.4
SATURATION DISTRIBUTION
 0.820 0.820 0.820 0.820 0.820 0.820 0.820 0.820 0.820 0.820


RESERVOIR AFTER      580.0 DAYS
TEMPERATURE PROFILE
 151.7 151.4 150.6 149.1 147.2 144.2 140.1 134.2 125.1 111.5  95.0
SOLUTION ERROR
 0.000-0.000 0.000 0.000 0.000 0.000 0.000 0.000 0.000 0.000
RATE      106.5
ELEMENT BY ELEMENT RESISTANCE
 0.068 0.069 0.070 0.072 0.075 0.080 0.087 0.099 0.123 0.168
INCREMENTAL AND TOTAL PRODUCTION      426.4   90518.8
SATURATION DISTRIBUTION
 0.820 0.820 0.820 0.820 0.820 0.820 0.820 0.820 0.820 0.820


RESERVOIR AFTER      584.0 DAYS
TEMPERATURE PROFILE
 151.5 151.2 150.4 148.9 147.0 144.0 139.9 134.1 125.0 111.4  95.0
SOLUTION ERROR
 0.000-0.000 0.000 0.000 0.000 0.000 0.000 0.000 0.000 0.000
RATE      106.3
ELEMENT BY ELEMENT RESISTANCE
 0.068 0.069 0.070 0.072 0.075 0.080 0.087 0.099 0.123 0.168
INCREMENTAL AND TOTAL PRODUCTION      425.6   90944.4
SATURATION DISTRIBUTION
 0.820 0.820 0.820 0.820 0.820 0.820 0.820 0.820 0.820 0.820
```

```
150052 EXAMPLE NO 2                                    IBLDR -- JOB   LEAL

OBJECT PROGRAM IS BEING ENTERED INTO STORAGE.
          42.790   118.800    61.730    52.250     0.230     0.260
           0.545    60.130    50.320   140.000     1.013     0.500
           0.230     0.042     1.500   445.000    74.000     0.765
           0.235  1600.000     0.362    10.000     0.945    54.945
           1.700     1.200  3000.000
     ORIGINAL SATURATION
      0.200 0.200 0.200 0.200 0.200 0.200 0.200 0.200 0.370 0.370
     TOTAL TIME OF INJECTION
      720.0 710.0 690.0 660.0 620.0 560.0 485.0 400.0 285.0 145.0


     INITIAL BACK PRODUCTION RATE=          103.64 BPD


     RESERVOIR AFTER        4.0 DAYS
     TEMPERATURE PROFILE
      436.7 432.6 433.2 432.4 432.2 431.6 430.7 429.0 422.7 375.4  74.0
     SOLUTION ERROR
      0.000 0.000 0.000 0.000 0.000 0.000-0.000 0.000-0.000 0.000
     RATE      103.3
     ELEMENT BY ELEMENT RESISTANCE
      0.000 0.000 0.000 0.000 0.000 0.000 0.000 0.000 0.000 0.000


     RESERVOIR AFTER        8.0 DAYS
     TEMPERATURE PROFILE
      373.9 347.5 349.5 344.4 340.7 333.7 323.7 309.1 279.2 207.2  74.0
     SOLUTION ERROR
     -0.000-0.000 0.000 0.000 0.000 0.000 0.000 0.000 0.000 0.000
     RATE      100.7
     ELEMENT BY ELEMENT RESISTANCE
      0.000 0.000 0.000 0.000 0.000 0.000 0.000 0.000 0.000 0.000
     INCREMENTAL AND TOTAL PRODUCTION      408.2     1236.7
          0.200     0.200     0.200     0.200     0.200     0.200
          0.435     0.200     0.370     0.630


     RESERVOIR AFTER       12.0 DAYS
     TEMPERATURE PROFILE
      307.1 301.0 303.0 297.6 295.2 289.5 281.8 270.0 246.4 192.9  74.0
     SOLUTION ERROR
     -0.000-0.000 0.000 0.000 0.000 0.000 0.000 0.000 0.000 0.000
     RATE       99.4
     ELEMENT BY ELEMENT RESISTANCE
      0.000 0.000 0.000 0.000 0.000 0.000 0.000 0.000 0.000 0.008
     INCREMENTAL AND TOTAL PRODUCTION      400.2     1636.9
          0.200     0.200     0.200     0.200     0.200     0.435
          0.435     0.200     0.630     0.630
```

```
RESERVOIR AFTER       16.0 DAYS
TEMPERATURE PROFILE
 290.0 287.5 286.5 282.0 279.0 272.5 263.8 250.7 225.3 170.9  74.0
SOLUTION ERROR
-0.000-0.000 0.000 0.000 0.000 0.000 0.000 0.000 0.000 0.000
RATE       98.1
ELEMENT BY ELEMENT RESISTANCE
 0.000 0.000 0.000 0.000 0.000 0.000 0.000 0.000 0.004 0.009
INCREMENTAL AND TOTAL PRODUCTION      394.9    2031.8
     0.200     0.200     0.200     0.200     0.200     0.435
     0.435     0.200     0.630     0.630
```

```
RESERVOIR AFTER       20.0 DAYS
TEMPERATURE PROFILE
 276.2 271.4 271.0 266.7 263.6 257.1 248.4 235.3 210.4 160.5  74.0
SOLUTION ERROR
 0.000-0.000 0.000 0.000 0.000 0.000 0.000 0.000 0.000 0.000
RATE       96.8
ELEMENT BY ELEMENT RESISTANCE
 0.000 0.000 0.000 0.000 0.000 0.000 0.000 0.000 0.005 0.009
INCREMENTAL AND TOTAL PRODUCTION      389.7    2421.5
     0.200     0.200     0.200     0.435     0.435     0.435
     0.435     0.630     0.630     0.630
```

```
RESERVOIR AFTER       24.0 DAYS
TEMPERATURE PROFILE
 262.9 260.6 259.7 255.5 252.3 245.7 236.9 223.7 199.2 151.4  74.0
SOLUTION ERROR
 0.000-0.000 0.000 0.000 0.000 0.000 0.000 0.000 0.000 0.000
RATE       95.5
ELEMENT BY ELEMENT RESISTANCE
 0.000 0.000 0.000 0.000 0.000 0.000 0.001 0.004 0.005 0.010
INCREMENTAL AND TOTAL PRODUCTION      384.6    2806.2
     0.435     0.435     0.435     0.435     0.435     0.435
     0.630     0.630     0.630     0.630
```

```
RESERVOIR AFTER       28.0 DAYS
TEMPERATURE PROFILE
 253.8 251.1 250.0 246.0 242.8 236.2 227.4 214.2 190.1 144.7  74.0
SOLUTION ERROR
 0.000-0.000 0.000 0.000 0.000 0.000 0.000 0.000 0.000 0.000
RATE       94.2
ELEMENT BY ELEMENT RESISTANCE
 0.000 0.000 0.000 0.000 0.000 0.001 0.004 0.004 0.006 0.010
INCREMENTAL AND TOTAL PRODUCTION      379.5    3185.6
     0.435     0.435     0.435     0.435     0.435     0.435
     0.630     0.630     0.630     0.630
```

```
RESERVOIR AFTER      120.0 DAYS
TEMPERATURE PROFILE
 173.3 172.7 171.4 168.9 165.9 160.7 153.9 143.8 127.5 102.9  74.0
SOLUTION ERROR
-0.000-0.000 0.000 0.000 0.000 0.000 0.000 0.000 0.000 0.000
RATE       67.2
ELEMENT BY ELEMENT RESISTANCE
 0.005 0.005 0.006 0.006 0.006 0.006 0.007 0.008 0.009 0.013
INCREMENTAL AND TOTAL PRODUCTION      271.0    10535.5
      0.630      0.630      0.630      0.630      0.630      0.630
      0.630      0.630      0.630      0.630
```

```
RESERVOIR AFTER      124.0 DAYS
TEMPERATURE PROFILE
 171.8 171.2 169.9 167.5 164.5 159.4 152.6 142.6 126.5 102.3  74.0
SOLUTION ERROR
 0.000-0.000 0.000 0.000 0.000 0.000 0.000 0.000 0.000 0.000
RATE       66.1
ELEMENT BY ELEMENT RESISTANCE
 0.006 0.006 0.006 0.006 0.006 0.006 0.007 0.008 0.009 0.013
INCREMENTAL AND TOTAL PRODUCTION      266.7    10802.2
      0.630      0.630      0.630      0.630      0.630      0.630
      0.630      0.630      0.630      0.630
```

```
RESERVOIR AFTER      128.0 DAYS
TEMPERATURE PROFILE
 170.4 169.8 168.6 166.1 163.1 158.1 151.4 141.4 125.5 101.7  74.0
SOLUTION ERROR
 0.000-0.000 0.000 0.000 0.000 0.000 0.000 0.000 0.000 0.000
RATE       65.0
ELEMENT BY ELEMENT RESISTANCE
 0.006 0.006 0.006 0.006 0.006 0.006 0.007 0.008 0.009 0.013
INCREMENTAL AND TOTAL PRODUCTION      262.3    11064.5
      0.630      0.630      0.630      0.630      0.630      0.630
      0.630      0.630      0.630      0.630
```

```
RESERVOIR AFTER      132.0 DAYS
TEMPERATURE PROFILE
 169.0 168.5 167.2 164.8 161.9 156.9 150.2 140.3 124.6 101.2  74.0
SOLUTION ERROR
 0.000-0.000 0.000 0.000 0.000 0.000 0.000 0.000 0.000 0.000
RATE       64.0
ELEMENT BY ELEMENT RESISTANCE
 0.006 0.006 0.006 0.006 0.006 0.006 0.007 0.008 0.010 0.013
INCREMENTAL AND TOTAL PRODUCTION      258.0    11322.5
      0.630      0.630      0.630      0.630      0.630      0.630
      0.630      0.630      0.630      0.630
```

```
RESERVOIR AFTER      360.0 DAYS
TEMPERATURE PROFILE
 132.9 132.7 131.8 130.2 128.0 124.6 119.9 113.0 102.9  89.1  74.0
SOLUTION ERROR
-0.000-0.000 0.000 0.000 0.000 0.000 0.000 0.000 0.000 0.000
RATE       42.6
ELEMENT BY ELEMENT RESISTANCE
 0.102 0.104 0.108 0.115 0.127 0.146 0.179 0.247 0.408 0.818
INCREMENTAL AND TOTAL PRODUCTION      170.5   22470.8
     0.830      0.830      0.830      0.830      0.830      0.830
     0.830      0.830      0.830      0.830
```

```
RESERVOIR AFTER      364.0 DAYS
TEMPERATURE PROFILE
 132.6 132.4 131.5 129.9 127.7 124.3 119.6 112.8 102.7  89.0  74.0
SOLUTION ERROR
-0.000-0.000 0.000 0.000 0.000 0.000 0.000 0.000 0.000 0.000
RATE       42.5
ELEMENT BY ELEMENT RESISTANCE
 0.103 0.105 0.110 0.117 0.128 0.147 0.181 0.249 0.411 0.820
INCREMENTAL AND TOTAL PRODUCTION      170.1   22640.9
     0.830      0.830      0.830      0.830      0.830      0.830
     0.830      0.830      0.830      0.830
```

```
RESERVOIR AFTER      368.0 DAYS
TEMPERATURE PROFILE
 132.3 132.1 131.2 129.6 127.4 124.0 119.3 112.6 102.5  88.9  74.0
SOLUTION ERROR
-0.000 0.000 0.000 0.000 0.000 0.000 0.000 0.000 0.000 0.000
RATE       42.4
ELEMENT BY ELEMENT RESISTANCE
 0.104 0.106 0.111 0.118 0.129 0.149 0.182 0.251 0.413 0.822
INCREMENTAL AND TOTAL PRODUCTION      169.7   22810.6
     0.830      0.830      0.830      0.830      0.830      0.830
     0.830      0.830      0.830      0.830
```

```
RESERVOIR AFTER      372.0 DAYS
TEMPERATURE PROFILE
 131.9 131.7 130.9 129.3 127.1 123.7 119.1 112.3 102.4  88.8  74.0
SOLUTICN ERROR
-0.000-0.000 0.000 0.000 0.000 0.000 0.000 0.000 0.000 0.000
RATE       42.3
ELEMENT BY ELEMENT RESISTANCE
 0.106 0.107 0.112 0.119 0.131 0.150 0.184 0.253 0.416 0.824
INCREMENTAL AND TOTAL PRODUCTION      169.3   22979.9
     0.830      0.830      0.830      0.830      0.830      0.830
     0.830      0.830      0.830      0.830
```